Author Response to Anonymous Referee #1 Comments

We thank the reviewer for her/his helpful comments. Referee comments are given in black and author comments/actions in red.

"The paper by Williams et al. "Characterising the Seasonal and Geographical Variability of Tropospheric Ozone, Stratospheric Influence and Recent Changes" utilises satellite and ozonesonde observations and two chemistry-climate models to investigate the stratospheric influence on tropospheric ozone. The authors conclude that the influence of stratospheric on tropospheric ozone is larger than previously thought. The authors also assessed the tropospheric ozone over the periods of 1980-89 and 2001-2010, and find an overall significant increase in tropospheric ozone, and attribute 25-30% changes at the surface and 50-80% in the upper troposphere to the stratosphere-troposphere exchange. The paper is well written, and the analysis is generally thorough, but some clarifications and improvements are needed before the paper can be accepted for publication in ACP. Detailed comments are listed below."

Thank you for your positive assessment of our manuscript. We hope to have clarified the issues raised with details on changes given below.

"General comments:

A major concern is that this study includes only two CCMI model results, which reduces the robustness of the finding, especially in that "the influence of STE in the tropospheric ozone is larger than previously thought". Furthermore, using only simulations constrained with prescribed dynamics might obscure the changes due to dynamical feedbacks, especially when assessing long-term changes in ozone. Therefore, I suggest that the authors tone down the conclusion mentioned above, and instead focus on the uncertainty in the contribution of STE to the tropospheric ozone. The limitation of using prescribed dynamics CCM simulations should also be noted and discussed. A wider usage of CCMI models would address the first comment. As a minimum, the authors should give a reason for using only the two chosen models."

We acknowledge your concern that there are caveats with confining the analyses to only two models (such as the robustness of findings) but we argue that such detailed analyses would not be possible in the context of a wider range of CCMI models, at least not within the scope of this paper alone. However the main reason for our choice of these two models is the availability of the O_3S tracer which is defined similarly. Whilst some (but not all) of the other CCMs in CCMI have O_3S tracer simulations, they are not defined equivalently. We also acknowledge your point regarding the use of the specified dynamics simulations and agree that the above conclusion needs to be toned down accordingly, with greater emphasis on the uncertainty in the contribution of STE to tropospheric ozone. Whilst we are fully aware that the use of specified dynamic simulations can supress chemistry-climate feedbacks, the constraint on dynamics is critical for our quantification of historical changes due to the primary influence of transport and dynamics on the chemical distribution of ozone VMR. We agree that the limitations of using only two CCMs and specified dynamics simulations needs to be noted and discussed more widely, which we now address in the revised manuscript. In response to the first comment, we now make clear the reason for our choice of the two models.

“Regarding previous studies, I doubt that the paper by Lamarque et al. (1999) is still a very relevant reference that the authors focus their comparisons on, given that the approach used in Lamarque et al. (1999) was very simplistic compared to what can be achieved using more recent state-of-the-art CCMs. Also, there are a few more studies that have investigated the impact of STE on tropospheric ozone which the authors failed to cite, for example, Lelieveld and Dentener (2000), Hess et al. (2013), etc. Jos Lelieveld and Frank J. Dentener, What controls tropospheric ozone? JGR, 105, P3531-3551 2000.

P. G. Hess and R. Zbinden, Stratospheric impact on tropospheric ozone variability and trends: 1990–2009, ACP, 13, 649–674, 2013.

Therefore, a more thorough review of the recent literature would be desirable.”

Our explicit reference to Lamarque et al. (1999) relates to the similarity of their analyses to ours and we would argue that the comparison to their results highlights how our understanding of the influence of the stratosphere on tropospheric ozone has changed in the last twenty years as models have become increasingly more complex. However, we certainly agree with your point and thus also feel that other more recent publications on the matter (such as the ones suggested above) need mentioning, which will help for a more thorough review of the recent literature on the impact of STE on tropospheric ozone. This has now been implemented.

“Specific comments:

P2, L13: add “large” before “number”

Done.

“P4, L17: please add references here”

A reference has been added to support this point.

“P5, L5-L20: Can you describe the models’ characteristics in a more objective way here? Why do you choose these two models specifically (there are quite a few other models from CCMI that you could include)? Also describe the main differences between these two models.”

Please see paragraph for amendments to help describe such characteristics more objectively. A sentence has been added to justify the use of only the two models (based on the definition of the O_3S tracer which is similar in both models and is either absent or defined different in other CCMI models. A sentence has also been added highlighting the main differences between the two models which is logically structured in more detail in the following specific model sub-sections (2.1.1 and 2.1.2).

“P5, L28: Pease provide more details in chemical schemes used in EMAC.”

Please see following added sentence detailing the chemistry included in the MECCA chemistry submodel which goes into EMAC.

“P6, L4 & L21: Please provide more detailed information on how the O3S tracer is defined in terms of its chemical and dynamical nature in both models.”

Please see manuscript for additional added information on the chemical and dynamical constraints on defining the O3S tracer.

“P7, L19-L21: Please clarify if the AKs have or have not been applied to the modelled and ozonesonde data when you compare these two. It only makes sense to apply AKs when compare model/sonde data to the satellite data.”

No AKs have been applied for this comparison and rightly so as it only makes sense to apply AKs for satellite-model/satellite-sonde comparisons as you state. The sentence describes satellite-sonde validation efforts as reported by another study (Miles et al., 2015). Although this was cited further up, it has been cited again to avoid any confusion.

“P7, L27-L29: I don’t understand why “The 1000-450 hPa (0-5.5 km) OMI subcolumn data is considered a representative approximation of the full tropospheric ozone column amount, due to vertical smearing of information from above 450 hPa (_ 5.5 km).” is the case. Is it possible to show AKs?”

We remove this claim as the accuracy of this representativeness is strongly latitude and seasonally dependent and due to lack of supporting literature to support this statement.

“P9, L1-L4: Please add references here. There are a series of publications on JOSIE by Smit et al.

Smit, H. G. J., and D. Kley (1998), JOSIE: The 1996 WMO International intercomparison of ozonesondes under quasi flight conditions in the environmental simulation chamber at JuÂ´llich, WMO Global Atmosphere Watch report series, No. 130 (Technical Document No. 926). World Meteorological Organization, Geneva.

Smit, H. G. J., and W. Straeter (2004a), JOSIE-1998, Performance of ECC Ozone Sondes of SPC-6A and ENSCI-Z Type, WMO Global Atmosphere Watch report series, No. 157 (Technical Document No. 1218), World Meteorological Organization, Geneva.

Smit, H. G. J., and W. Straeter (2004b), JOSIE-2000, JuÂ´llich Ozone Sonde Inter-comparison Experiment 2000, The 2000 WMO international intercomparison of operating procedures for ECC-ozonesondes at the environmental simulation facility at JuÂ´llich, WMO Global Atmosphere Watch report series, No. 158 (Technical Document No. 1225), World Meteorological Organization, Geneva.”

Many thanks, these references have been added.

“P10, L19: Ozone is not at its minimum in SON in the SH, but maximum. Biomass burning emissions and STE usually dominate the seasonality of SH O3.”

We acknowledge this is the case already for the SH as a whole, but this sentence refers only to Antarctica and the Southern Ocean where the influence of stratospheric ozone depletion is ‘likely’ dominant.

“P11, L21-23: can you provide more details on the difference between these two NOx emission datasets?”

Further details added courtesy of the Hoesly et al. (2018) reference.

“P12, L1-L2: This seems slightly mis-leading on the function of the AKs. The purpose of applying the AVKs is to compare like with like.”

We use Fig.2 (Table S1) to show and describe the importance of applying AKs and the effect it has on tropospheric ozone which we would argue is informative for an uninitiated reader to AKs and the necessity of its application for like for like model-satellite measurement comparisons. Sentenced revised slightly to avoid misleading the reader.

“P12, L4-L7: Similar features seem exist in both models; it seems more likely due to transport barrier than STE (which the STE maximises in winter).”

We agree with this statement and revise this rather speculative sentence to allude to this as a possible cause, as well as the magnitude of the stratospheric ozone hole which could explain the retention of this feature after applying AKs.

“P12, L7-L9: Does the difference in chemical schemes between the two models play a role here?”

There could be differences due to disparities in the implementation of emissions in the model schemes and different treatments (e.g. bulking of species in CMAM) but we cannot disentangle such influence apart from dynamics here in our evaluations. We now acknowledge this as having a possible influence in the biases in each model here and allude to the need for further investigation.

“P13, Fig 3: It is impossible to discern the RSD of ozonesonde data denoted as circles, due to a uniformed colour scale.”

We have revised the colobar scale down from 0-20 % to 0-14 % to make clearer structure in the RSD plots. Ozonesonde RSD is now made more easily distinguishable (white outline) but note that the RSD for sondes is uniformly low with few exceptions. The reason for this unclear and would warrant further investigation.

“P14, Fig 4: The value of 100 ppbv O3 seems a bit too low for defining the tropopause. Using 100 ppbv O3 also deviates from the definition by Bethan et al. (1996) (cited in caption), which is based on the ozone gradient, defined as the minimum altitude where the vertical gradient of the O3 VMR is greater than 60 ppb/km, remains so for a further 200 m, and the O3 mixing ratio is greater than 80 ppbv, exceeding 110 ppbv immediately above the tropopause.”

Thank you for spotting this error, we now remove the citation to Bethan et al. (1996) and simply state that we choose the 100 ppbv ozone isopleth as a rough approximation of the chemical tropopause height.

“P15, L16-L32: Please note the figures that you are discussing throughout this paragraph.

Also, the description/discussion in this paragraph can be simplified to focus on the main points."

All discussion in this paragraph refers to Fig. 4 and we now remind the reader at the start of this paragraph. We have revised and shortened this paragraph for easier reading and to make clearer the main points.

"P16, L1-L2: again, please can you refer to the figure(s) that you are discussing."

Done.

"P16, L27: Do you also apply AVKs to model data when compare them with ozonesonde data? If so, it is not necessary."

No we do not. We merely use the model-ozonesonde comparison to infer how the biases arise/change between OMI and the models as a result of applying AKs to the models in these comparisons (Fig. 1 and 2).

"P16, L28: do you mean "simplified" tropospheric chemistry scheme? It is unusual to use the word "conservative"."

Yes, word changed.

"P16, L29-L31: which comparison/figures you are talking about here? Please make it clear by referring to figures."

The additional smearing (increase in subcolumn ozone due to AK application) can be seen in Fig. 2 but the conclusion is made based on the model-ozonesonde comparison (Fig. 4) as should be clear from the previous few sentences. We however remind the reader that the influence of the AK can be seen in Fig. 2 to make this clearer.

"P16, L32-L33: It seems lacking context regarding "since vertical smearing of information is far more limited due to a higher tropopause.". Could you be specific? Where is the information regarding a higher tropopause?"

We base our statement on the higher climatological mean position of the tropopause in the tropics/sub-tropics compared with the extratropics which will result in less smearing of information from the stratosphere. Sentenced revised for clarity.

"P17: L1: "must induce" should be "must have induced""

Changed.

"P17: L3-L7: Showing the AKs might help with the discussion here."

We add in an example of the OMI monthly mean AKs for August 2007 (~ 47°S) to illustrate this point in to the supplement (new Fig. S2), which importantly shows that the 1000-450 hPa

subcolumn is sensitive to influence from ~ 150-450 hPa pressure range. This indicates where the smearing of information can originate from. We refer the reader to this figure and emphasise this point in the manuscript.

“P21, L31: Please provide details on how you map the model data to ozonesonde measurements shown in Fig 7?”

Additional detail has been added. Ozonesonde profile measurements were aggregated for each month and for 10 degree latitude bands, which were then subsequently averaged over all 31 years (1980-2010) over all longitudes (zonal average). Similarly to Fig. 4, measurements were interpolated and averaged between ±20 hPa for each pressure level (350, 500 and 850 hPa).

“P23, L1: it is too general to say that “… are evident in the contemporary CCM simulation” while only two CCMs are used here.”

Dropped the word “contemporary”.

“P24, L11: What do you mean "even lower tropospheric ozone"?”

We refer to the lower troposphere but can see how such confusion may arise. The phrase “even lower” has been removed and we refer now to such influence extending down into the lower troposphere.

“P24, L20: What is the rationale for choosing these longitudes?”

Whilst the choice is a little arbitrary to illustrate that calculated changes are very much height-dependent, both the 30°W and 30°E transects intersect the small region of negative change over central Africa, which varies according to model and pressure level in terms of magnitude and location. The 30°W transect also intersects Greenland where there is significant model disparity at 350 hPa during MAM (Fig. 8a and 10a), although the cross-sectional view (Fig. 9a and 11a) shows such large differences to be confined only to the uppermost part of the domain near to the tropopause). We find this to be consistent with differences in tropopause height found by Hegglin et al. (2010) and our own finding that the lower branch of the BDC is stronger in CMAM. The 90°W transect (Fig. 9c and 11c) intersects the Himalayas where there are some interesting differences in the calculated changes on either side of this mountain range for both O_3 and O_3S and between each model. Overall the selected transects help the discussion in this section to understand the upper level of stratospheric contribution to changes in near-surface ozone (largest across the Eurasian continent) and the source of such features such as the negative trend region over Africa (not evident in O_3S). A shorter version of this rationale is now added here in the manuscript for clarity.

“P25, Fig 8: There are large areas in the SH that are denoted significant in CMAM (SON 500 hPa and SON surface plots), which are not reflected in the relevant discussion. Please check.”

We now acknowledge this in the manuscript but do not discuss in depth as changes are small. The modest increase would appear to be related to long range transport from the SH

subtropics and entrainment hemispherically by upper level winds especially. O_3S shows no such significant changes implying this increase is driven by changes in the troposphere.

"P27, L22: Please note which figure(s) you are discussing here? Is Fig 8?"

It is Fig. 8, yes. This has been added.

"P30, L10-L12: is "subtle shifts in the height of tropopause" shown anywhere?"

We do not show it anywhere but we do refer to Hegglin et al. (2010) earlier on in 4.1 (page 19, line 8) which finds that the CMAM tropopause is lower (some 30-50 hPa higher in pressure) than EMAC. This citation is now mentioned here also to support this statement.

"P34, L10-L12: What are the reference variables for these percentage changes?"

The percentage change values relate to the change values in ppbv we summarised earlier in 5.1 – e.g. The O_3 (Fig. 8) increase in the NH mid-latitudes during MAM/SON in the upper troposphere, being on the order of some 4-6 ppbv is seen to equate to a 1-3 ppbv increase in O_3S (Fig. 10) over the time period considered, hence we arrive at a ~ 25-50 % stratospheric contribution to the total change. We now mention here that such values are arrived at in conjunction with use of the tagged stratospheric (O_3S) tracer.

"P35, L2: Please specify re "some regions of the world"."

We now give examples where the increase is substantial and generally significant for both models in one or more seasons: W. Eurasia, E. North America, S. Pacific Ocean and the S. Indian Ocean.

Author Response to Anonymous Referee #2 Comments

Thank you for your comments. Referee comments are given in black and author comments/actions in red.

"The manuscript titled "Characterising the Seasonal and Geographical Variability of Tropospheric Ozone, Stratospheric Influence and Recent Changes" presents a very interesting analysis on the stratospheric influence on tropospheric ozone using two chemistry-climate models CMAM and EMAC, as part of the IGAC/SPARC CCMI activity. The manuscript first shows that both models agree quite well with the observations from Satellite with the Ozone Monitoring Instrument (OMI) and from ozonesondes. Then the manuscript focuses on the models to study the variability of tropospheric ozone, stratospheric ozone and the stratospheric intrusions in order to assess how much stratospheric ozone impact tropospheric ozone. A statistically significant increase in tropospheric ozone is found across much of the world. The role of the stratosphere-troposphere exchange to such ozone changes ranges from 25-30% at the surface and 50-80% in the upper troposphere-lower stratosphere.

Although the manuscript is not so easy to read and follow, it is well structured; in particular, the summaries of each main section are very much appreciated.
I would suggest minor revisions, mainly clarifications, before the manuscript could be published."

Thanks for your feedback. Hopefully implementation of the suggested minor revisions/clarifications will help to improve the legibility of the manuscript.

"General comments:

I found one general information missing about the models. It is the inferred stratospheric influx as mentioned in Young et al., 2013 (Table 2) for other CCMI models. Could the authors add this information?

Young, P. J., Archibald, A. T., Bowman, K. W., Lamarque, J. F., Naik, V., Stevenson, D. S. et al.: Pre-industrial to end 21st century projections of tropospheric ozone from the Atmospheric Chemistry and Climate Model Intercomparison Project (ACCMIP). Atmos. Chem. Phys., 13(4), 2063-2090, doi:10.5194/acp-13-2063-2013, 2013".

This information is only from ACCMIP (a subset of CCMI models) and therefore we summarise such information instead from table 8.1 from the IPCC WG1 AR5 report which includes the mean stratospheric influx from this subset of models, in addition to a range of other models and observational estimates. Sentence added in opening paragraph of section 2.

"Specific comments:

Line 1 p. 2: Could the authors give the period of time on which the change in ozone was calculated: 4-6 ppbv (5-10%)".

This information should have been implicit as the time period was mentioned in the previous sentence (line 34-35, p. 1). Have omitted this detail here and given the period of time the change was calculated over at the end of the above sentence (line 2, p. 2) for clarity.

"Line 24 p.2: "background ozone" is used here, when I think it refers to "baseline ozone". According to the Hemispheric Transport of Air Pollution 2010 Part A paper and Cooper et al.

(2014), “Baseline concentrations refer to observations made at a site when it is not influenced by recent, locally emitted or produced anthropogenic pollution. The term global or hemispheric background concentration is a model construct that estimates the atmospheric concentration of a pollutant due to natural sources only.

Cooper, O. R., Parrish, D. D., Ziemke, J., Cupeiro, M., Galbally, I. E., Gilge, S., ... & Oltmans, S. J. (2014). Global distribution and trends of tropospheric ozone: An observation-based review.

HTAP, T., 2010. Hemispheric Transport of Air Pollution 2010 Part A: Ozone And Particulate Matter, Air Pollution Studies No. 17”.

Thanks for pointing this out. We indeed misuse the term ‘background ozone’ as referring to the ‘baseline ozone’ when citing Cooper et al. (2014) and so have corrected this and added in the additional HTAP (2010) reference. Our reference to studies which refer to ‘background ozone’ remain, but we keep these citations separate from the two above.

“Line 12-14 p. 3: I am not sure to understand where “seasonal minimum’ comes from. According to Tang et al. (2016), the STE ozone flux in the Northern Hemisphere shows a maximum in late spring and early summer as well. Could the authors clarify the sentence?”

The phrase “seasonal minimum” on line 13 relates to the STE mass flux, not the STE ozone flux which we acknowledge has a seasonal maximum in late spring and early summer (in agreement with Yang et al. (2016)?) on line 12. Have revised this sentence, which hopefully clarifies this better and improves readability.

“Line 9 p. 5: [Typo] In “24, 6, 48 and 24 h”, “24” is written twice”.

This is an actual fact not a typo. These times refer to the nudging to temperature, vorticity, divergence, and surface pressure respectively. These are now listed following a colon and taken out of parentheses to avoid confusion.

“Line 26 p. 5: [Typo] Change “Langrangian” to “Lagrangian””

Typo corrected.

“Line 1 p. 9: Could the authors add references about the intercomparison campaigns between 1970 and 1990, for example Beekman et al. (1994). I would have the same comment for the “evidence that the ECC sondes have greater precision […]”.

Beekmann, M., Ancellet, G., Megie, G., Smit, H., Kley, D., 1994b. Intercomparison campaign of vertical ozone profiles including electrochemical sondes of ecc and brewer-mast type and a ground based uv-differential absorption lidar. J. Atmos. Chem. 19, 259e288.”

References added, many thanks.

“Line 18 p. 9: The authors wrote, “A seasonal maximum in tropospheric ozone is evident in each hemisphere during spring, which is more pronounced in the Northern Hemisphere and extended in many regions through summer”. According to Figure 1a, the Northern Hemisphere shows a seasonal maximum in spring and summer. In spring the maximum is rather seen

above 80N. How confident are you on the retrieval of tropospheric ozone above 80N? Wouldn't be rather a stratospheric signal?
Could the authors add this particular polar region (>80N) where the spring maximum is seen?"

We make no change to the manuscript as the retrieval should not be trusted at these latitudes due to the influence of the OMI row-anomaly (rows on the 2-D detector which have become damaged or blocked by insulation blankets – mentioned on page 8, L6-9). We have instead extended the grey masking to cover this region in MAM/JJA.

"Line 21 p. 9: Use of the parenthesis: "northward (southward)". This is not really a good structure and the authors tend to overuse it through the manuscript. I would suggest writing it without the parenthesis. That would be better English and more fluent for the reader.

Sentence revised and we limit use of this structure elsewhere to only sentences where we deem appropriate and fluency is not compromised for the reader.

Figure 1 (p. 10): I would suggest to change the maximum limit of the colorbar. Tropospheric ozone (1000-450 hPa sub-column) barely reach 35 DU at a maximum. I would suggest to change 50 DU to 35 DU. The geographical variability of tropospheric ozone will then be easier to see.
Would the authors know what is happening above South Africa for JJA and SON? There is ozone values around 30 DU on the cost and above the ocean around but rather 20 DU on the continent, as there would be a continent/ocean barrier. It does not seem real."

We have revised this colour scale accordingly. We believe advection of precursor-rich air from the continent (due to biomass burning) and later formation of photochemically formed ozone to explain the higher values offshore, together with the reduced depth of the subcolumn over the relatively elevated South African mainland.

"Line 23 p. 12: Could the authors explain more, maybe with an equation, how they link the "interannual variability" and the "seasonal aggregates of the computed relative standard deviation (RSD) of the monthly mean O3". It is not obvious. The interannual variability seems to be the variability year to year. Why would the authors study seasonal composites of RSD as a metric for the interannual variability?"

We have added an equation immediately below this sentence for clarity in how we calculate seasonal composites of RSD. The standard deviation is normalised with respect to the mean of each individual month over all years (2005-2010) to compute the monthly RSD which we then aggregate by calendar season. This metric therefore captures variability with respect to the monthly resolved seasonality over all years which we infer here as the interannual variability.

"Line 14 p. 17: Section 4. Could the authors explain more the difference between O3S and O3F? If there is any equation used, I would suggest adding them to the text. It is not so clear."

We now make this clear through revising this sentence and have also added the O_3F equation in line (in addition to the Fig. 5 caption).

“Line 18 p. 33: “RSD values of over 10%”. How does 10% compare with other values? It is not a clear evidence for the reader that it shows an influence of ENSO and QBO.”

According to Lee et al. (2010), a study that was originally cited in section 3.2, the QBO is estimated to induce anomalies of as much as 10-20 % in tropical tropospheric ozone, which would scale with the 10-20 % variability in RSD found in both OMI and the models. This is again referred to here to ensure the reader makes this connection but ‘ENSO’ is dropped as the study found that the influence from ENSO is likely much smaller (~ 3 %).

“Line 24 p. 33: “Taking this information into account”. To which information do the authors refer?”

This refers to the findings of section 3 (summarised in the paragraph above in section 6: conclusions). This is made clearer to the reader.

“Line 33 p. 33: The sentence started at this line and finishes line 2 p. 34, I think the sentence could be shortened.”

This sentence has been split in two.

“Line 34 p.33: “(no larger than 20%)”, I would suggest removing the parenthesis and writing “with biases no larger than 20%”.”

This has been revised.

“Line 13 p. 34: What does “high sensitivity to the tropopause” mean?”

This refers to the height of the tropopause being key to the calculated changes (due to the associated sharp vertical gradients in ozone). Changed to ‘known discrepancies in tropopause height’ as found in Hegglin et al. (2010).

“Figure S4 p. 6: [TYPO] in the caption change “CMAN” to “CMAM””

Thanks, typo corrected.

Author Response to Anonymous Referee #3 Comments

Thank you for your comments. Referee comments in black and author comments/actions in red.

"This is an interesting and useful analysis, but needs to be put in context and contrasted with other recent work before it is published. The authors would also be well-advised to better qualify the limitations of their study, in particular with regard to tropospheric chemistry."

Thanks, we agree with these comments and now have added more references to contemporary work and better pointed out the limitations of our study, particularly relating to tropospheric chemistry and the specified dynamics simulations used.

"Detailed remarks:

Page 3, lines 21-25: (and elsewhere) the authors focus on Lamarque et al. (1999), a 20-year old study. There are much more recent modeling studies that show larger net influence of STE. For example, Figure 6 of Banerjee et al. (2016) looks very much like Figure 5 of this manuscript. Doubtless similar plots for other models exist. If the authors wish to make the case for their result "that the stratospheric influence on tropospheric ozone is larger than previously thought", they need to quote recent studies that show smaller influence."

We agree. The statement has been toned down to reflect the important role of the stratosphere more generally. The influence of STE on tropospheric ozone is now updated here in accordance with more recent studies (including a reference to Banerjee et al., 2016). However, we keep the reference to Lamarque et al. (1999) in places to emphasise the similarity of their analyses to ours and the focus of the paper.

"Line 34: Similarly, the authors cite only one observational study, and for the Southern Ocean. There have been many such studies, e.g. Dibb et al. (1994); Elbern et al. (1997); Stohl et al. (2000); Zanis et al. (2003); Colette and Ancellet (2005); Cooper et al. (2006); Thompson et al. (2007a,b); Cristofanelli et al., (2010); Tarasick et al., (2018). Citing some of these would not only be appropriate, but would support the authors' point, as in general they find modest influence of STE on lower tropospheric ozone levels."

Thanks for these additional references. We now summarise and discuss this literature in a separate paragraph which immediately follows on from the discussion of stratospheric influence according to model studies.

"Page 4, lines 10-11: While I agree that there are certainly major limitations with the accuracy of retrieved tropospheric ozone from spaceborne instruments, I take issue with the statement "…scientists must instead rely on tools such as chemistry climate models (CCMs) to fill in the gaps in our understanding of the global distribution of tropospheric ozone". NO, NO, NO! Models are sophisticated data visualization tools: they contain (at best) all that we know about the atmosphere. They allow us insights and interpretation that would not be possible without them, but they do not contain anything that we don't, collectively, already know."

Whilst we largely agree with this point, we would argue that quantification of the stratospheric contribution (O_3S) to both the vertical and global distribution of tropospheric ozone is not

possible from observations alone. Additionally, specific model simulations and diagnostics can help to disentangle various feedbacks/mechanisms that could not be inferred from observations alone. We have rewritten this statement to now better explain the added scientific value we can gain from CCMs in comparison with observations.

“Page 8, lines 10-11: I thought the main problem was lack of photons that actually penetrate this far, as well as lack of contrast in the scattered spectrum, compared to a few km higher up.”

We agree that this is the main issue with the retrieval of particularly lower tropospheric ozone (with errors in the retrieval due to albedo and aerosols for instance of secondary importance). This detail has been added into the manuscript.

“Page 8, line 18: It seems odd to cite satellite papers for generic facts about the global ozonesonde network. Liu et al. (2013b) has a good discussion, with a map and table of sites. In line 26, the proper reference here is Smit et al. (2007), although the others are fine as additional references. On the next page (line 2), citations are required for the WMO & JOSIE campaigns.”

We agree with this point and omit some of this detail, referring the reader to the suggested Liu et al. (2013b) reference. Citations have been added for the WMO and JOSIE campaigns. Many thanks for these references and clarification.

“Page 9: I find the statement in lines 28-30 quite remarkable. I believe there are many studies showing that long-range transport of ozone and its precursors are the dominant source of ozone in remote areas.”

We agree that this argument is valid but more applicable to the lower troposphere. We thus revise this sentence to refer to the free troposphere and tone down our assertion of the dominant role of STE to avoid any contradiction.

“Page 17 (top paragraph), and elsewhere: the authors put a lot of effort into explaining the effects of “vertical smearing”. Of course they need to consider OMI AKs when comparing to OMI data, but perhaps they would find it easier to use a 3D ozonesonde based dataset, like Liu et al. (2013a,b).”

We believe our paper will serve to highlight the importance of AKs for model-satellite measurement comparisons which is sometimes not fully understood or appreciated within the CCMI community. We agree that comparisons with an ozonesonde-based dataset using trajectory mapping would provide further insight but of course such products have their limitations. Such analysis we would suggest is beyond the scope of this study but we now mention such approach could be warranted to further establish and confirm the presence of such model biases we found in our model-ozonesonde comparison (Fig. 4).

“Page 22 (Figure 7a): How are these plots produced from ozonesonde data?”

This is now made clear in the opening sentence to sub-section 4.3. Ozonesonde profile measurements were aggregated for each month and for 10 degree latitude bands, which were

then subsequently averaged over all 31 years (1980-2010) over all longitudes (zonal average). Similarly to Fig. 4, measurements were interpolated and averaged between ±20 hPa for each pressure level (350, 500 and 850 hPa).

"Page 23, line 22: The "significant difference in the strength and dominance of the shallow branch of the BDC in each model" needs more explanation. It is first mentioned here, in the Summary."

The build-up and burden of ozone in the extratropical lowermost stratosphere is directly related to strength of the lower BDC branch (since the equatorial region is where most ozone is produced). We add in this additional detail and include citations.

"Page 31 (Summary): The authors should consider, and discuss, the differences between their results and the much smaller STE response found by Neu et al. (2014). In particular, Neu et al. claim that larger responses of tropospheric ozone to STE are found in models without comprehensive tropospheric chemistry."

We have added a few sentences discussing our findings in relation to the earlier study by Neu et al. (2014) and note this important caveat.

"Page 32, lines 31-34: Discussing the comparison before the AKs are applied makes little sense, and should be omitted."

Actually, we feel this finding highlights an important trade-off in applying AKs to models that have known stratospheric biases for model-measurement comparisons of tropospheric ozone. In the case of CMAM, we can infer through our analyses (Fig.2 and Fig. 4 in section 3) that the closer agreement to OMI arises due to the competing influence of the relatively simple tropospheric chemistry scheme (underproduction of in situ photchemical formation of ozone) and excessive smearing of stratospheric ozone due to a high bias in the lower stratosphere (~ +20-60 %). Such analyses therefore show that CMAM is more deficient in its representation of tropospheric ozone than EMAC, whereas the opposite might be inferred from Fig. 1 alone. We expand this point to argue our case and make the reader aware that in a limit number of cases, where stratospheric biases are sufficiently large, application of AKs for model-measurement comparisons of tropospheric ozone would not be advocated, particularly if the model representation of tropospheric ozone is known to be good.

"Page 33, line 26: See previous comment, page 23, line 22."

Sentence expanded to explain this conclusion again.

"Minor points:

Page 5, lines 11, 12: Typographical errors."

Sentence has since been removed.

"Page 5, line 34: The solar cycle evolves?"

We refer to the 11-year solar cycle which we now state explicitly for clarity.

“Page 6, line 9: Typographical error.”

Removed ‘have’.

“Page 6, line 19: “Compared with EMAC”?”

Changed to ‘In contrast to EMAC’

“Page 8, line 20: Actually the WOUDC also has data for Indian, Brewer-GDR, carboniodine and Regener sondes.”

Thanks for this clarification. We however remove such detail and direct the reader elsewhere (e.g. Liu et al., 2013b) as suggested by yourself.

Author Additional Comments

Referee comments in black and author comments/actions in red.

Further amendments to the manuscript have been made in accordance with an internal review procedure within the Canadian Centre for Climate Modelling and Analysis department of Environment Canada, of which is the host institution of co-author *David A. Plummer*. These amendments are listed below:

"P1, L32: With the model biased high in the lower strat and underproducing photochemical O3 in the troposphere, the conclusion that stratospheric O3 intrusions are larger than previously thought is cast in doubt, since that may just be because of the model biases.

Can more explanation be added here to explain why the authors still feel confident in that conclusion? For example, was a correction applied to the model before coming to that conclusion?"

Changed "larger than previously thought" to "significant". Although we can be confident that the real influence of the stratosphere is larger than that found by Lamarque et al. (1999), which is the main study we base this assertion on, we have to appreciate it is a twenty year old study that was based on a much simpler model. We therefore include new references throughout the manuscript as suggested by the reviewers and tone down statements such as that above. We see no reason to alter the estimated influence exceeding 50 % in the wintertime high latitudes however, as both model show this (it was only CMAM which had the high (low) bias in the lower stratosphere (troposphere) and if anything the inverse was found for EMAC). However, it is an important point and does suggest there is some uncertainty still in our understanding of the stratospheric influence.

"P2, L25: Fiore et al (2002, JGR) and references therein could be added as older (more seminal) references of the increase in background tropospheric O3.

Fiore, A. M., D. J. Jacob, I. Bey, R. M. Yantosca, B. D. Field, A. C. Fusco, and J. G. Wilkinson (2002), Background ozone over the United
States in summer: Origin, trend, and contribution to pollution episodes, J. Geophys. Res., 107(D15), ACH 11–1–ACH 11-25, doi:10.1029/2001JD000982."

Done.

Here's another reference for transpacific transport of O3:

"P2, L28-29: Zhang, L., et al. (2008), Transpacific transport of ozone pollution and the effect of recent Asian emission increases on air quality in North America: An integrated analysis using satellite, aircraft, ozonesonde, and surface observations, Atmos. Chem. Phys."

Reference added.

"P4, L7: Lines 5-11 read as a little dismissive of the many excellent tropospheric O3 measurements from satellites such as TES, OMI/Trop-OMI, TOMS, MLS, etc - many of which have *long* term (> decade), global datasets, and are well validated by ground-based remote sensing, in situ, and inter-satellite comparisons.

If just trying to motivate the use of models to fill in the gaps in measurements, one may mention that the satellite measurements are usually limited to just a couple of overpass times per day at each location, and often have large errors in retrieved O3 (but are those uncertainties more than those from the mode??).
However, the second point about assessing and quantifying the causes and processes of trop O3 is good".

These lines have been rewritten to sound less dismissive, with greater acknowledgement of the value such satellite datasets provide and their contribution to our understanding of tropospheric ozone. The paragraph as a whole has also been modified to highlight the value of CCMs in terms of providing insights and interpretation (mechanisms, feedbacks and quantification of the stratospheric influence) that cannot be inferred from observations alone, as opposed to the filling in of gaps in the measurements, which is not such a valid point for such a reason you mention.

"P4, L7-8: add references"

Reference added.

"P4, L16-17: do you have a reference or other proof (e.g., your own calculations) of emissions being the largest source of model uncertainty?"

No, but we add in a reference which supports this claim.

"P4, L27: what does F stand for? Is O3F the total O3? ...Ok, coming back to this, I think I understand what O3F is, and "F" may stand for "fraction", perhaps?

Ideally O3S and O3F would be changed to something clearer like: O3_strat and O3_%strat (use subscript instead of "_")

The F indeed refers to fraction. This has been made clearer in the manuscript and indeed should have been defined as such here (the first instance it is mentioned).

"P6, L9: EMAC also extends to 0.01 hPa, but above you haven't given the altitude. Either move to first mention of 0.01 hPa, or remove the km altitude altogether, since that's highly variable depending on latitude".

Removed 95 km reference.

"P13, Fig. 3: The RSD from the ozonesondes looks to be much lower than that from OMI (and that from the models too), but this is not discussed in Section 3.2."

The scale range has been revised to show more structure in the RSD plots, however the ozoneosnde RSD is significantly lower than OMI in particular with few exceptions. This will require further investigation.

"P14, L25-29: I think the ppbv goes with Fig S1, but this method of using brackets is confusing b/c there is also left, middle, and right in brackets in the same sentence. I suggest describing Fig 4 in one sentence, and then adding a second sentence, saying that Fig S1 shows the same thing, but absolute differences of VMRs instead of percent differences."

Correct but agreed that the use of brackets is excessive in this sentence so have revised this and split into two sentences in accordance with your suggestion. Many thanks.

“P15, L31: change "should be" to "are"”

Done.

“P17, L23: It's not clear to me what O3S is. From the wording, it sounds like it is just O3. But from the equation given in the caption, O3S seems to be the tagged stratospheric O3. If the latter, this sentence needs to be changed to say "Seasonal composites of the monthly mean, zonal-mean vertical distribution of stratosphere-originating ozone (O3S)" or "...tagged-stratospheric ozone (O3S)".

This comes back to my earlier comment that O3F and O3S are not described clearly enough, and was confusing to me (and possibly other readers). Ideally, "O3F" and "O3S" would be replaced by
"O3_%strat" and "O3_strat"”

This has been clarified and sentence broken up to avoid excessive use of brackets and enhance readability.

“P17, L24: How is Fig. S2 different from Fig 5? I don't see any corresponding bracketed statement that goes with S2 rather then Fig 5...
Please add the explanation in these brackets, and make it clearer in the caption for Fig S2. For example, the caption to Fig S2 could be "Figure S2 - same as Fig 5, but for ...[whatever is diffferent]."

...Ok, it took me a while, but now I see that the above sentence referring to O3 corresponds to Fig 5, and the bracketed "(O3S concentration)" corresponds to Fig S2. This method of using brackets to try to save wording makes it unnecessary confusing for the reader, and could be written just as efficiently as follows:

"Seasonal composites of [....] ozone concentrations (is it concentrations or VMR? clearly state one without using brackets) from 1000-80 hPa are shown in Figure 5 for EMAC (a), ... together with ... . The same is shown for the stratospheric-tagged O3 (O3S) in Figure S2.”"

This has been remedied following the action taken immediately above.

P17, L33: There are alot of these bracketed inverse statements that I think should just be restated for clarity. For example, here it doesn't cost too many extra words to say:

"with the former clearly a greater influence near the surface, and the latter in the upper troposphere."

I would reword most, if not all, cases like this in the paper to improve clarity when it can be done so efficiently.”

Done. We appreciate your point and make such revisions where necessary elsewhere to enhance readability and avoid reader confusion.

“P19, L25: Although this is a straightforward sentence using the bracket method, rewording to "when O3_%strat reaches a maximum in winter and minimum in summer." only adds one word ("and") and is clearer to the reader.”

Done.

“P20, Fig. 6: what is the gray? Please mention what it is in the caption.”

The grey shaded regions represent where surface pressure values are lower than the plotted pressure level (i.e. where each pressure level would be below ground). This is now indicated in the figure caption.

“P23, L1: "in the present study"”

Phrase added.

“P24, L11: what is meant by "even lower"? Meaning the models are biased even lower? Or meaning even lower in altitude? This should be clarified b/c if interpreted the first way, then a low-biased tropospheric O3 will given erroneously high biased O3F in the troposphere.

I would remove "even lower" from the sentence.”

We were referring to the influence exceeding 50 % as far down as the lower troposphere and hence we revise the sentence to make this clearer and avoid reader misinterpretation.

“P24, L19: just say "modelled O3 VMRs", remove the word "concentration" b/c VMR is not a concentration.”

Done.

“P24, L19: again I'm confused: does Fig S5 correspond with O3 VMR and Fig 8 correspond to O3 concentration? The brackets are confusing and unnecessary.”

Fig. S5 refers to the seasons DJF/JJA (also brackets at end of sentence). We agree that this method could confuse the reader so have clarified this.

“P24, L21: re-write to clearly state that Fig S6 is for DJF/JJA - if that's the case.”

Again, this has now been clarified.

“P24, L22: (and Fig. S7 for ...)”

Again meaning for DJF/JJA. This is now clearer.

“P24, L23: ditto”

Also for DJF/JJA but for the cross-sections. This is now made more obvious for the reader.

“P24, L29: by what measure? ...The paired t-test p-value threshold should be interpreted with caution, and I suggest the authors add a caveat (e.g., reference to Waserstein & Lazar paper that I mention in a different comment).”

We now reference this citation and make the reader aware that such stippling needs to be interpreted with caution.

“P25, Fig. 8: A word of warning about interpreting the t-test threshold this way. The American Statistical Association (ASA) has thrown out the idea of using p-value thresholds to confirm or deny the null hypothesis, saying that you have to look at the broader picture and additional data to determine significance. Please see: “The ASA’s Statement on p-Values: Context, Process, and Purpose”, by Wasserstein, R.L., and Lazar, N.A., The American Statistician, 70:2, 129-133, 2016. https://www.tandfonline.com/doi/full/10.1080/00031305.2016.1154108 ...and consider revising wording in this paper to be less definitive about statistical significance based on the p<0.05 threshold.”

Thank you for bringing this to my attention. We add in the necessary caveats when discussing the stippled regions in relation to statistical significance.

“P30, L9: explain what's in Fig S8 in the brackets”

Specified the two different seasons presented in each of Fig. 11 (MAM/SON) and Fig. S8 (DJF/SON) for clarity.

“P31, L31: ....4-6 ppbv over the Northern Hemisphere and 2-6 ppbv over the Southern Hemisphere subtropics..."

Revised for greater clarity.

“P32, L3: too many brackets! Reword to remove as many as possible.”

Most of these brackets have now been removed.

“P33, L6: why would a complex chemistry scheme cause a high bias? Do you mean "inaccuracies in the complex chemistry scheme"?”

You are right, it should not unless inaccuracies exist but I would not know if this is the case. The implication here is that the emission inventories will have an error attached and this might manifest more prominently in EMAC’s modelling of ozone due to the complexity of the chemistry scheme. This would favour a high bias in this model if such inventories are an overestimate of the truth as implied by Hoesly et al., 2018. Sentence has been revised to reflect this.

“P33, L6: but both models used the same emissions, no?”
Correct, this has now been stated as so.

“P33, L16: Is there a paper on OMI's long-term performance that you can reference?”

We have added a reference that discusses the long-term performance of OMI – Levelt et al. (2018).

“P34, L4: due to ... ?”

Further detail from the Bonisch et al. (2011) reference has been added regarding the cause of reduced transit times in the lower stratosphere.

Characterising the Seasonal and Geographical Variability of Tropospheric Ozone, Stratospheric Influence and Recent Changes

Ryan S. Williams[1], Michaela I. Hegglin[1], Brian J. Kerridge[2], Patrick Jöckel[3], Barry G. Latter[2] and David A. Plummer[4]

[1] *University of Reading, Reading, UK*
[2] *Rutherford Appleton Laboratory (RAL), Harwell Oxford, Didcot, UK*
[3] *Deutsches Zentrum für Luft- und Raumfahrt (DLR), Institut für Physik der Atmosphäre, Oberpfaffenhofen, Germany*
[4] *Canadian Centre for Climate Modelling and Analysis, Environment and Climate Change Canada, Montréal, QC, Canada*

Correspondence to: Ryan S. Williams (r.s.williams@pgr.reading.ac.uk)

Formatted: German (Germany)
Formatted: German (Germany)

Abstract. The stratospheric contribution to tropospheric ozone (O_3) has been a subject of much debate in recent decades, but is known to have an important influence. Recent improvements in diagnostic and modelling tools provide new evidence that the stratosphere has a much larger influence than previously thought. This study aims to characterise the seasonal and geographical distribution of tropospheric ozone, its variability and changes, and provide quantification of the stratospheric influence on these measures. To this end, we evaluate hindcast specified dynamics chemistry-climate model (CCM) simulations from the ECHAM/MESSy Atmospheric Chemistry (EMAC) model and the Canadian Middle Atmosphere Model (CMAM), as contributed to the IGAC/SPARC Chemistry Climate Model Initiative (CCMI) activity, together with satellite observations from the Ozone Monitoring Instrument (OMI) and ozonesonde profile measurements from the World Ozone and Ultraviolet Radiation Data Centre (WOUDC) over a period of concurrent data availability (2005-2010). An overall positive, seasonally dependent bias in 1000-450 hPa (~ 0-5.5 km) subcolumn ozone is found for EMAC, ranging from 2- to 8 Dobson Units (DU), whereas CMAM is found to be in closer agreement with the observations, although with substantial seasonal and regional variation in the sign and magnitude of the bias (~ -4 to +4 DU). Although the application of OMI averaging kernels (AKs) improves agreement with model estimates from both EMAC and CMAM as expected, comparisons with ozonesondes indicate a positive ozone bias in the lower stratosphere in CMAM, together with a ~~n underestimation of photochemical ozone production (negative bias) in the troposphere.~~negative bias in the troposphere resulting from a likely underestimation of photochemical ozone production. This has ramifications for diagnosing the level of model-measurement agreement. Model variability is found to be more similar in magnitude to that implied from ozonesondes, in comparison with OMI which has significantly larger variability. Noting the overall consistency of the CCMs, the influence of the model chemistry schemes and internal dynamics is discussed in relation to the inter-model differences found. In particular, it is ~~shown~~ inferred that CMAM simulates a faster and shallower Brewer-Dobson Circulation (BDC) ~~relative~~ compared to both EMAC and observational estimates, which has implications for the distribution and magnitude of the downward flux of stratospheric ozone, over the most recent climatological period (1980-2010). Nonetheless, it is shown that the stratospheric influence on tropospheric ozone is ~~larger than previously thought~~significant and is estimated to exceed 50 % in the wintertime extratropics, even in the lower

troposphere. Finally, long term changes in the CCM ozone tracers are calculated for different seasons ~~between 1980-89 and 2001-10.~~ An overall statistically significant increase in tropospheric ozone is found across much of the world, but particularly in the Northern Hemisphere and in the middle to upper troposphere, where the increase is on the order of 4-6 ppbv (5-10 %) between 1980-89 and 2001-10. Our model study implies that attribution from stratosphere-troposphere exchange (STE) to such ozone changes ranges from 25-30 % at the surface to as much as 50-80 % in the upper troposphere-lower stratosphere (UTLS) across ~~many~~ some regions of the world, including western Eurasia, eastern North America, the South Pacific and southern Indian Ocean. These findings highlight the importance of a well-resolved stratosphere in simulations of tropospheric ozone and its implications for the radiative forcing, air quality and oxidation capacity of the troposphere.

Key Words: Tropospheric ozone, stratosphere-troposphere exchange (STE), chemistry climate models (CCMs), ozone monitoring instrument (OMI), ozone variability and changes.

1 Introduction

Tropospheric ozone (O_3) has wide ranging implications for air quality, radiative forcing and the oxidation capacity of the troposphere (Fiore et al., 20~~10~~2a; Myhre et al., 2013). Whilst ozone is typically regarded as a pollutant at ground level, adversely affecting human health and ecosystems (Paoletti et al., 2014), it is a primary source of the hydroxyl (OH) radical which acts to cleanse the troposphere by breaking down a large number of pollutants, along with some greenhouse gases (Seinfeld and Pandis, 2006; Cooper et al., 2010). Despite this, ozone is also a greenhouse gas itself, exerting the largest radiative forcing in the upper troposphere due to the ~~characteristic~~ inherent low temperatures in the upper troposphere (Lacis et al., 1990). Since ozone has a relatively short global mean lifetime in the troposphere (~ 3 weeks), along with spatially and temporally highly varying sources and sinks (Lelieveld et al., 2009), it is not well mixed, ~~and~~ with large spatial and temporal variations in ozone abundance ~~thus occur~~ as a result over seasonal, interannual and decadal timescales. This is reinforced by the strong dependence on sunlight as well as precursor emissions, which have both natural and anthropogenic sources (Cooper et al., 2014).

A large fraction of the ozone in the troposphere is formed through photochemical reactions of precursor molecules such as carbon monoxide (CO), nitrogen oxides (NO_x) and volatile organic compounds (VOCs), which have both natural and anthropogenic emission sources. Since the late 19th century however, changes in the tropospheric ozone burden can be largely attributed to anthropogenic precursor emissions, which have led to a significant increase in ~~background~~ baseline (HTAP, 2010; Cooper et al., 2014) and also background (Fiore et al., 2002b; Zhang et al., 2008; Stevenson et al., 2013) ozone ~~concentrations~~ volume mixing ratios (VMRs), particularly in the Northern Hemisphere mid-latitudes ~~(Fiore et al., 2002b; Zhang et al., 2008; Cooper et al., 2010, 2014; Stevenson et al., 2013). However,~~ (although it should be noted that this attribution is derived purely from modelling studies). Ozone may be produced either in situ or non-local to precursor source regions, as determined by the

synoptic meteorology, with the potential for long distance advection prior to photochemical destruction or deposition, given a lifetime of several weeks in the troposphere (Lelieveld et al., 2009). For instance, tropospheric ozone levels across western North America are particularly susceptible to increasing Asian emissions due to long range transport across the Pacific (Hudman et al., 2004; Cooper et al., 2010; Lin et al., 2014, 2015). An additional influence is that of exchange of stratospheric and tropospheric air masses, which leads to a net downward flux of ozone and a subsequent enhanced tropospheric ozone burden (Holton and Lelieveld, 1996; Lamarque et al., 1999), especially in mid-latitude regions (Miles et al., 2015).

Stratosphere-troposphere exchange (STE) of air is governed non-locally by the wave-driven large-scale meridional circulation, the Brewer-Dobson Circulation (BDC) (Holton et al., 1995; Shepherd, 2007; Butchart, 2014). The BDC induces preferential troposphere-to-stratosphere transport (TST) in the tropics, in contrast to mid to high latitude regions where stratosphere-to-troposphere transport (STT) must prevail to conserve mass continuity (Holton et al., 1995). The BDC, and thus STE, exhibits strong seasonality in both hemispheres with the circulation strongest during wintertime, but especially in the ~~n~~Northern Hemisphere, due to the largest wave-induced forces occurring at this time (Holton et al., 1995). Given a photochemical lifetime of several months in the lower stratosphere, analogous to transport timescales, seasonality in the BDC results in a significant enrichment of ozone and other chemical tracers in the extratropical lower stratosphere over winter (Hegglin et al., 2006; Krebsbach et al., 2006); with the largest ~~mixing ratios~~VMRs achieved close to the tropopause in early summer (Prather et al., 2011; Škerlak et al., 2014). Whilst it is recognised that the ~~cross-tropopause downward~~ STE flux of ozone in the extratropics reaches a seasonal maximum in late spring and early summer (~~T~~Yang et al., 2016), this incidentally coincides ~~with the downward STE mass flux being close to a seasonal minimum~~ closely to the seasonal minimum in the downward STE mass flux of air (Škerlak et al., 2014; Yang et al., 2016). This strongly implies that the ozone ~~concentration~~ VMR at the tropopause controls the seasonality in the downward ozone flux. Staley (1962) was the first to note that it is in fact the displacement of the tropopause altitude seasonally in each hemisphere that primarily governs the downward mass flux; maximum in spring as the tropopause rises and minimum in autumn as the tropopause falls relative to the ~~background~~ average state. Analysis of deep STE events, where direct entrainment of stratospheric air into the planetary boundary layer (PBL) occurs, indicates that the downward transport of ozone is primarily controlled by the mass flux for these events, with a peak in early spring (Škerlak et al., 2014).

Whilst it is accepted that STE is an important and significant source of upper tropospheric ozone (e.g. Holton et al., 1995), the influence on near-surface ozone levels is poorly understood. Globally, Lamarque et al. (1999) estimated that STE increases the average tropospheric column amount by only a modest ~ 11.5 % using a three-dimensional global chemistry transport model. However on a monthly resolved basis, this influence was shown to increase to ~ 10-20 % in the lower troposphere and ~ 40-50 % in the upper troposphere. More recent modelling studies however show a much larger influence. The annual mean estimated influence of the stratosphere is shown to range between 25 and 50 % in the lower and middle extratropical troposphere, with the largest influence in the Southern Hemisphere where other sources of ozone provide a smaller contribution

to the tropospheric ozone budget, according to various modelling studies (e.g. Lelieveld and Dentener, 2000; Banerjee et al., 2016). Hess and Zbinden (2013) found from observations that lower stratospheric (150 hPa) ozone explains nearly 70 % of the variance in mid-troposphere (500 hPa) ozone trends and variability over Northern Hemisphere mid-latitude regions, including Canada, the Eastern US and Northern Europe. Furthermore, a number of mid-latitude case studies have demonstrated that STT events may provide a much larger contribution to surface ozone in some seasons (typically spring), and more locally on timescales of hours to days given favourable meteorological conditions. Over a three month period between April and June 2010, Lin et al. (2012) concluded that the stratosphere was the source of 20-30 % of surface O_3 across the western US using the high resolution (~ 50 x 50 km^2) GFDL AM3 ~~chemistry climate model~~(CCM), with episodic enhancements of some 20-40 ppbv of the surface maximum 8-hour average (MD8A) ozone estimated from 13 identified stratospheric intrusion events. Similarly, model-based studies find evidence for a significant stratospheric contribution to the pronounced tropospheric summertime ozone maximum over the eastern Mediterranean and the Middle East (EMME) (Zanis et al., 2014; Akritidis et al., 2016) and the Persian Gulf (Lelieveld et al., 2009), with influence as far down as the PBL where near-surface ozone levels are known to frequently exceed EU air quality standards.

Observational based studies show a wide range in the level of stratospheric influence. In conjunction with a Beryllium (Be) based mixing model, Dibb et al. (1994) showed that the stratosphere has a maximum influence during spring in the Canadian Arctic of a mere 10-15 % at the surface. ~~In contrast using ozonesonde observations,~~ Greenslade et al. (2017) also found only a small stratospheric contribution (1-3.5 %) to the mean tropospheric ozone burden for three sites neighbouring the Southern Ocean, although with exceedances of 10 % during individual events. A number of European focussed studies highlight the significance of the stratosphere during episodic events, particularly over Alpine regions where elevated regions are sometimes directly impacted by stratospheric intrusions (e.g. Stohl et al., 2000; Zanis et al., 2003; Colette and Ancellet, 2005). This influence is typically largest in winter and spring (smallest in summer), although the seasonality exhibits greater complexity at some high altitude locations which is largely site-dependent. Significant enhancements in surface ozone, in association with stratospheric intrusions, have also been detected across the Himalayas during winter especially (up to 25 % contribution), in direct contrast to minimal influence during the summer monsoon season (e.g. Cristofanelli et al., 2010). Summertime ozonesonde campaign measurements over the northeastern US (Thompson et al., 2007a; 2007b) imply a stratospheric contribution of ~ 20 to 25 % to the tropospheric column ozone during summer 2004, which is comparable to the budget inferred from European profiles (Colette and Ancellet, 2005). A similar level of influence is found on average in the middle and upper troposphere ~~over~~ for 18 North American sites based on summer ozonesonde campaign data between 2006 and 2011 (Tarasick et al., 201~~8~~9). Ozonesonde measurements from all seasons between 2005 and 2007 reveal a larger influence still (34 % or 22 ppbv) over southeastern Canada, decreasing to 13 % (5.4 ppbv) and 3.1 % (1.2 ppbv) in the lower troposphere and boundary layer respectively, with typical occurrence of STT of 2-3 days (4-5 days) during spring and summer (autumn and winter).

Current understanding of the seasonal and regional climatology of tropospheric ozone is severely constrained by the paucity of in situ measurements from ozonesondes and aircraft measurements, which are spatially and temporally biased, although the advent of satellite remote sensing platforms in recent years for inference of global tropospheric ozone abundance has reduced uncertainty to ~~some~~ a significant extent (Parrish et al., 2014). Relatively long (~ decadal) global satellite datasets of tropospheric ozone now exist from several platforms (e.g. OMI, TES, TOMS, MLS) that have been extensively validated with respect to in situ and ground-based remote sensing measurements, as well as inter-satellite comparisons. ~~However,~~ Nonetheless, there are inherent limitations with retrieving tropospheric ozone from spaceborne instruments and this has implications for the accuracy of resultant satellite-based climatologies (Gaudel et al., 2018). ~~Although the validation of such satellite data with any limited in situ data available increases confidence in our estimates of the climatology and short term trends, scientists must instead rely on tools such as chemistry climate models (CCMs) to fill in the gaps in our understanding of the global distribution of tropospheric ozone, as well as longer term changes (Cooper et al., 2014).~~ Scientists however require tools such as chemistry climate models (CCMs), which offer sensitivity simulations and specific diagnostic variables that are not available from observations alone, ~~to be able to disentangle and~~ to elucidate the drivers of variability and longer term changes in the global distribution of tropospheric ozone, which includes quantification of the stratospheric influence. ~~different mechanisms and feedbacks, in addition to quantification of stratospheric influence, in influencing the global distribution of tropospheric ozone, as well as longer term changes, that cannot be understood from observations alone.~~ Additionally, CCMs can be used to assess and quantify the causes of tropospheric ozone features through analysis of photochemical production and loss rates, together with transport tracer simulations. The latter can serve to identify the relative importance of in situ photochemical production, long range transport and stratospheric influence. Nonetheless, such simulations are subject to a number of constraints, including limitations in model horizontal and vertical resolution, complexity of the implemented chemistry scheme and the realism of simulated transport characteristics. Above all however, the largest ~~uncertainty~~ unknown by far is the accuracy of the precursor emission inventories used in CCM simulations (Hoesly et al., ~~(~~2018).

In this study, the seasonal climatology, inter-annual variability and long term evolution of the influence of stratospheric ozone on tropospheric ozone and its geographical dependencies is investigated with the aim to update and extend the findings of Lamarque et al. (1999). A summary of the different data sources used is given in section 2. As a first step in section 3, we test the realism of two state-of-the-art CCMs by comparing their ozone estimates with the ozone distributions derived from the Ozone Monitoring Instrument (OMI) satellite measurements over a common baseline period, together with spatially and temporally limited vertical profile information provided by ozonesondes. Noting the model biases with respect to the observations, the fine scale vertical resolution offered by the CCMs is then exploited to analyse regional and seasonal variations in the vertical distribution of O_3 in section 4, together with ozone of stratospheric origin (O_3S) and the relative contribution of O_3S to the total amount of O_3 (the stratospheric ozone fraction: O_3F) to infer the importance of the stratosphere in determining tropospheric ozone levels. Finally, height resolved seasonal changes in model O_3 and O_3S are examined globally between

1980-1989 and 2001-2010 in section 5. The findings presented in both sections 3 and 4 are ~~also~~ discussed ~~here~~ within the context of the wider literature. Finally, section 6 will provide a summary of the findings, along with an overview of the utility of the models for improving our understanding of the spatial distribution and changes in tropospheric ozone.

2. Data Sources

2.1 Chemistry Climate Model (CCM) Simulations

This study uses RefC1SD specified dynamics ~~(SD)~~ hindcast simulations, conducted for the Chemistry Climate Model Initiative (CCMI-1) (Morgenstern et al., 2017), of both ozone (O_3) and stratosphere-tagged tracer ozone (O_3S) for the period 1980-2010 inclusive from two state-of-the-art CCMs: EMAC (Jöckel et al., 2016) and CMAM (Hegglin and Lamarque, 2015). These two models were primarily selected due to the close similarity in the O_3S tracer definition (detailed below in 2.1.1 and 2.1.2 respectively), which is either absent or defined differently in other CCMI models, and is fundamental to the quantification of the stratospheric influence and attribution to recent changes in tropospheric ozone in this study. O_3S decays according to the same reactions used in the O_3 simulations, although the reactions leading to photochemical production of ozone are omitted for the O_3S tracers (Roelofs and Lelieveld, 1997). ~~For~~ In each simulation, the prognostic variables: ~~(~~temperature, vorticity, and divergence, ~~and~~ as well as (logarithm of) surface pressure~~)~~ for ECHAM only (the coupled general circulation model in EMAC), from the ERA-Interim reanalysis dataset, ~~are~~ have been used to nudge the CCM towards the observed atmospheric state through Newtonian relaxation, with corresponding relaxation times of 24, 6, 48 and 24 h respectively for EMAC (Jöckel et al., 2016) and 24 h for all ~~four~~ three variables in CMAM (McLandress et al., 2013). ~~Variability in sea surface temperatures (SSTs) and sea ice concentration directly accounted for from ERA-Interim in the case of EMAC, but is instead derived from the HadISST dataset provided from the UK Met Office Hadley Centre for CMAM (Morgenstern et al., 2017; Rayner et al., 2003).~~ Variability in sea surface temperatures (SSTs) and sea ice concentration is directly accounted for in both EMAC and CMAM; from ERA-interim and HadISST (provided by the UK Met Office Hadley Centre) respectively (~~Morgenstern et al., 2017;~~ Rayner et al., 2003; Morgenstern et al., 2017). Furthermore, each model includes either prescribed decadal emissions or lower boundary conditions of anthropogenic and natural greenhouse gas (GHG) and ozone precursor emissions (which act as a forcing) from the MACCity inventory, which is based on ~~the~~ Coupled Model Intercomparison Phase 5 (CMIP5) ~~database~~ inventory and Representative Concentration Pathway (RCP) projections (Lamarque et al., 2010; Hoesly et al., 2018), alongside variability induced by other natural forcings such as solar activity and volcanic eruptions in most simulations (Brinkop et al., 2016). All simulations used are compliant with the ~~Chemistry-Climate Model Initiative (~~CCMI~~)~~ definitions specified by the IGAC and SPARC communities (Eyring et al., 2013). The stratospheric influx for CCMI models ranges from ~ 400-650 Tg yr^{-1}, which is within the range estimated from observational studies (IPCC, 2013). For full details of the model chemistry treatments and emission inventories used, the reader is directed to the CCMI review paper by Morgenstern et al. (2017), as well as Jöckel et al. (2016) for EMAC and the relevant section of Pendlebury et al. (2015) for CMAM. The main difference between the two models is the complexity of the tropospheric chemistry scheme, namely that CMAM simulates no non-methane hydrocarbon

Formatted: Not Superscript/ Subscript

chemistry, with additional differences in the model transport schemes; treatment of heterogeneous chemistry ~~calculations~~; accounting~~ance~~ of NO_x and isoprene emissions and representation of the Quasi Biennial Oscillation (QBO). ~~Only the main differences between the two models are briefly summarised here.~~ A brief overview of the two models and these differences is provided below (2.1.1 and 2.1.2).

Formatted: Subscript

2.1.1 EMAC

Formatted: Font: Bold

Formatted: Normal, Line spacing: single

RC1SD-base-10 simulation results (without nudging of the global mean temperature) from the interactively coupled European Centre for Medium-Range Weather Forecasts – Hamburg (ECHAM)/Modular Earth Submodel System (MESSy) Atmospheric Chemistry (EMAC) model are used in this study, which have a T42 (triangular) spectral resolution, equating to a ~~Q~~quadratic Gaussian grid of ~ 2.8° by 2.8°, and 90 vertical hybrid sigma pressure levels up to 0.01 hPa (Jöckel et al., 2016). EMAC uses the flux-form semi La~~n~~grangian (FFSL) transport ~~(FFSTL)~~ scheme for chemical ~~and meteorologically active~~ constituents, ~~physical tracers,~~ water vapour, cloud liquid water and cloud ice ~~as well as other chemical tracers~~ (Lin and Rood, 1996), with the chemistry submodels MECCA ~~(Sander et al., 2011a)~~ (Sander et al., 2011a) and SCAV (Tost et al., 2006) ~~providing the source of chemistry integrated into the model~~describing the kinetic systems in gaseous and aqueous/ice phase, respectively. ~~A~~ cComprehensive atmospheric reaction mechanisms that include~~s~~ basic O_3, CH_4, HO_x and NO_x chemistry; non-methane hydrocarbon (NMHC) chemistry up to C_4 and isoprene; halogen (Cl~~,~~ and Br ~~and I~~) chemistry; and sulphur chemistry is all included in the ~~MECCA~~ chemical scheme~~s~~ ~~(Sander et al., 2011a).~~ Relevant for representation of heterogeneous chemistry in the stratosphere, deviations from thermodynamic equilibrium are accounted for, which has implications for the distribution of polar stratospheric clouds (PSCs) and associated ozone depletion. In the troposphere, an offline representation of aerosol (dust, sea salt, organic carbon, black carbon, sulphates and nitrates) provides surfaces for heterogeneous chemistry. Emissions of ~~L~~lightning NO_x, soil NO_x and isoprene (C_5H_8) are parameterised online for EMAC using the submodel ONEMIS (Kerkweg et al., 2006; Jöckel et al., 2016). The model provides a consistent handling of the photolysis (submodel JVAL, Sander et al., 2014) and shortwave radiation schemes (submodel FUBRAD, Kunze et al., 2014), with particular regard to the evolution of the 11-year solar cycle (Morgenstern et al., 2017). The ~~The Quasi Biennial Oscillation (~~QBO~~)~~ is internally generated by the model, although zonal winds near the equator are nudged towards a zonal wind field (Brinkop et al., 2016) with a 58 day relaxation timescale to ensure realistic simulation of the QBO magnitude and phasing (Jöckel et al., 2016). For tracing stratospheric ozone, an additional diagnostic tracer O_3S is reset to the standard ozone tracer above the tropopause ~~Ozone is tagged as stratospheric in the O_3S tracer simulation above the tropopause (as defined by~~ using the World Meteorological Organisation (WMO) thermal definition equatorward of 30°N/S and using the 3.5 potential vorticity unit (PVU) dynamical tropopause definition poleward of 30°N/S) as defined in every model time step. The O_3S tracer is transported across the tropopause and subject to the tropospheric ozone sink reactions. The corresponding chemical loss of O_3S (LO_3S) is diagnosed and integrated, and in addition to its dry deposition, provides a direct measure for the stratosphere-to-troposphere exchange of ozone (Jöckel et al., 2006; 2016).

2.1.2 CMAM

Simulations from the atmosphere-only Canadian Middle Atmosphere Model (CMAM) are used here with a T47 spectral resolution (equivalent t~~e~~o ~ 3.75° by 3.75°) on the linear Gaussian grid used for the physical parameterisations in CMAM, with 71 vertical hybrid sigma pressure levels which ~~have~~ extend to 0.01 hPa ~~(~ 95 km altitude)~~ (Hegglin et al., 2014; Pendlebury et al., 2015). The model uses spectral advection of 'hybrid' moisture for transport (Merryfield et al., 2003) and a similar spectral advection of 'hybridized' tracers for chemically active tracers exhibiting strong horizontal gradients (Scinocca et al., 2008). Whilst a representation of heterogeneous chemistry on PSCs is provided, the model does not account for Nitric Acid Trihydrate (NAT) or PSC sedimentation (resulting in denitrification). Heterogeneous chemistry calculations are also made in the troposphere through prescribing sulphate aerosol surface area densities. Chemistry is calculated throughout the troposphere, although the only hydrocarbon considered is methane. To account for isoprene (C_5H_8) oxidation in CMAM, an additional 250 Tg-CO/year in emissions (including an additional 160 Tg-CO/year from soils) is included, distributed as Guenther et al. (1995) isoprene emissions. Unlike EMAC, soil NO_x emissions are not calculated online for CMAM and are instead prescribed, with lightning NO_x emissions parameterised from the Allen and Pickering (2002) updraft mass flux scheme (Morgenstern et al., 2017). ~~Compared with~~ In contrast to EMAC, consistency in the radiation and photolysis schemes has not specifically been imposed. Although CMAM does not generate a QBO internally, a representation of the QBO is induced in the ~~SD~~ specified dynamics simulations through nudging to ERA-Interim. The stratospheric ozone (O_3S) tracer uses the WMO thermal tropopause definition as the threshold for tagging of ozone as stratospheric across all latitudes, with an additional criterion that the tropopause must be < 0.7 in hybrid-sigma coordinates to prevent erroneous identification at high latitudes, during winter especially. Every timestep, the O_3S tracer is set equal to the model ozone above the tropopause, while below the tropopause the O_3S tracer has an imposed first-order loss rate equal to the model calculated first-order chemical loss rate of O_x defined as $O_x = O_3 + O(^1D) + O(^3P) + NO_2 + HNO_4 + 2NO_3 + 3N_2O_5$. The O_3S tracer also undergoes dry deposition at the surface with the same dry deposition velocity as calculated for ozone”.

2.2 Observations

2.2.1 OMI

The ozone monitoring instrument (OMI) is a Dutch/Finnish UV/VIS nadir-viewing solar backscatter spectrometer aboard the NASA-Aura satellite launched in July 2004. The satellite has a retrograde, sun-synchronous polar orbit (inclination of 98.2°) at an altitude of 705 km, providing some 14 orbits a day with a local equatorial crossing time in the ascending node of 13:45

Formatted: Font: Bold
Formatted: Font: Bold
Formatted: Comment Text, Line spacing: 1.5 lines
Formatted: Font: 10 pt
Formatted: Font: 10 pt
Formatted: Font: (Default) +Body (Times New Roman)
Formatted: Font: (Default) +Body (Times New Roman)
Formatted: Font: (Default) +Body (Times New Roman), Subscript
Formatted: Font: (Default) +Body (Times New Roman)
Formatted
Formatted: Font: (Default) +Body (Times New Roman)
Formatted
Formatted: Font: (Default) +Body (Times New Roman)
Formatted
Formatted: Font: (Default) +Body (Times New Roman)
Formatted
Formatted: Font: (Default) +Body (Times New Roman)
Formatted
Formatted: Font: (Default) +Body (Times New Roman)
Formatted
Formatted: Font: (Default) +Body (Times New Roman)
Formatted
Formatted: Font: (Default) +Body (Times New Roman)
Formatted
Formatted: Font: (Default) +Body (Times New Roman)
Formatted
Formatted: Font: (Default) +Body (Times New Roman)
Formatted
Formatted: Font: (Default) +Body (Times New Roman)
Formatted
Formatted: Font: (Default) +Body (Times New Roman)
Formatted
Formatted: Font: (Default) +Body (Times New Roman)
Formatted
Formatted: Font: (Default) +Body (Times New Roman)
Formatted: Font: 11 pt

local time (Levelt et al., 2006). OMI operates in the 270-500 nm spectral interval and has a spectral resolution of 0.42-0.63 nm (Foret et al., 2014). OMI is the first of a generation of instruments which use 2-D detector arrays, providing concurrent sampling at all across-track positions, as opposed to platforms which use a 1-D detector array to scan across track. OMI supplements the observational knowledge of ozone from other longstanding satellite platforms, such as NASA's Total Ozone Mapping Spectrometer (TOMS) instrument and ESA's Global Ozone Monitoring Experiment (GOME) instrument, at a much enhanced spatial resolution (e.g. 13 km x 24km for OMI compared with 40 km x 320 km for GOME in the along track and across track directions nominally at nadir). The across track resolution however becomes significantly coarser away from nadir; reaching 13 km x 150 km towards the edge of the swath (corresponding to an angle of 57° from nadir). The swath is 2600 km wide at the surface resulting from a wide field of view of 114°, with a near global coverage time of one day (Levelt et al., 2006; Foret et al., 2014). Temperature-dependent spectral structure in the region between 320 and 345 nm (the Huggins Band) contains the information required for retrieval of ozone in the troposphere region (Miles et al., 2015). The logarithm of the ozone ~~volume mixing ratio~~(VMR) on a fixed pressure grid (surface pressure, 450, 170, 100, 50, 30, 20, 10, 5, 3, 2, 1, 0.5, 0.3, 0.17, 0.1, 0.05, 0.03, 0.017, 0.01 hPa) provides the basis for the retrieved profiles (Miles et al., 2015).

This study uses 1000-450 hPa (0-5.5 km) subcolumn ozone values retrieved from OMI ~~by~~, as derived using the Rutherford Appleton Laboratory (RAL) height-resolved optimal estimation profiling scheme (Miles et al., 2015; Gaudel et al., 2018)~~,~~ for one in four 50 x 50 km samples in every 100 x 100 km bin, which has been further optimised to increase sensitivity to tropospheric ozone. These "Level-2" (L2) data have been averaged into monthly mean 2.5° x 2.5° (~ 275 km) gridded "Level-3" (L3) data between 2005 and 2010. This resolution is more comparable with the resolution of the CCM simulations used in this study for model comparisons (section 3). Validation against ozonesondes for this subcolumn, after applying averaging kernels (AKs) to account for vertical smearing associated with the satellite retrieval, yields a relatively low retrieval bias of ~ 1.5 Dobson Units (DU) (6 %) (Miles et al., 2015). The sign of the bias is latitude dependent for lower tropospheric ozone – underestimation in the southern hemisphere by ~ 15-20 % (1-3 DU) and overestimation in the northern hemisphere by ~ 10 % (2 DU). These systematic biases can be attributed to inaccuracies in the radiative transfer modelling, which are partially rectified through use of a priori information to shift the erroneous retrieved profiles towards the true values (Mielonen et al., 2015). An additional monthly mean, (linearly interpolated) latitude dependent bias, identified with respect to the global ozonesonde ensemble, was also corrected for in the OMI data used in this study. Other filtering criteria used to enhance the quality of the dataset include omission of observations with a cloud fraction greater than 0.2 and a solar zenith angle exceeding 80°. ~~The 1000-450 hPa (0-5.5 km) OMI subcolumn data is considered a representative approximation of the full tropospheric ozone column amount, due to vertical smearing of information from above 450 hPa (~ 5.5 km).~~ This estimation differs from other techniques such as cloud slicing (e.g. Ziemke and Chandra, 2012) and residual methods such as total column ozone (TCO) from OMI minus vertical profile measurements from the Microwave Limb Sounder (MLS) (e.g. Ziemke et al., 2011). In comparison with the OMI-MLS method, the OMI-RAL profiling scheme is more (less) sensitive to the lower (upper) troposphere (Gaudel et al., 2018). ~~Therefore t~~To ensure a direct comparison with other datasets, in order to test the level of

agreement with models and ozonesonde observations, averaging kernels (AKs) should be applied ~~to these datasets~~ to induce such smearing of information that inherently occurs in UV-nadir satellite measurements. The influence of AKs is critically evaluated for the 1000-450 hPa subcolumn for both the models and ozonesondes in section 3.

OMI is regarded as a very stable platform, with the radiometric degradation during the instrument's lifetime estimated to have been just ~ 2 % in the UV and ~ 0.5 % in the VIS channel, which is significantly lower than other comparable instruments (Levelt et al., ~~2017~~2018). Despite this, the quality of radiance data began to decline from 2007 onwards (but particularly starting from 2009) across all wavelengths in a progressively larger number of across-track views, corresponding to rows in the 2-D detector arrays; suspected to be blocked by insulation blankets covering the instruments which have become damaged. This one main anomaly is subsequently referred to as the row-anomaly (Schenkeveld et al., 2017). Although OMI has relatively high sensitivity to the troposphere, sensitivity is much weaker near the surface ~~(Sellitto et al., 2011),~~ due to the limited penetration of photons and subsequent reduced signal in the backscattered radiance spectrum (Sellitto et al., 2011)~~,~~, with factors such as surface albedo and aerosols in the PBL also ~~causing~~ resulting in additional interference (Liu et al., 2010).

2.2.2 Ozonesondes

Vertical ozone profile data over the period 1980-2010 was derived from the World Ozone and Ultraviolet Radiation Data Centre (WOUDC); an archive of balloon-borne in situ measurements of ozone, together with other variables such as temperature, humidity and pressure. Ozonesondes typically provide a vertical resolution of ~ 150 m from the surface up to a maximum altitude of approximately 35 km, although not in all cases (Worden et al., 2007; Nassar et al., 2008). Most sonde stations launch ozonesondes on a weekly basis, but a number of European sites provide measurements 2-3 times a week (Worden et al., 2007). The WOUDC archive contains measurements from primarily electrochemical concentration cell (ECC) sondes, but also from two other instruments: ~~from three different instruments:~~ the Brewer-Mast (BM)~~, the electrochemical concentration cell (ECC)~~ and the Japanese ozonesonde (KC) (SPARC, 1998), which all yield measurements of ozone equivalently. ~~The vast majority of the WOUDC sonde profile measurements were however obtained from ECC ozonesondes, although all three instruments yield measurements of ozone equivalently (in units of partial pressure using atmospheric pressure as a vertical coordinate) through detection of the oxidation reaction between ozone and potassium iodide (KI) in an aqueous solution (Komhyr et al., 1995; WMO, 1998). Differences can however arise due to instrument type (two different manufacturers), procedures and the strength of the KI solution (Thompson et al., 2003; 2007).~~ The reader is directed to Liu et al. (2013b) for further details of the WOUDC measurement network, including a map and table of all observation sites. The accuracy of sonde measurements is typically estimated to be within the range of ± 5 %, depending on various factors. Precision between the various sonde types is estimated to be within ± 3 %, with systematic biases of less than ± 5 % within the lower to middle stratosphere (12-27 km altitude range), provided that profile measurements have been normalised with respect to ground based total ozone measurements (WMO, 1998).

Uncertainties are however much larger in the troposphere due to lower ~~concentrations of ozone~~ ozone VMRs, yielding a relatively low signal-to-noise ratio, which increases the susceptibility to both instrumental errors and instrumental variability. Sonde performance can additionally be affected by local air pollution, which can further enhance the level of uncertainty. Systematic differences between different instruments in the troposphere were estimated to vary between 10 and 15 % in various intercomparison campaigns between 1970 and 1990 (Beekman et al., 1994; Smit et al., 1998). There is evidence that the ECC sondes have greater precision and consistency than either the BM or KC sondes here (e.g. WMO-III, JOSIE campaigns); precision of ± 5-10 % for ECC compared with a range of 10-20 % for BM/KC. A small positive bias of 3 % is noted for ECC with no evidence of biases exceeding ± 5 % for BM/KC (Smit et al., 2004a; 2004b).

3. Tropospheric Ozone (Model-Measurement Comparison)

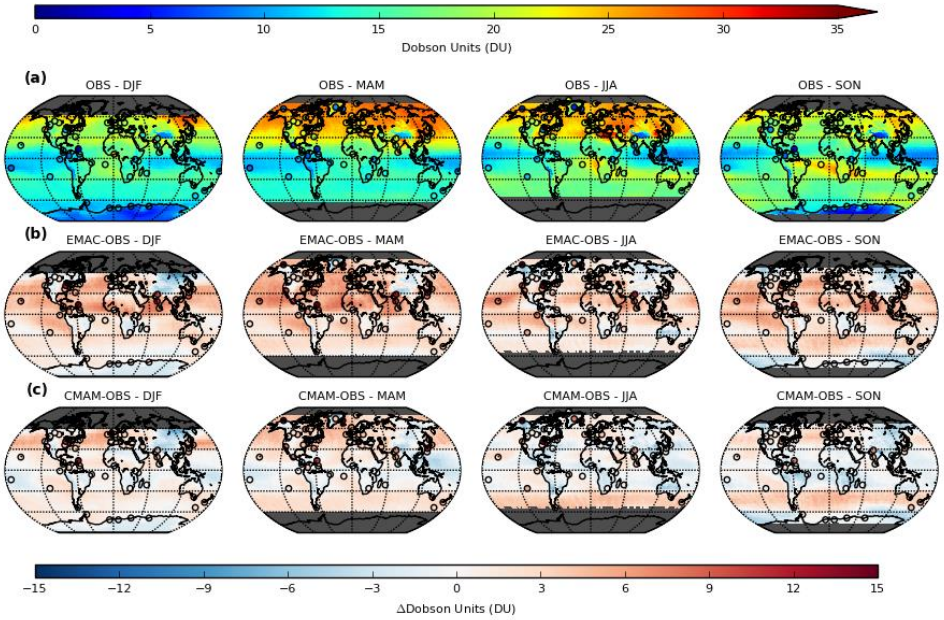

Figure 1 – Seasonal composites of monthly averaged 1000-450 hPa (0-5.5 km) subcolumn O_3 (DU) for 2005-2010 (left to right) from (a) OMI, (b) EMAC minus OMI and (c) CMAM minus OMI. Circles denote (a) equivalent ozonesonde-derived subcolumn O_3 (DU), (b) EMAC minus ozonesonde differences and (c) CMAM minus ozonesonde differences. All data was regridded to 2.5° resolution (~ 275 km). All model and ozonesonde subcolumn data has been modified using AKs to ensure a direct comparison.

In order to evaluate the utility of the models in assessing tropospheric ozone and estimating stratospheric influence, the CCM simulations (EMAC and CMAM) are first validated here against the OMI observations, in addition to the spatially and temporally limited, height resolved ozonesonde measurements. This is achieved through a combined model-measurement characterisation of the seasonal and geographical variability of tropospheric ozone (section 3.1), together with the interannual variability (section 3.2) over the 2005-2010 period. Lastly, a vertically resolved assessment of the CCMs is provided for three different mid-latitude regions (Europe, eastern North America and the Tasman Sea) from ~~combined~~aggregated ozonesonde profile measurements between 1980 and 2010 (section 3.3).

Seasonal composites of monthly mean 1000-450 hPa (0-5.5 km) subcolumn ozone from OMI, together with available ozonesonde-derived AK-fitted subcolumns, and the respective differences for each AK-fitted CCM are shown in Fig. 1. A seasonal maximum in tropospheric ozone is evident in each hemisphere during spring, which is more pronounced in the Northern Hemisphere and extended in many regions through to summer (JJA). In contrast to the extratropics, tropospheric ozone remains low year-round (< 20 DU) at low-latitudes although some seasonality is apparent; notably a northward ~~(southward)~~ shift in the region of lowest ozone from boreal winter ~~(summer)~~ into summer ~~(winter)~~, and the reverse from boreal summer back to winter. This is likely associated with the seasonal migration of the Inter Tropical Convergence Zone (ITCZ) which closely follows the region of maximum solar insolation. In this region, strong upwelling occurs which leads to the transport of ozone depleted air from the tropical PBL upwards towards the tropopause. This is most pronounced across the Maritime Continent where convective activity is climatologically most intense (e.g. Thompson et al., 2012).

The BDC, which leads to meridional transport in ozone and other constituents in the stratosphere, is strongest ~~(weakest)~~ during winter (weakest during summer) and it is this annual variability which ~~primarily governs~~exerts a major influence over the seasonality of free tropospheric ozone (through changes in STE), ~~-~~in regions of the extratropics where emissions of tropospheric ozone precursors are at a relatively low background level (Roscoe, 2006). This is invariably the case across much of the Southern Hemisphere, where anthropogenic precursor emissions are substantially lower and more spatially confined in comparison with the Northern Hemisphere. In some regions such as the South Atlantic, it is evident that tropospheric ozone is similarly high in winter (JJA) (~ 25-30 DU) but it is known that this is a result of biomass burning activity in western Africa and resultant plumes which are advected offshore during the dry season in particular (e.g. Mauzerall et al., 1998). Across Antarctica and the Southern Ocean however, halogen-~~-~~induced stratospheric ozone depletion is likely the dominant driver of the seasonality; leading to a minimum in spring (SON), although no observations from OMI are available during the polar night (MAM and JJA). In the Northern Hemisphere, the strong influence of emission precursors from widespread anthropogenic activity serves to delay and broaden the maximum, since the peak in the in situ photochemical formation of ozone is driven by solar insolation. This is particularly apparent in subtropical regions such as ~~in~~ the eastern Mediterranean, due to favourable photochemical conditions for the production and subsistence of ozone during the summer months.

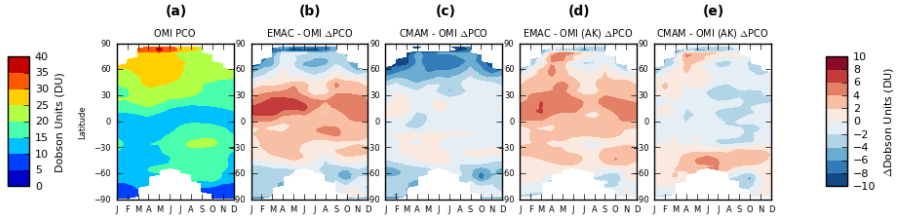

Figure 2 – Zonal-mean monthly averaged 1000-450 hPa (0-5.5 km) subcolumn O_3 (DU) for 2005-2010 from (a) OMI, (b) EMAC minus OMI without AKs, (c) CMAM minus OMI without AKs, (d) EMAC minus OMI with AKs and (e) CMAM minus OMI with AKs.

A corresponding zonally averaged monthly mean evolution, together with the respective differences for each CCM (both with and without AKs) is additionally shown in Fig. 2 and further summarised as 30° latitude band averages in Table S1. Whilst the AK-fitted EMAC differences with respect to OMI (Fig. 1 and Fig. 2d) show an overall year-round, albeit seasonally varying positive bias, particularly within the 0° to 30° latitude band (~ +2-8 DU), the difference is largely negative in CMAM (~ 0 to -4 DU), except during spring (MAM) in parts of the Northern Hemisphere (~ 0 to +4 DU) and within the 30°S to 60°S latitude band (~ +2-6 DU). Although such differences on a zonally averaged basis are relatively small (on the order of 10-20 %), the systematic nature and seasonal dependence of such biases is important to consider. Regional differences are evidently larger however, with differences of up to 10 DU (50 %), such as over mid-latitude oceanic regions where both CCMs show a positive bias relative to OMI and also with respect to limited available ozonesonde data from maritime locations. Some continental regions such as eastern Asia on the other hand show a negative bias in most seasons; largest in winter (DJF) (5-10 DU or 20-40 %). A recent study by Hoesly et al. (2018) shows discrepancies between the CMIP5 NOx emissions database (used in CCMI emission inventories) and an updated, refined database over the timeframe considered, the Community Emissions Data System (CEDS), which could explain the pattern of biases between the continental regions of the Northern Hemisphere. Whilst the CMIP5 emissions dataset is composed of "best available estimates" from many different sources, the dataset has limited temporal resolution (10-year intervals), contains inconsistent methods across emission species and lacks uncertainty estimates and reproducibility. The CEDS dataset addresses some of these shortcomings by also factoring in activity data to estimate country, sector and fuel-specific emissions on an annual basis, which is further calibrated to existing inventories through emission factor scaling. The sign of the biases is more complex and spatially variable in summer (JJA) but are typically low (-3 to +3 DU), implying that the CCMs are reasonably consistent overall with the OMI measurements during this season. In the Southern Hemisphere, the general positive bias is weaker (particularly in austral winter and spring) and most regions show a negative bias in at least one season. Model-measurement agreement here is typically higher compared with the Northern Hemisphere, particularly for latitudes where O_3 precursor emissions are lower and in the less photochemically active seasons (i.e. autumn and winter). This could indicate that CCMs ~~include excessive emissions~~ simulate excessive photochemical production of ozone in the Northern Hemisphere particularly (Young et al., 2013; Shepherd et al., 2014) or that the role of

tropospheric sinks (e.g. through wet and dry deposition or other loss reactions) is underestimated (Revell et al., 2018), with our results indicating regionally differing magnitudes in these biases.

Both Fig. 2 and Table S1 show the importance of applying AKs (on a monthly mean zonally-averaged basis) in order to diagnose the agreement between the two datasets, by enabling a like-for-like comparison, since it is clear that both CCMs significantly underestimate the amount of tropospheric ozone overall at both middle and high latitudes, relative to the OMI observations (Fig. 2b-2c). The effect of applying the AKs (Fig. 2d-2e) is shown to significantly reduce or even eradicate the negative bias (poleward of 30ºN/S), and it is this difference which indicates the approximate magnitude of the influence vertical smearing has on the retrieved OMI subcolumn measurements. A residual negative bias (~ -2 to -6 DU) also exists in the Southern Hemisphere during spring (SON) over the Southern Ocean south of 60°S (adjacent to Antarctica). ~~This could reflect greater stratospheric influence than captured by the models (particularly EMAC) or perhaps more likely an offset in jet stream positioning, as supported by the zonally-structured positive bias northward of 60°S, which strongly influences both STE and long-range transport.~~ This might relate to differences in the representation of a transport barrier such as the ~~surf zone region~~edge of the wintertime polar vortex, which influences mixing in the surf zone region~~, which~~ and is eradicated in this season, ~~or perhaps also~~ together with disparities in the magnitude of the Antarctic ozone hole, which has implications for vertical smearing, influencing the resultant tropospheric ozone burden. Indeed, a cold-pole bias which leads to a delayed onset in the seasonal breakdown of the polar vortex is an inherent bias common to most CCMs (McLandress et al., 2012). Biases in much of the tropics appear also to be connected to dynamics which favour long-range transport (e.g. trade wind circulations) originating from regions of known precursor emissions (e.g. biomass burning from South America)~~.~~, although differences in the chemical schemes may also be influential and would require further analysis.

Differences with AKs show that EMAC is in slightly better agreement with OMI across the Southern Hemisphere extratropics, although CMAM is in closer or comparable agreement over the tropics and the Northern Hemisphere. The model is especially consistent during JJA and SON over the continents in particular (Fig. 1b and 1c). Furthermore, a high level of agreement between the ozonesonde and OMI observations is apparent in all four seasons (Fig 1a), confirming that the OMI retrieval algorithm correctly captures the regional and seasonal climatological features in tropospheric ozone. Some sonde sites however show consistently smaller amounts of ozone (e.g. western North America and Greenland), although this may be attributed to the high elevation (e.g. mountain summit locations) of these sites~~,~~ relative to the average topographical elevation of a 2.5º grid cell within which the OMI observations are averaged over, which inherently leads to lower amounts of ozone within the partial column.

3.2. O_3 Interannual Variability

As a metric of interannual variability, seasonal aggregates of the computed relative standard deviation (RSD) of the monthly mean ~~O_3~~ozone for ~~both~~ OMI ~~and,~~ each CCM and ozonesondes ~~sites~~ are shown in Fig. 3, as calculated in equation 1 below:

$$RSD = \sum_{i=0}^{N} \frac{\sigma_i}{\mu_i} / N \quad (1)$$

Formatted: Keep with next

where N is the number of months in a season, σ_i is the standard deviation of each month calculated over all years and μ_i is the multiannual monthly mean of each month. Variability in the tropics is enhanced due to the significantly lower mean tropospheric ozone, in comparison with the extratropics. It should be noted that the calculated RSD is significantly lower for ozonesondes compared to each CCM and particularly the OMI measurements, which is currently being investigated further. Although OMI shows much higher variability than the models, there is good agreement in regions of high RSD across much of the tropics (> 10 %), which is largest during SON, at least from the OMI observations. The highest RSD is consistently found over the western Pacific and the Maritime Continent close to the equator, where it approaches 20 % for both OMI and the CCMs (particularly CMAM). The region is strongly influenced by some of the main drivers of natural variability, including the El Niño Southern Oscillation (ENSO) and the Madden Julian Oscillation (MJO). Throughout the tropics, high variability may also be associated with the ~~Quasi Biennial Oscillation (~~QBO~~)~~. Although the QBO is a stratospheric phenomenon, studies

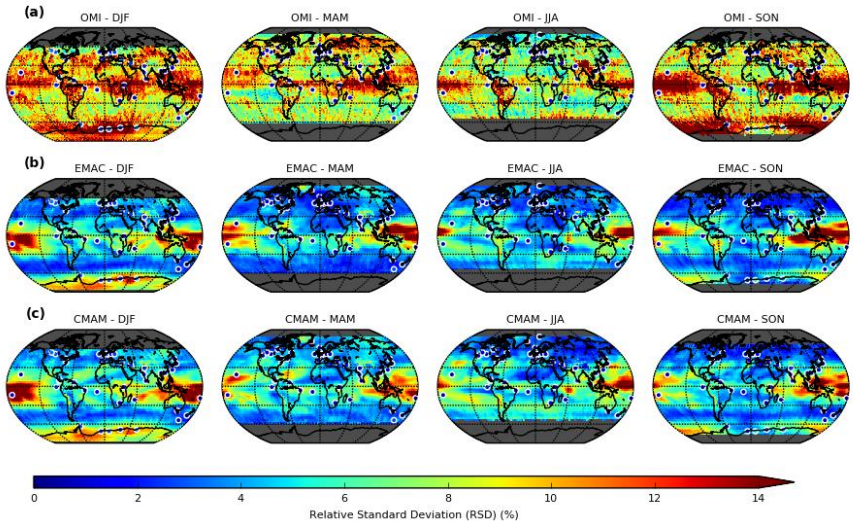

Figure 3 – Seasonal composites (left to right) of monthly 1000-450 hPa (0-5.5 km) subcolumn O_3 relative standard deviation (RSD) (%) for 2005-2010 for (a) OMI, (b) EMAC and (c) CMAM. ~~RSD calculated as the standard deviation (SD) divided by the mean (multiplied by 100).~~ Circles denote (a-c) the seasonal RSD calculated from ozonesonde measurements. Model and ozonesonde subcolumn data ~~has~~ have ~~again~~ been modified using AKs to ensure a direct comparison.

show that the alternating phases of the zonal equatorial wind can influence tropospheric ozone by as much as 10-20 % (~ 8 ppbv) (e.g. Lee et al., 2010). The RSD is generally lower for OMI outside of the tropics, although significant variability (> 10 %) is still evident for some regions in different seasons. The CCMs in contrast show very low RSD over much of the extratropics (< 5 %), with only subtle spatial structures evident in the seasonal composites. Equivalent composites of the absolute standard deviation (SD) (not shown) show some variability however at mid-latitudes during winter and spring in each hemisphere (up to 2 DU), principally in oceanic regions, and this may indicate sensitivity to the main extratropical cyclone tracks. Higher RSD is however shown across Antarctica during the polar day and over the Southern Ocean (up to 10 %), which is collocated in the corresponding OMI seasonal composites. This may largely be a retrieval artefact caused by vertical smearing, which is highly dependent on the tropopause height, since comparative RSD fields from the CCMs without AKs show no such structure (not shown).

3.3. O_3 Vertical Distribution Assessment

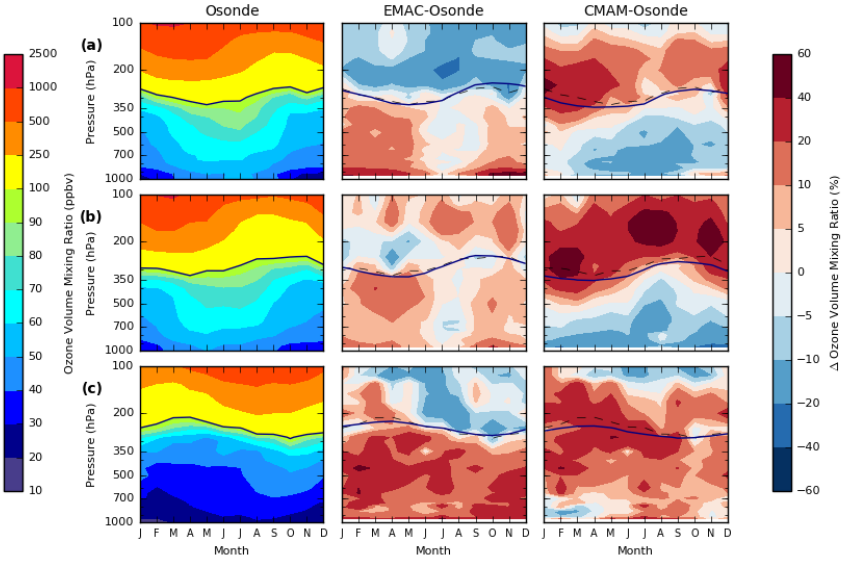

Figure 4 – Monthly evolution of the vertical distribution of mean O_3 volume mixing ratio (VMR) (ppbv) derived from ozonesonde measurements (left column); EMAC minus ozonesonde differences (%) (middle column) and CMAM minus ozonesonde differences (%) (right column) over the period 1980-2010 inclusive for three different world regions: (a) Europe (n = 18), (b) eastern North America (n = 14) and (c) Tasman Sea (n = 6). The ozonesonde/model 100 ppbv contour (the ozone defined extratropical tropopause as identified in Bethan et al. (1996)) is additionally highlighted in bold (ozonesonde 100 ppbv contour indicated again by dashed line – middle and right column).

To evaluate the vertical agreement of the CCM O_3 VMR tracer simulations, monthly mean ozonesonde-derived measurements were interpolated and averaged between ±20 hPa of the 22 different model pressure levels between the surface (~ 1000 hPa) and the lower stratosphere (100 hPa) for three different extratropical regions. Fig. 4 ~~(Fig. S1)~~ shows the monthly mean evolution averaged over all sites (left), together with the respective percentage ~~(ppbv)~~ differences relative to the nearest model grid columns in EMAC (middle) and CMAM (right), within each bounding box~~es~~ (region): (a) Europe (30° N - 65° N, 15° W - 35° E), (b) eastern North America (32.5° N - 60° N, 92.5° W - 55° W) and (c) the Tasman Sea (55° S - 15° S, 140° E - 180° E). The absolute differences are also shown in Fig. S1. Tables S2a-c additionally provide~~s~~ a summary of this information on a seasonal basis for six selected pressure levels ~~for~~in each region. These regions were selected for the assessment due to the relatively high number of ozonesonde sites in close proximity. Furthermore, the variability in emissions of ozone precursors and stratospheric influence, due to varying UTLS dynamics in these predominantly extratropical regions, make these regions suitable for evaluating the realism to which the CCMs simulate these influences.

The seasonality in ozone ~~concentration~~ VMR is shown to be very similar in both Europe (Fig. 4a) and eastern North America (Fig. 4b) as expected for two regions of similar latitude in the same hemisphere. In the stratosphere, a springtime maxima (autumn minima) is clear, although the timing is not synchronous at all pressure levels, with a tendency for a delayed maximum (minimum) in each region with increasing pressure (decreasing altitude). This is also apparent for the Tasman Sea region (Fig. 4c), albeit the seasonality is reversed. This can be attributed to the BDC in the lower stratosphere, which leads to a gradual accumulation of ozone during wintertime in the lowermost stratosphere and a subsequent gradual depletion of ozone during summertime as the circulation weakens (~~Holton et al., 1995;~~ Logan et al., 1985; Holton et al., 1995; Hegglin et al., 2006). For all regions, this delayed signal in the maximum (minimum) in ozone ~~concentration~~ VMR propagates down into the troposphere (identified here as the region < 100 ppbv), with the exception of the springtime maximum over the Tasman Sea which peaks earlier with increasing pressure (decreasing altitude) from the tropopause (around late September) towards the surface (early August). Clearly though, there is a large difference in the climatological ozone ~~concentration~~ VMR throughout the year between this region and both Europe and eastern North America; the Tasman Sea region reflecting only a very limited influence from emission precursors. The composite produced for this region likely provides a reasonable representation of the natural background influence of the stratosphere on tropospheric ozone in the extratropics, in contrast to the other two regions.

The computed model-ozonesonde monthly mean differences (Fig. 4) reveal notable differences both between each model and each region in the troposphere (~ 300-1000 hPa); as high as 20-30 ppbv (> 50 %). ~~between each model in the lower troposphere over Europe and between both eastern North America and the Tasman Sea in the lower troposphere in CMAM.~~ EMAC shows an almost universal positive bias between 0 and 40 % (0-20 ppbv) throughout the year for all three regions which contrasts with the overall negative bias in the stratosphere (~ 100-300 hPa) (except over eastern North America). Some seasonal dependence in the tropospheric bias is evident over Europe and eastern North America, with the largest (smallest) difference between ~~January~~ September and May (June and August)~~.~~; on the order of ~ +20-60 % (+10-20 ppbv) outside of boreal summer.

~~A less pronounced secondary peak in the magnitude of the bias is also evident during autumn (SON). An exception to this is in the lower troposphere (> 850 hPa) over Europe, where the largest differences are evident (~ +20-60 % equating to some +10-20 ppbv) from autumn (SON) through to spring (MAM).~~ In contrast, no obvious seasonal variation in the bias is apparent over the Tasman Sea region. For CMAM, a generally negative, seasonally dependent bias (~ 5-20 % or 5-10 ppbv) is apparent in the lower to middle troposphere over Europe and particularly eastern North America, most pronounced during summer (JJA), whereas an overall positive bias (up to 10-40 % or 5-20 ppbv) exists over the Tasman Sea, largest in the free troposphere. Both the seasonal character of the negative bias over Europe and eastern North America (largest during the most photochemically active months), together with the difference in the sign of the bias between the troposphere and the UTLS, strongly implies a difference in the implementation of the tropospheric chemistry scheme in CMAM compared with EMAC, since prescribed emissions ~~should be~~ are equivalent in ~~each~~ both models. Specifically, the omission of non-methane VOCs (NMVOCs) in CMAM likely accounts for much of this underestimation.

The largest absolute differences (Fig. S1) are however indeed evident in the lower stratosphere (100-300 hPa), with a systematic positive bias in CMAM in most seasons (widely between +50 and +200 ppbv, ranging from 10-50 %). A slight negative bias (~ -10 to -50 ppbv or -0-10 %) is however apparent between 100 and 150 hPa over Europe, largely during summer (JJA), and also more pronounced over the Tasman Sea from March through to November (> 50 ppbv or 5-20 %). Over eastern North America, a very large positive bias is evident in CMAM throughout the year ranging between 20 and 60 % (+50 to +200 ppbv), with a seasonal shift in the height of the largest differences, similarly to over Europe yet more pronounced. In contrast, the differences between EMAC and the ozonesonde measurements have a very different character, with a general negative bias over Europe, particularly in summer (JJA) (~ -20 to -100 ppbv or -10-20 %). Over eastern North America and the Tasman Sea, the pattern and magnitude of the biases is more complex with both pressure (altitude) and month. An overall positive bias is found over eastern North America (typically +20 to +50 ppbv or +5-20 %), except from January to May between ~ 170 and 250 hPa, whilst an overall negative bias (generally between -20 and -50 ppbv or 5-20 %) is evident over the Tasman Sea except between January and May and for a small region (120-180 hPa) during August-September. The general negative bias in EMAC (positive bias in CMAM) might indicate an underestimation (overestimation) in the strength of the BDC but the seasonal dependence of the bias, and in particular the complexity in EMAC, suggests influence from other factors.

3.4 Summary

In summary, the CCM simulations are broadly in agreement with both sets of observations, capturing both the extent and magnitude of geographical and seasonal features in tropospheric ozone over the concurrent period of data availability (2005-2010). There is very close agreement overall in the global mean seasonal composites of tropospheric subcolumn (1000-450 hPa) ozone between ~~each~~ both CCMs, although differences relative to OMI show that there is an overall significant, systematic positive bias in the EMAC model (Fig. 1 and 2), particularly over the Northern Hemisphere (~ 2-8 DU), whereas no overall

bias is apparent in CMAM despite some meridional and seasonal differences (~ -4 to +4 DU). An evaluation of the model-ozonesonde differences in the vertical distribution of ozone ~~volume mixing ratios~~VMRs (ppbv) over both Europe and eastern North America (Fig. 4) indicates a different origin for the biases in each model compared with OMI. In EMAC, the positive bias is predominantly a result of excess in situ photochemical production from emission precursors, whereas biases in CMAM are largely determined by the relative influence of excessive vertical smearing of ozone (induced by applying the OMI AKs). This results from a large positive ozone bias in the lower stratosphere (not present in EMAC), as well as the much more ~~conservative~~ simplified tropospheric chemistry scheme implementation. The additional smearing from AKs is concluded to overcompensate for the reduced in situ production of ozone to yield a larger positive or comparable bias in CMAM (poleward of 30°S/N) (Fig. 2), where the application of AKs has a disproportionally larger effect on the estimated subcolumns. In contrast, a larger positive bias is found in EMAC over low latitudes (30°N-30°S) but primarily in the Northern Hemisphere where precursor emissions are more abundant, ~~since vertical smearing of information is far more limited due to a higher tropopause.~~ which is understandable due to the higher climatological mean position of the tropopause in this region (with respect to the extratropics), leading to less vertical smearing of information from the stratosphere when AKs are applied. The zonal average monthly mean integrated subcolumn OMI-model differences without AKs (figure 2b-c) would be consistent with this interpretation and it is obvious that application of the OMI AKs must have induced additional vertical smearing of ozone in CMAM in the equivalent latitude range (~ 30-65°N) compared with EMAC (figure 2d-2e) due to the likely presence of a high ozone bias in the lower stratosphere compared with both ozonesondes and EMAC. Such factor is also suspected to be influential in also explaining the transition from a negative to a positive bias after applying AKs in the Southern Hemisphere between May and December in the region between 30°S and 60°S in CMAM. The sensitivity of the 1000-450 hPa subcolumn to the lowermost stratosphere is exemplified in a plot of the monthly mean AKs for August 2007 over the Southern Ocean (~ 47°S, 0°E) (Fig. S2), which shows influence from the ~ 150-450 hPa pressure range. It is known that CCMs tend to have inherent biases in ozone in the lower stratosphere (e.g. Jöckel et al., 2006, 2016; Pendlebury et al., 2015; Kolonjari et al., 2017), so it is likely that the results found here are applicable hemisphere-wide but again further investigation is warranted, perhaps using an ozonesonde trajectory-based mapping approach (e.g. Liu et al., 2013b). The interannual variability (Fig. 3) in the models seems to be consistent with that from the OMI measurements and as reported in the literature, at least in the equatorial region where the magnitude of interannual variability is typically on the order of ~ 10-20 %. In the extratropics, both ozonesondes and models show smaller variability (< 5 %), in contrast to OMI. Whether such differences arise due to model inadequacies in capturing the magnitude of natural variability, or simply as a result of measurement noise in the OMI observations is a subject for further investigation.

4. Stratospheric Influence

Having assessed the ability of the CCMs to represent key features of the global climatology of tropospheric ozone with respect to both in situ and satellite observations, model simulations of the vertical distribution in ozone ~~concentration~~ VMR are now

investigated globally over the 1980-2010 climatological period, together with the role of stratospheric ozone in influencing both regional and seasonal variations.

4.1 O_3 Vertical Distribution, Seasonality and Stratospheric Contribution (O_3F)

Seasonal composites of the monthly mean, zonal-mean vertical distribution of ozone VMR ~~concentration (O_3S concentration) (VMR)~~ in the troposphere and lower stratosphere (1000-80 hPa) are shown in Fig. 5 ~~(Fig. S2)~~ for (a) EMAC ~~(a)~~, (b) CMAM ~~(b)~~ and (c) CMAM-EMAC ~~(c)~~, together with the percentage contribution of mean ozone of stratospheric origin (O_3F (%) = (O_3S / O_3) x 100: dashed lines). The equivalent seasonal composites of tagged-stratospheric ozone (O_3S) ~~concentration~~ VMR are also shown in Fig. S~~2~~3. The meridional distribution in the tropospheric seasonal mean ozone ~~concentration~~VMR corresponds closely to the latitudinal variability in the integrated 1000-450 hPa subcolumn seasonal composites produced from both the CCM and OMI data (Fig. 1 and 2). The highest ozone VMR according to both CCMs can be found over mid-latitudes, with consistent seasonality to that identified in section 3; a maximum in the Northern Hemisphere during spring into summer

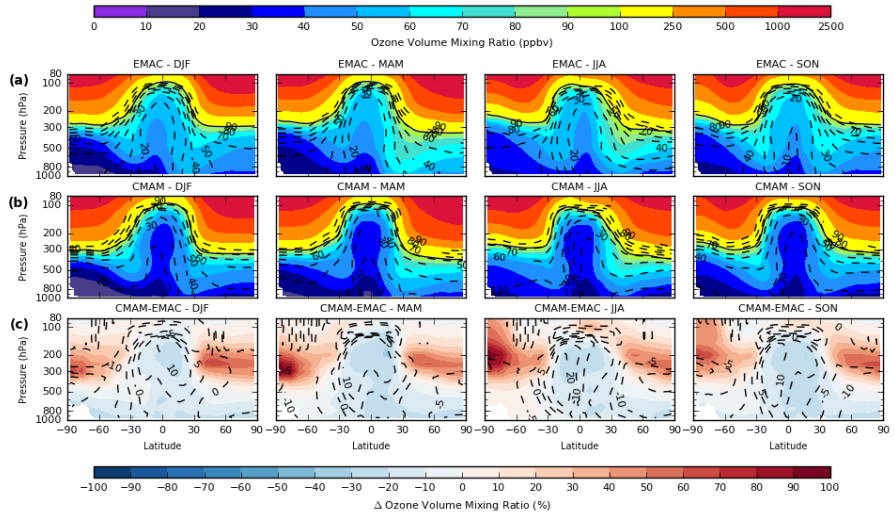

Figure 5 – Zonal mean seasonal composites of monthly mean O_3 ~~concentration~~ VMR (ppbv) for the troposphere and lower stratosphere (1000-80 hPa) from (a) EMAC, (b) CMAM and (c) CMAM and EMAC (CMAM-EMAC) percentage differences over the period 1980-2010. Dashed lines indicate the stratospheric contribution (%) calculated using both ozone tracers in each model: O_3F (%) = (O_3S / O_3) x 100. The 100 ppbv contour (bold line) is included as a reference for the tropopause altitude (top and middle row).

(MAM and JJA) and in spring (SON) over the Southern Hemisphere. It is obvious that ~~the concentration of~~ ozone VMR is significantly greater year-round in the Northern Hemisphere. This is due in part to the large difference in precursor emissions from the surface but also due to a stronger BDC in the Northern Hemisphere and subsequent enhanced STE of ozone, with the former ~~(latter)~~ clearly a greater influence near the surface, ~~(upper troposphere)~~ and the latter in the upper troposphere. As indicated by the dashed contours, the stratospheric influence increases with altitude for all latitudes across all seasons. However, there is a significant meridional gradient in the stratospheric influence, with values ranging from < 30 % over the tropics in all four seasons throughout the troposphere, to maximum values between 40 and 75 % during the winter months at high latitudes in both hemispheres from the surface to 350 hPa. Towards summertime, this fraction decreases sharply across middle and high latitudes (particularly near the surface) due to a combination of reduced STE and increasing importance of precursor emissions during the photochemically active months. Thus in relative terms, the stratosphere has a smaller contribution outside the winter months (lowest in summer). Despite this, the stratosphere has the largest contribution during spring in absolute terms (see supplement Fig. ~~S2~~S3), extended through to summer in the Northern Hemisphere upper troposphere, which is well established in the literature (e.g. Richards et al., 2013; Škerlak et al., 2014; Zanis et al., 2014). This further implies that the influence of the stratosphere becomes secondary to precursor emissions during the photochemically active months, away from the upper troposphere.

The inter-model difference in the zonal mean ozone ~~concentration~~ VMR for each season is shown in Fig. 5 (c). With respect to EMAC, CMAM shows lower values overall throughout the tropical troposphere, and also over the Northern Hemisphere lower and middle troposphere in all seasons (~ 0-30 % or between 0 and -20 ppbv). In contrast, CMAM shows much higher values in the extratropical upper troposphere (up to +50 ppbv or 50-100 % in relative terms) in all seasons, with smaller positive differences extending towards the surface in the Southern Hemisphere, particularly in winter (JJA). The large difference in the extratropical upper troposphere, in conjunction with the vertically extensive negative bias in the tropics, may be partially attributed to a difference in the large scale dynamics in each model. Notably, a modest downward shift in the height of the extratropical tropopause would lead to such large differences apparent in Fig. 5, due to the existence of a very sharp gradient in ozone ~~concentration~~ VMR at this boundary.~~,~~ Indeed, it has been identified previously that tropopause pressures in EMAC are lower than CMAM (by as much as 30-50 hPa) in free running simulations, equating to a smaller total mass of the lowermost stratosphere (Hegglin et al., 2010), although the actual difference is likely smaller in the case of the specified dynamics simulations analysed here. Apart from over the Southern Hemisphere high latitudes, the negative difference in CMAM (relative to EMAC) throughout much of the troposphere would appear to be related to both a difference in the implementation of the tropospheric chemistry scheme in each model and the amount of simulated O_3S, which is evidently some 0-10 ppbv (up to 20 %) lower in CMAM despite a much larger ozone burden in the extratropical UTLS region (Fig. ~~S2c~~S3c). An exception to this is over the Southern Hemisphere subtropics during wintertime (JJA) especially where a significantly larger amount of O_3S (~ 0-20 %) is transported down towards the surface in CMAM compared with EMAC (indicative of greater STE). The absence of a positive difference in Fig. 5c in this region however suggests an overwhelming influence of the reduced in situ

photochemical formation of ozone in CMAM due to the simplicity of the tropospheric chemistry scheme in this model, despite an obvious larger stratospheric ozone fraction here (O_3F > 20 % larger in CMAM in the mid-troposphere).

4.2 O_3F Global Distribution and Seasonality

The global distribution of ozone of stratospheric origin is next investigated, in order to quantify the relative contribution to tropospheric ozone, as well to help identify preferential pathways of stratosphere-troposphere transport. The climatological fraction of stratospheric sourced ozone (O_3F) is shown globally for EMAC and CMAM, together with the difference between both models (CMAM-EMAC) in Fig. 6 at (a) 350 hPa, (b) 500 hPa and (c) 850 hPa for both DJF and JJA (see Fig. S~~3~~4 for MAM and SON) over the period 1980-2010, when O_3F reaches a maximum ~~(minimum)~~ in ~~the respective~~ winter ~~(summer) hemisphere~~ and minimum in summer. Both CCMs are broadly consistent at each pressure level, with a clear decrease in the O_3F towards the surface as already indicated in Fig. 5. The meridional gradient is largest in the upper troposphere at 350 hPa with low values across the tropics (< 40 % between 30°N and 30°S) associated with both convective upwelling and the short photochemical lifetime of ozone in the tropics, with higher values in the extratropics but particularly in the winter hemisphere (> 70 %). In the Northern Hemisphere mid-latitudes where the gradient is largest, a planetary-scale wave pattern is evident (particularly at 350 hPa) which is consistent with longitudinal variability in the climatological positioning of the upper level jet streams induced by orography (e.g. the Rocky Mountains in North America) (Charney and Eliassen, 1949; Bolin, 1950), particularly in winter (DJF). Although the O_3F is relatively high during summer in each hemisphere at 350 hPa as well, the O_3F is much lower at 500 hPa and 850 hPa (which is consistent with Fig. 5) and reflects the relative minimal role of the stratosphere during this season (with strong influence from precursor emissions instead). At 850 hPa, the stratospheric influence is typically largest over oceanic regions which further reflects the importance of emission precursors over continental regions, particularly in the Southern Hemisphere where biomass burning is prevalent over Africa and South America.

Large differences in O_3F are apparent at high latitudes (poleward of 60°N and 60°S) during summer in each hemisphere at 350 hPa, with CMAM showing a significantly smaller fraction in ozone of stratospheric origin (~ 40-50 %) compared with EMAC (~ 70-80 %). This is despite a positive bias of ~ 20-50 % (20-30 ppbv) in the seasonal mean ozone VMR in CMAM compared with EMAC (Fig. 5c), although this bias exists across all seasons whereas the O_3F bias is seasonally dependent. Inspection of model tracer values (not shown) indicates slightly lower stratospheric ozone (O_3S) in CMAM compared with EMAC, along with higher O_3 values (ozone of non-stratospheric origin) at 350 hPa which gives rise to this difference; although the exact origin of this discrepancy would require further investigation. During wintertime in the Southern Hemisphere (JJA) subtropics, a large positive difference in O_3F also exists over a relatively narrow latitude range between 0°S and 30°S, which is indicative of an equatorward displacement in the position of the subtropical jet stream in CMAM compared with EMAC. The differences show some variation longitudinally, with the largest differences extending from east Africa towards Indonesia and northern

Australia and out across the South Pacific. Reference to seasonal composites of the model O_3S VMR tracer (Fig. ~~S2~~S3) confirms that the positive bias is related to larger STE in CMAM relative to EMAC, at least over the Southern Hemisphere

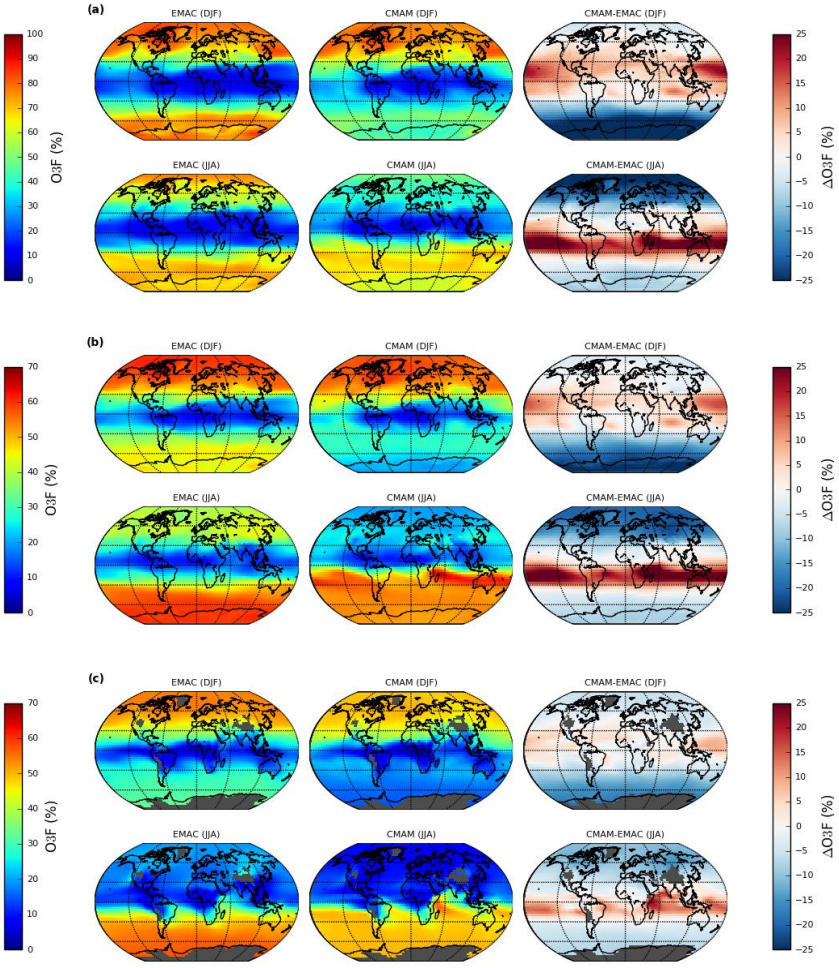

Figure 6 – Seasonal (DJF/JJA) composites of (a) 350 hPa, (b) 500 hPa and (c) 850 hPa monthly mean stratospheric ozone fraction (O_3F) for EMAC (left), CMAM (middle) and CMAM-EMAC (right) over the period 1980-2010. Note the scale difference between (a) and (b-c). Grey shaded regions represent regions where the surface pressure is lower than the plotted pressure level.

subtropics. The effect of greater STE, even locally across this latitude range, in CMAM would propagate eastwards due to the influence of upper level winds, leading to transport of ozone-rich air on intercontinental scales. Both the highest O_3S (not shown) and O_3F values in CMAM are apparent over a relatively small geographical area of the Indian Ocean north of Madagascar (adjacent to the east African coastline) which signifies preferential stratosphere-to-troposphere transport in this region which extends deep into the lower troposphere (O_3F > 50 % at 850 hPa). Although EMAC shows relatively high O_3F in the wider region during this season, evidence of a preferential STE pathway here is lacking in this model and indeed no such feature has been widely recognised in the literature. Such differences are non-existent during DJF, although CMAM shows generally higher O_3F over part of the Indian Ocean and the South Pacific and relatively lower O_3F over South America, the South Atlantic and over Africa. The differences described at 350 hPa are very similar at 500 hPa, albeit the negative difference at high latitudes during summer is lower (~ 10-20 %). Although the spatial distribution of the biases is broadly consistent at 850 hPa as well, there is much greater variability regionally in the tropics and the negative bias at high latitudes is relatively low (> 10 %).

4.3 Monthly Evolution of Stratospheric Influence

The zonal-mean monthly evolution of mean ozone (O_3) ~~concentration~~ VMR at 350, 500 and 850 hPa is shown in Fig. 7 based on (a) the monthly mean aggregated ~~available global measurement network of~~ in situ ozonesonde observations from the WOUDC database, interpolated and averaged for 10° latitude intervals and within ±20 hPa of each pressure level ~~(a)~~, (b) as simulated ~~from~~ by EMAC ~~(b)~~, and (c) subsequently for EMAC O_3S ~~(c)~~ and (d) EMAC O_3F ~~(d)~~.The ozonesonde measurements are in broad agreement with that simulated by EMAC (and CMAM; see Fig. ~~S4~~S5), in terms of both the seasonality and meridional variability in the climatological mean ozone ~~concentration~~ VMR at each of the three different pressure levels. However, the ozone ~~concentration~~ VMR across the Northern Hemisphere high latitudes at both 500 and 850 hPa during the broad spring and summer maximum is somewhat higher (~ 0-10 ppbv) in EMAC, whereas closer agreement with the ozonesonde climatology is apparent for CMAM (Fig. ~~S4~~S5). At the 350 hPa level on the other hand, CMAM overestimates ozone in the extratropics relative to both EMAC and ozonesondes by as much as 10-20 ppbv, which is consistent with the identified high ozone bias in the UTLS in CMAM over three different extratropical regions in section 3 (Fig. 4), whereas EMAC is in closer agreement with the ozonesonde-derived composites. Furthermore, there is very high variability with latitude in the tropics compared with EMAC (and CMAM), although this is almost certainly an artefact of both the paucity and poor spatial representativeness of ozonesonde stations. This figure is similar to that produced by Lamarque et al. (1999, Fig. 2., p. 26368) and their model results bear some resemblance to Fig. 7 (Fig. ~~S4~~S5) in terms of the characterisation of the zonal mean evolution of ozone VMR and calculated O_3F, although significantly higher ~~concentrations of~~ O_3 and O_3S VMRs are evident in the ~~contemporary~~ CCM simulations, as well as higher stratospheric fraction (O_3F) values in this study.

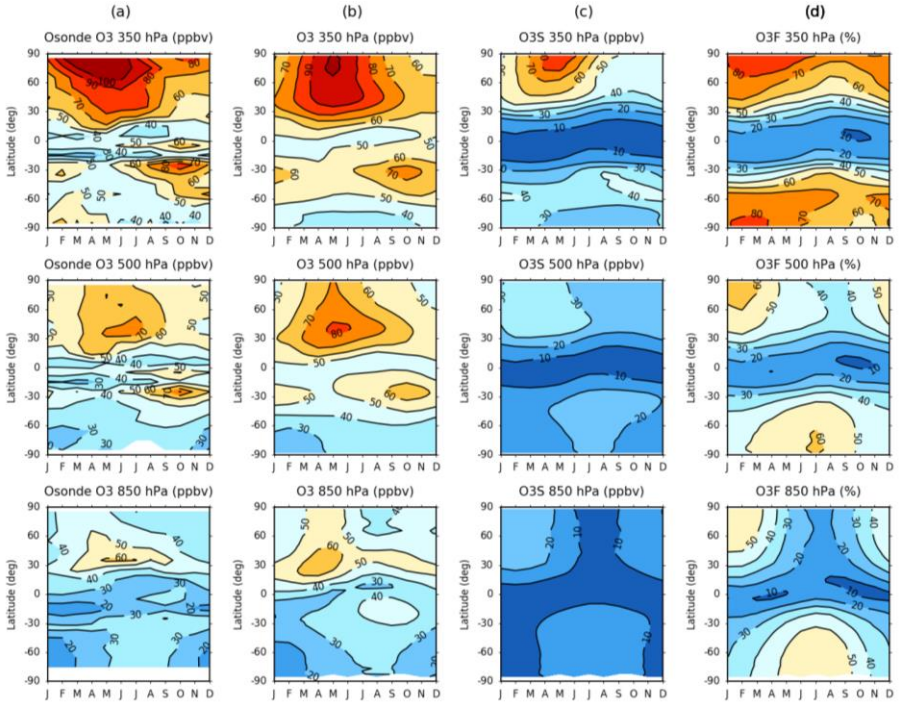

Figure 7 – Zonal-mean monthly mean evolution of O_3 VMR ~~concentration~~ (ppbv) derived from (a) ozonesondes and (b) EMAC O_3 model tracer. The evolution of the (c) EMAC stratospheric O_3S tracer and (d) O_3F stratospheric fraction (%) are additionally included over the period 1980-2010 for 350 hPa (top row), 500 hPa (middle row) and 850 hPa (bottom row).

The EMAC O_3S evolution corresponds closely to the O_3 evolution at 350 hPa, reflecting the large contribution of the stratosphere in the upper troposphere ozone burden (shown also in the O_3F evolution), but this correspondence falls sharply towards the surface (850 hPa) as noted in section 4.2 from Fig. 6. It is important to note that a pronounced spring maximum in O_3S (> 60 ppbv at 350 hPa) is only evident in the Northern Hemisphere, with a much smaller, short-lived maximum between 30° S and 60° S (~ 40 ppbv at 350 hPa), due to the combined influence of the springtime Antarctic ozone hole and a weaker BDC in the Southern Hemisphere which constrains the seasonality. The ozone hole influence is particularly apparent at 350 hPa in each model O_3F evolution fields (d), where the strong symmetry between each hemisphere is briefly interrupted during SON when the ozone hole readily develops over the Southern Hemisphere high-latitudes. The O_3F evolution shows again the sharp meridional gradient in the stratospheric influence, particularly in the upper troposphere, which separates the tropical

zone of convective upwelling from the region of net subsidence in both hemispheres where net STE is downward. The seasonality in extratropical O_3F is greater towards the surface due to the competing influence of precursor emissions. Despite this, Fig 7. (bottom row) shows that the stratosphere still contributes about half (~ 50 %) of the amount of ozone during winter at high latitudes at 850 hPa, implying that the stratosphere has a significant influence on near-surface ozone levels, and in turn air quality. This fraction is slightly higher in the Southern Hemisphere due to the lower abundance of precursors compared with the Northern Hemisphere.

4.4 Summary

In summary of this section, use of the model stratospheric ozone (O_3S) tracers reveals a significant difference in the strength and dominance of the shallow branch of the BDC in each model, which is intrinsically related to the burden of ozone in the extratropical lowermost stratosphere through transport from the primary ozone production (equatorial) region (Hegglin et al., 2006). ~~which~~ This has implications for both the simulated downward flux of ozone from the stratosphere and its influence on the relative contribution of stratospheric ozone to tropospheric ozone. CMAM simulates a faster, shallower BDC as inferred from Fig. 5 (section 4.1) which shows between 50-100 % more ozone in the extratropical UTLS region (equating to as much as a +50 ppbv difference), which contrasts with a negative difference in the tropics of between 0 and 30 % (0 to -20 ppbv difference) relative to EMAC within this region (~ 200-400 hPa). This inference is supported by a recent finding of a maximum decrease in the AoA between 1970 and 2100 in the mid-latitude lower stratosphere in CMAM, whereas EMAC shows a decrease in stratospheric mean AoA which is more pronounced with both latitude and altitude, due to acceleration of the BDC due to climate change (Eichinger et al., 2019). It is inferred from characterisation of the vertical ozone distribution biases in Fig. 4 (section 3) that EMAC more accurately depicts the BDC and its effects on the meridional variation in stratospheric ozone, although it is likely that this model is still too conservative in this aspect compared to reality, given a smaller, but general negative stratospheric ozone bias (up to 10-20 %) in the extratropics with respect to ozonesondes. The same inference is in turn made for STE of ozone; a larger proportion of the downward flux of ozone is ~~modelled~~ simulated over the subtropics in comparison with EMAC, which simulates a larger flux in the extratropics (Fig. 6 and Fig. ~~S3~~S4~~)~~. The difference is particularly large in the Southern Hemisphere subtropics (0°-30° S), with a typically larger fraction of stratospheric ozone ranging from 10-25 % from the lower to upper troposphere in CMAM relative to EMAC during austral winter (JJA). There is indication of a preferential STE pathway over the western Indian Ocean and neighbouring east Africa which is active during this season as far down as the PBL according to CMAM, although any preferential pathway or STE 'hotspot' in this region is ~~not~~ neither obvious in EMAC nor widely established in the literature. Further work is necessary to understand how realistic the representation of STE is in each model, together with the simulated in situ photochemical production of ozone from precursor emissions. Reference to the earlier work of Lamarque et al. (1999) shows that the contemporary CCM simulations analysed in this study more closely match the ozonesonde-derived climatology, which is remarkably consistent in both this study and that produced by Lamarque et al. (1999, Fig. 1, p. 26367), compared to the chemistry transport model (CTM) selected

in their study, which underestimated tropospheric ozone ~~concentrations~~ VMRs by as much as 20-50 %. Both the stratospheric ozone and derived stratospheric fraction fields in their study show very conservative numbers relative to that calculated in this study for both EMAC and CMAM, indicating that the stratosphere has a much larger influence than previously thought, although differences in the stratospheric tracer definitions might explain some of this difference. Both contemporary simulations suggest a significant stratospheric influence on ~~even lower~~ tropospheric ozone, of over 50 % during wintertime in the extratropics (extending down into the lower troposphere), ~~which~~ is significantly higher than the 10-20 % estimated from the CTM in Lamarque et al. (1999) and still considerably higher than more recent studies, which imply an influence in the range of 30-50 % (e.g. Lelieveld and Dentener, 2000; Banerjee et al., 2016).

Formatted: Pattern: Clear

5. Recent Changes in Tropospheric O_3 and O_3S

Seasonal changes in the global mean tropospheric ozone distribution between 1980-89 and 2001-10 are next quantified using the CCM simulations, together with changes in attribution from the stratosphere. The changes in the ~~modelled~~ simulated ozone (O_3) ~~concentration (~~VMR~~s)~~ ~~tracers~~ between these two periods are shown globally in Fig. 8 ~~(Fig. S5)~~ at 350 hPa, 500 hPa and the surface model level, as well as throughout the troposphere for three different latitudinal cross sections (30°W, 30°E and 90°E) in Fig. 9 ~~(Fig. S6)~~ for MAM/SON ~~(DJF/JJA)~~. Changes for DJF/JJA are also shown globally in Fig. S~~5~~6 and for these latitude cross-sections in Fig. S~~6~~7. These latitudinal transects help show that regional ~~e vertical distribution of~~ changes in O_3 and O_3S are strongly height-dependent, particularly along these selected longitudes where notable features are observed, ~~and around notable observed features along these longitudes~~ which differ in each model and season. The respective changes in the ~~modelled~~ simulated stratospheric ozone (O_3S) ~~concentration (~~VMR~~s)~~ ~~tracers~~ are then shown globally in Fig. 10 (Fig. ~~S7~~S8) for each level and as a function of pressure for each latitudinal cross section in Fig. 11 ~~(Fig. S8)~~ for MAM/SON and Fig. S9 for ~~(~~DJF/JJA~~)~~. Zonal-mean changes in each model tracer are additionally summarised in Table S3 (O_3) and Table S4 (O_3S) for 30° latitude bands. Statistical significance is inferred where the paired t test p-value is less than 0.05 (stippled regions), although the distribution of such regions should be interpreted only as an approximation, in the absence of additional data (Waserstein & Lazar, 2016).

5.1 O_3 Change (1980-89 to 2001-10)

It is evident in Fig. 8 that both models simulate an overall increase in ozone, which is typically largest (in absolute terms) and most robust (statistically significant) in the upper troposphere (350 hPa) and across the Northern Hemisphere in both seasons. The increase here in both MAM and SON is on the order of some 4-6 ppbv (5-10 %), although in excess of 6 ppbv across some regions during MAM and in CMAM especially, with only a slightly ~~lesser~~smaller overall increase evident at 500 hPa (mid-~~-~~troposphere). Greater spatial variability is evident at 350 hPa (at least in MAM) due to enhanced sensitivity to changes in the tropopause altitude at this level. This can be inferred from Fig. 9 in the Northern Hemisphere for the 30°W latitudinal

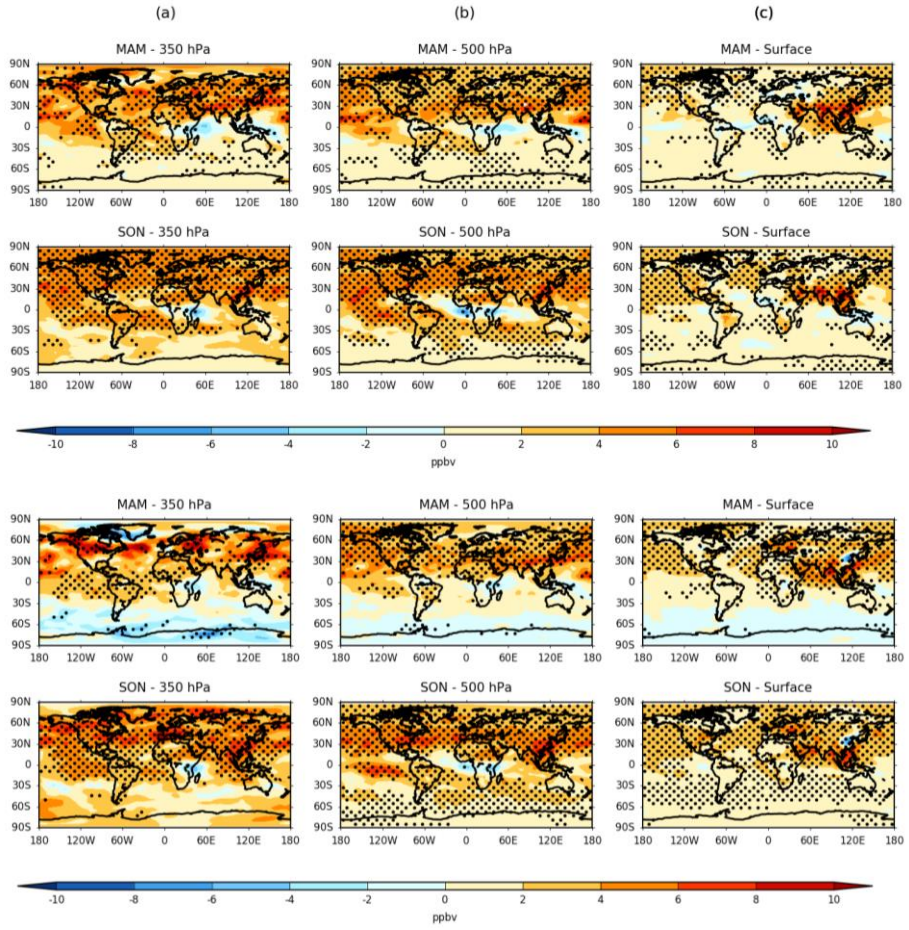

Figure 8 – Seasonal change in EMAC (top) and CMAM (bottom) ozone (O_3) VMR ~~concentration~~ (ppbv) between 1980-89 and 2001-10 for MAM and SON at (a) 350 hPa, (b) 500 hPa and (c) the surface model level. Stippling denotes regions of statistical significance according to a paired two-sided t-test ($p < 0.05$).

cross section in particular, where relatively large apparent model disagreement at 350 hPa can be attributed to a slight downward shift in CMAM relative to EMAC; consistent with that found in sections 3 and 4. Relative to CMAM, the largest

increases in EMAC are shifted equatorward (~ 10-40°N) and are collocated more closely with the region influenced by the subtropical jet stream (e.g. Manney and Hegglin, 2018), particularly in spring (MAM). In contrast, the largest changes in

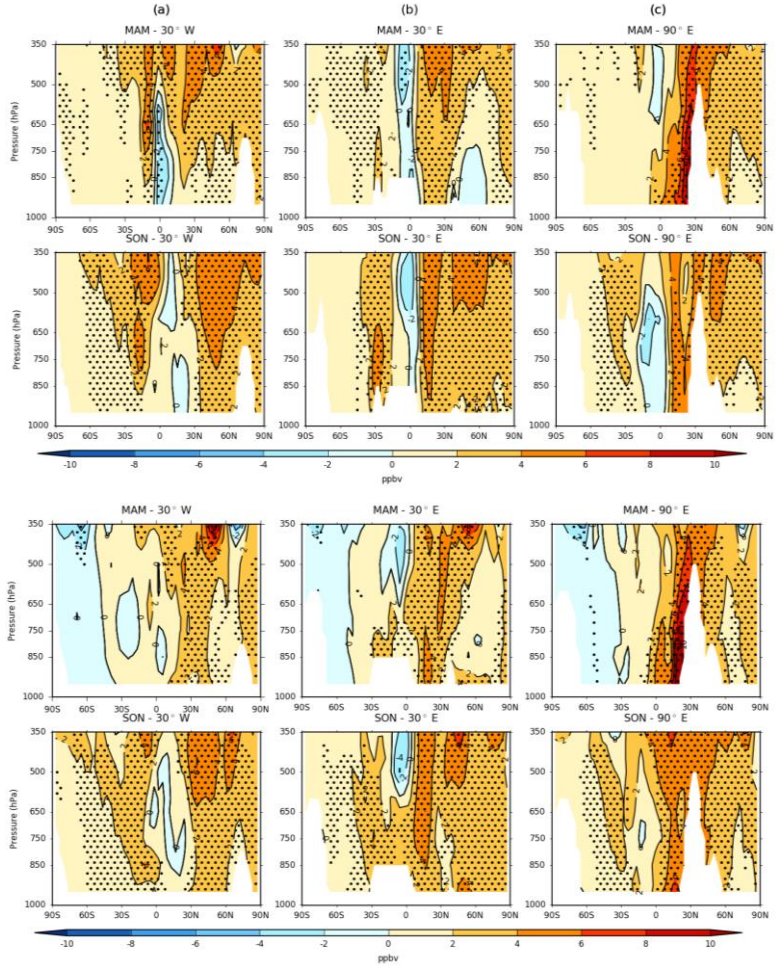

Figure 9 – Longitudinal cross-sections of the seasonal change in the vertical distribution of ozone (O_3) VMR (ppbv) from EMAC (top) and CMAM (bottom) between 1980-89 and 2001-10 for MAM and SON at (a) 30° W, (b) 30° E and (c) 90° E. Stippling denotes regions of statistical significance according to a paired two-sided t-test ($p < 0.05$).

CMAM are generally poleward of 30°N, particularly at the 350 hPa level. The spatial distribution in the changes is also less zonally consistent than for EMAC, and this could reflect a greater influence in the eddy-driven (polar) jet stream in modulating such spatial variability.

Northern Hemisphere surface changes show greater regional variability due to the strong dependence of the surface environment as both a source of emission precursors and as a sink of ozone. In both seasons, the largest statistically significant increases can be found over south east Asia (exceeding 6 ppbv locally), except for a small region of decrease over north-east China apparent only in CMAM. The 90°E latitudinal cross section in Fig. 9 intersects this region, showing the largest increase close to the southern flank on the Himalayas in each model during both MAM (+6-10 ppbv) and SON (+4-6 ppbv), extending from the surface upwards towards the UTLS (350 hPa). A significant increase is also evident widely over oceanic regions, particularly in CMAM and in SON where values exceed 2 ppbv. This could be attributable to a number of factors, including increases in emissions from international shipping, long range transport from upstream precursor emission sources as well as enhanced subsidence in mid-latitudes due to the influence of subtropical high pressure systems (e.g. the Azores High and the North Pacific High) which may have expanded and intensified in recent decades (Li et al., 2011~~;~~ 2012). Long range transport has a clear dominant influence over the Pacific sector, as expected due to the rapid advection from this region. Given recent emission controls in North America, and therefore smaller changes in surface ozone, this factor would be less influential over the Atlantic. Across Europe, there is a large discrepancy in the long term changes between the two models, with negligible change in EMAC (or even slightly negative in MAM) but considerable increase (~ 2-6 ppbv) in CMAM in both seasons. Fig. 10 later shows that this difference is at least partly related to the simulated downward flux of stratospheric ozone in each model during spring (MAM) but not in autumn (SON), with the remaining difference likely related to the chemistry schemes in each model. It is however noted from Jöckel et al. (2016) that the timing of road traffic emissions is offset in this EMAC simulation, leading to a slight underestimation of tropospheric partial column ozone (up to ~ 1.5 DU in Northern Hemisphere mid-latitudes during boreal summer between 2000 and 2013), but any impact on calculated ozone changes or trends has not yet been quantified.

Smaller, ~~largely statistically insignificant~~ changes are typically found over the tropics and across parts of the Southern Hemisphere in both models (Fig. 8), but particularly in CMAM and during autumn (MAM) when changes are near-zero or even negative. Between 0°N and 30°S, a continuous region of statistically significant increase in ozone (~ 2-6 ppbv) is however apparent along a north-west to south-east axis over the Pacific, South America and South Atlantic at both 350 and 500 hPa; largest and most coherent in EMAC and during SON, particularly over the Pacific Ocean. The geographical orientation of this feature is consistent with the climatological positioning of the Southern Hemisphere subtropical jet stream. Over Africa, a relatively small region of decrease (along or slightly south of the equator) is present in both seasons, in both models at 350 and 500 hPa. The largest decreases are evident in SON, where locally ozone has decreased at a rate of 4-6 ppbv. This feature is not always statistically significant, likely due to its small-scale and subsequent enhanced sensitivity to interannual variability. The

latitudinal cross section through 30°E in Fig. 9 shows this feature to be most pronounced in the mid- to upper- troposphere in each model (even absent in CMAM in the lower troposphere). The bimodal structure of the changes in ozone (with an increase to the south of this region) is again consistent with a poleward shift in the subtropical upper tropospheric jets as found ~~in~~by Manney and Hegglin (2018) and the location of STE. During autumn (MAM), CMAM shows a decrease over much of the extratropics (statistically significant in places at 350 hPa) which could be related to the effects of stratospheric ozone depletion, and the influence this may have on STE of ozone. Ozone depletion principally occurs however during spring (SON) so any apparent delayed impact on tropospheric ozone would need to be investigated further. Indeed, both models (but particularly CMAM) show widespread, statistically significant increases across much of the Southern Hemisphere extratropics during this season at 500 hPa, and to a lesser extent at the surface, which appears related to the larger, regional increases in the subtropics, likely through long-range transport and entrainment around the hemisphere by upper level winds. The relatively insignificant changes at 350 hPa and changes in O_3S (section 5.2) imply that this increase is tropospheric driven.

5.2 O_3S Change (1980-89 to 2001-10)

The long term changes in the corresponding stratospheric ozone (O_3S) model tracers shown in Fig. 10 and 11 ~~(Fig. S7 and S8)~~ for MAM/SON (and Fig. S8 and S9 for DJF/JJA) help attribute the long term changes in O_3 described above primarily to either changes in STE or due to changes occurring in the troposphere, such as the photochemical production of ozone from precursors as well as changing tropospheric transport regimes. Similarly to the changes in O_3, both the largest spatial variability and changes in O_3S are evident towards the upper troposphere (350 hPa), particularly in the Northern Hemisphere where an overall increase can again be seen between both periods. The largest increases in O_3S span across the mid-latitudes in the Northern Hemisphere particularly during MAM), with extensive regions of +3-5 ppbv or greater and +2-4 ppbv in both models during spring (MAM) and autumn (SON) respectively, although statistical significance is often lacking in CMAM especially; indicating the high level of interannual variability in upper tropospheric dynamics. This can again be inferred from the spatial change patterns in the upper troposphere in the latitudinal cross sections in Fig. 11 (Fig. ~~S8~~S9) but most notably along the 30°W meridian, where subtle shifts in the height of tropopause, tropopause pressures of up to 30-50 hPa higher in CMAM (Hegglin et al., 2010), and associated sharp gradients in ozone ~~concentrations~~ VMR ~~can~~ may at least partly explain the large discrepancies between the models in both the sign and magnitude of changes for any given region at the 350 hPa pressure level. Both models are however consistent in showing statistically significant increases in the regions of the subtropical jet, but particularly in EMAC, which is also evident in the mid-troposphere (500 hPa). In contrast, the models differ significantly at high latitudes, especially in MAM when CMAM shows a large decrease (>-5 ppbv) over parts of NE Canada, Southern Greenland and Northern Siberia.

Although EMAC shows a few localised regions of slight decrease, which are spatially collocated with CMAM, the model is dominated by an increase in O_3S at these latitudes. Together with intermodel discrepancies in tropopause height, the spatial

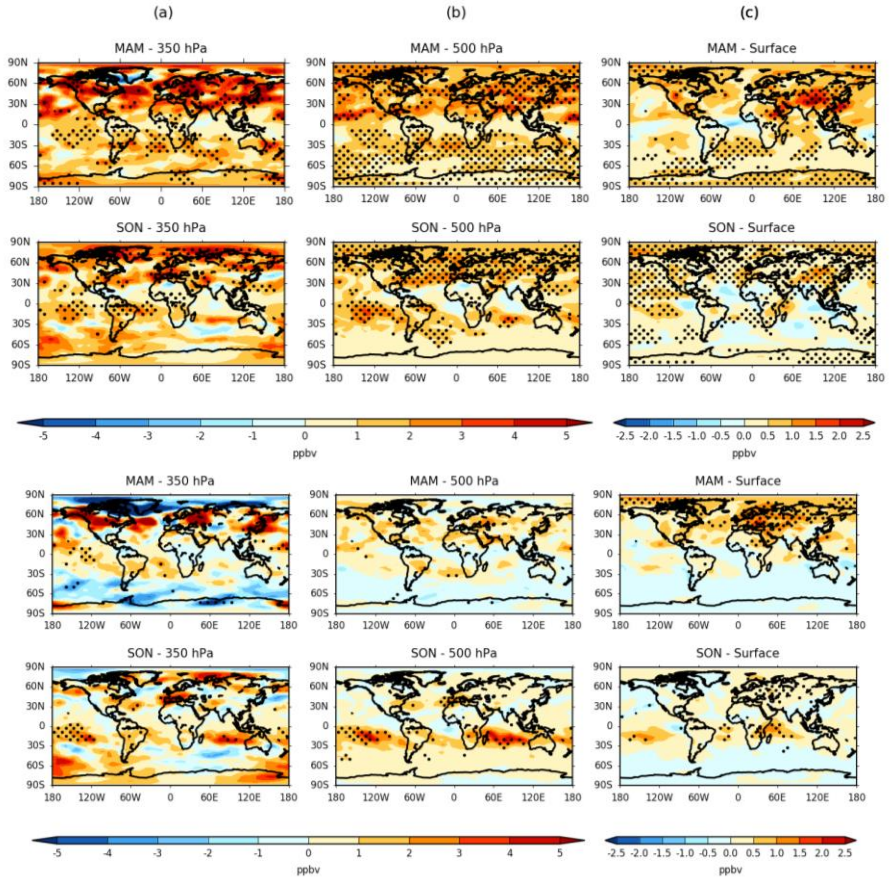

Figure 10 – Seasonal change in EMAC (top) and CMAM (bottom) stratospheric ozone (O_3S) VMR ~~concentration~~ (ppbv) between 1980-89 and 2001-10 for MAM and SON at (a) 350 hPa, (b) 500 hPa and (c) the surface model level. Stippling denotes regions of statistical significance according to a paired two-sided t-test ($p < 0.05$). Note the scale difference between (a-b) and (c).

distribution in changes during MAM (most notably in CMAM) could reflect an equatorward shift in the mean position of the eddy-driven polar jet stream over time, and the subsequent area of preferential downward STE, which has been identified through trend analyses using reanalysis datasets (Manney and Hegglin, 2018). Indeed, an equatorward trend of ~ -0.4° dec^{-1} in

Formatted: Font: (Default) Times New Roman

the jet latitude has also been calculated for both models for the period 1960-2000 in a recent study by Son et al. (2018), as determined by the maxima in the 850 hPa zonal mean zonal wind, although this trend is typically poleward for most other

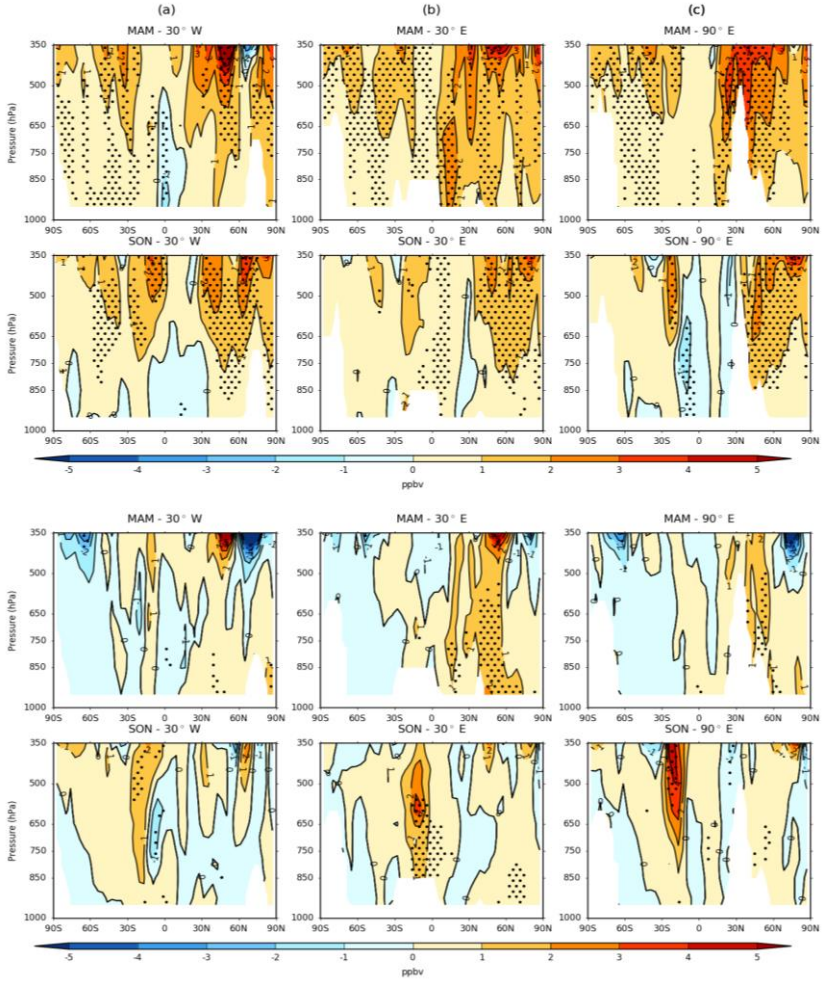

Figure 11 – Longitudinal cross-sections of the seasonal change in the vertical distribution of stratospheric ozone (O_3S) VMR (ppbv) from EMAC (top) and CMAM (bottom) between 1980-89 and 2001-10 for MAM and SON at (a) 30° W, (b) 30° E and (c) 90° E. Stippling denotes regions of statistical significance according to a paired two-sided t-test ($p < 0.05$).

CCMI models. Conversely, changes at 500 hPa are much more spatially uniform, although large differences remain between the two models. Surface changes in O_3S on the other hand are generally modest, with the large role of precursor emissions in contributing to the increase in O_3 (Fig. 8) obvious across many regions, most notably over SE Asia, when comparing such changes with the calculated changes in the model O_3S tracers. Nonetheless, some regions (e.g. western North America and Eurasia) show an increase of 1-2 ppbv in MAM (locally significant), which represents a large fraction of the corresponding increase in O_3 (or even an offset of a slight negative change over parts of Europe in EMAC) as previously shown in Fig. 8. The main difference between the two models is the larger relative increase in O_3S in EMAC across much of the Middle East and central southern Asia, and conversely across much of Europe and western Eurasia in CMAM. The former difference is additionally highlighted in the 90°E transect (Fig. 11) which intersects the Himalayan region, although both models show a statistically significant increase (> 1 ppbv) in spring (MAM) along the northward flank of the mountain range which represents a minimum contribution of ~ 25-30 % to the surface ozone change of 2-4 ppbv (Fig. 9) Regional discrepancies are smaller in SON with a general, albeit smaller, increase in O_3S (~ +0-1 ppbv) apparent, which is most pronounced in EMAC. ~~Interestingly, changes during this season are widely statistically significant in direct contrast with MAM across most regions, although the climatological influential of the stratosphere is least during this season.~~

Changes in O_3S across the tropics at both 350 and 500 hPa are generally small, consistent and of similar magnitude between each model, during both MAM and SON, reflecting the absence of influence from the stratosphere (typical tropical tropopause altitude of ~ 100 hPa in the tropics) and a general upwelling regime. In the Southern Hemisphere subtropics however, both models show hemispheric-wide, sometimes statistically increases in O_3S on the order of ~ +1-4 ppbv centred between 10-30°S, except in CMAM during MAM when any increase is confined over South America and adjacent oceanic regions. Such zonal structure in the spatial trend patterns is strongly supportive of influence from the subtropical jet stream, with the largest changes offset slightly equatorward of the climatological mean position in both seasons as identified in the literature (Langford, 1999; Manney and Hegglin, 2018). Indeed, preferential transport from the stratosphere to the troposphere has a known tendency to occur on the equatorward side of the jet (Lamarque and Hess, 2003). The calculated changes in the O_3S tracer confirms that the O_3 changes (Fig. 8) are primarily driven (> 50 %) by an enhanced influence from the stratosphere, with the increase largest in CMAM during austral spring (SON) in likely association with an increased lower branch in the BDC in this model, which is more pronounced in the Southern Hemisphere (Hegglin et al., 2014; Haenel et al., 2015). Poleward of 30°S, changes are weak and generally insignificant at 500 hPa, with CMAM exhibiting an overall slight decrease during MAM and also in SON over Antarctica, whilst EMAC displays a slight increase generally (only exceeding 1 ppbv on a local basis), most pronounced in MAM where changes are significant in places. The spatial change patterns are broadly similar at 350 hPa, although spatial variability is considerably larger and complex patterns emerge, with particularly large discrepancies during MAM between each model. The differential spatial change patterns in each model at this height could be attributable to a range of factors such as the simulation of stratospheric ozone depletion, changes in the BDC between the two time periods, as well as differences in tropopause altitude in each model. Surface changes in O_3S across the Southern Hemisphere are small (and

insignificant in places), although two localised regions of statistically significant increase (locally > 1 ppbv in CMAM) emerge in SON in the tropics; in the central South Pacific and over part of the western Indian Ocean and eastern Africa. The latter region is captured in the 30°E latitudinal cross section (Fig. 11) in CMAM especially, with a clear downward pathway in evidence coupling changes in O_3S from the tropopause to the surface. Both regions are collocated spatially with the area of largest increase in O_3S at both 350 and 500 hPa in the Southern Hemisphere, indicating that the influence of enhanced STE of ozone during SON between 1980-89 and 2001-10 is able to penetrate deep into the PBL in these regions, explaining most of the increase in the model O_3 tracers locally here.

5.3 Summary

To summarise, changes in seasonal mean tropospheric ozone are generally positive between 1980-89 and 2001-10 in both models, with a maximum increase of ~~approximately~~ ~ 5-10 % corresponding to approximately 4-6 ~~(2-6)~~ ppbv ~~(~ 5-10 %)~~ over the Northern Hemisphere ~~(~~and 2-6 ppbv over the Southern Hemisphere subtropics during springtime in both the middle (500 hPa) and upper troposphere (350 hPa). A significant stratospheric contribution to such increase is found here of up to 3-5 (1-4) ppbv during this season (~ 50-80 %), although significant intermodel disagreement exists in the magnitude and sometimes the sign of the attributable change in ozone due to the stratosphere for any given region or season. This is particularly the case in the extratropics, where different responses to transport likely arise in each model resulting from nudging to specified dynamics as captured in ERA-Interim. Both the ozone (O_3) and stratospheric ozone (O_3S) tracers exhibit a preferential increase in the subtropics ~~(extratropics)~~ in EMAC ~~(~~and extratropics in CMAM) which may reflect the relative importance of the subtropical ~~(~~and polar~~)~~ jet streams respectively. This difference is however larger in the former case, which implies that the higher amounts of simulated ozone from precursor emissions in EMAC, particularly in the Northern Hemisphere subtropics, propagates upward from the surface and longitudinally due to influence of these two jet streams, contributing to this difference. In the tropics and Southern Hemisphere extratropics on the other hand, estimated changes are typically small and insignificant, with some indication of a decrease over high-latitudes in CMAM. This ~~is likely~~ could be attributable to the influence of stratospheric ozone depletion but this requires further investigation given the lack of model agreement and largest decrease in autumn (MAM), which is not consistent with the timing of the springtime stratospheric ozone hole. Although surface ozone changes are dominated by regional changes in precursor emissions between the two periods – the largest, statistically significant increases (> 6 ppbv) over south-east Asia – the changing influence from the stratosphere is also shown to be highly significant. Indeed, the global area of statistical significance in the calculated O_3S changes typically increases from the upper troposphere (350 hPa) to the surface. Increases in surface ozone driven by the stratosphere are estimated to be up to 1-2 ppbv between the two periods in the Northern Hemisphere, although this is highly variable both regionally and seasonally and between each model. In relative terms, the stratosphere can be seen to typically explain ~ 25-30 % of the surface change over some regions such as the Himalayas, although locally it may represent the dominant driver (> 50 %) where changes in emission precursors are negligible or even declining due to the enforcement of air quality regulations over regions such as Western

Europe and Eastern North America. ~~The stratospheric influence over changes in tropospheric ozone according to these models may however be overestimated, due to deficiencies in either the representation of the stratosphere or tropospheric chemistry: the latter of which is applicable to CMAM especially. This is highlighted in a recent study by Neu et al. (2014), which shows only a modest 2 % change in northern hemisphere mid-latitude tropospheric ozone to a ~ 40 % variation in the strength of the stratospheric circulation on interannual timescales due to ENSO and the QBO (considered to approximate the mean change due to climate change this century) from observations, with a similar muted response according to a simulation from the Community Atmosphere Model with Chemistry (CAM-Chem). This CCM is largely unique in having both a well-resolved stratosphere and comprehensive tropospheric chemistry scheme, but still lacks the tagged stratospheric ozone tracers necessary for vertically-resolved estimates of the stratospheric contribution to tropospheric ozone presented here.~~ The stratospheric influence over changes in tropospheric ozone could be overestimated in the case of CMAM, which has deficiencies in the representation of tropospheric chemistry, although both models contain a well resolved stratosphere and in the case of EMAC, a comprehensive tropospheric chemistry scheme. It is claimed by Neu et al. (2014) that models without comprehensive tropospheric chemistry cannot be used to estimate stratospheric influence, since a much larger response to tropospheric ozone is found in such models, although we find that EMAC shows a larger increase in stratospheric-tagged ozone (O_3S) which challenges this statement. The much smaller STE response found in their study, which shows only a modest 2 % change in northern hemisphere mid-latitude tropospheric ozone to a ~ 40 % variation in the strength of the stratospheric circulation, is also inferred from variability that occurs on interannual timescales due to ENSO and the QBO, which is used a proxy for the mean change in the stratospheric circulation this century. Therefore, the calculated changes presented here would also question the assumption that interannual variations in ENSO and the QBO constitute a representative surrogate for long-term changes anticipated due to climate change.

6. Conclusions

Seasonal variability, stratospheric influence and recent changes in tropospheric ozone are evaluated in this study using two state-of-the-art CCMs, which have the added provision of tagged stratospheric ozone tracer simulations. This study finds evidence that both CCMs are broadly consistent and agree with satellite (OMI) observations and limited in situ (ozonesonde) profile measurements over the 2005-2010 common baseline period, in simulating both the geographical variability and seasonality in tropospheric subcolumn (1000-450 hPa) ozone. Inherent, systematic biases (with a strong seasonal dependence) are however shown to exist in each model. EMAC is characterised by an overall positive bias with respect to OMI, largest in Northern Hemisphere low latitudes during springtime (~ +2-8 DU or +10-30 %). In contrast, CMAM shows no obvious overall bias (~ -4 to + 4 DU or -20 to +20 %) but with significant regional, latitudinal and seasonal variability in both the sign and magnitude of the bias relative to OMI. In CMAM, the mid-latitude seasonal evolution of the biases ~~between~~ relative to OMI (Fig. 2) ~~and with respect to ozonesondes for three different extratropical regions~~ show larger consistency prior to the application of the satellite (OMI) AKs, with respect to ozonesondes for three different extratropical regions (Fig. 4), which is contrary to

that expected through accounting for the observation geometry of the satellite. Whilst the application of AKs serves to mitigate slightly the positive tropospheric bias in mid-latitudes in EMAC, the negative bias in CMAM is converted to a positive bias generally in mid- to high-latitudes. Comparisons with ozonesondes indicates that the low tropospheric bias in CMAM, likely related to the simplicity of the model chemistry scheme, is offset due to an inherent high ozone bias in the lowermost stratosphere (as high as 40-60 %). This leads to excessive downward smearing of ozone into the troposphere as a result of applying satellite (OMI) AKs, necessary to compare both model simulation and OMI satellite measurements equivalently. This highlights an important trade off in the application of satellite AKs for model-measurement comparison analyses of tropospheric ozone where biases in lower stratospheric ozone are known to exist. This evaluation implies that in certain circumstances, the application of AKs would not be advocated where model biases in lower stratospheric ozone are sufficiently large~~, particularly if the model representation of tropospheric ozone is known to be comprehensive,~~ due to anomalous vertical smearing. However, such a detailed quantitative evaluation would be needed to identify such cases. The high bias in mid-latitudes in EMAC could be explained by an overestimation of emissions in MACCity (a CMIP5 based inventory)~~ics~~ (Hoesly et al., 2018), which although ~~are~~ used in both models, leads to a higher bias in EMAC due to the comparatively complex tropospheric chemistry scheme in this model ~~is likely explained by a combination of the relatively complex tropospheric chemistry scheme and possible overestimation of emissions~~. Given the largest tropospheric biases are equatorward of the region ~~greater~~ influenced by vertical smearing from the lowermost stratosphere, the two influences are more independent in this model. The relative importance of these drivers is regionally and seasonally dependent but serves to yield an overall lower bias in CMAM compared with EMAC. The influence of applying AKs is typically to increase the subcolumn amount of tropospheric ozone (1000-450 hPa) in the extratropics by ~ 1-5 DU or ~ 2-8 DU in EMAC and CMAM respectively, depending on season, whereas a slight decrease (~ 0-1 DU) is induced in the tropics in all seasons. An exception to this is over the Southern Hemisphere high latitudes, where the increase is significantly lower due to influence of the ozone hole, particularly in austral spring (SON) when any increase is negligible (0-1 DU). It is important to note that like models, satellite retrieval platforms such as OMI have their own limitations, such as the susceptibility to instrument noise or retrieval errors (Levelt et al., 2006; Mielonen et al., 2015; Schenkeveld et al., 2017; Levelt et al., 2018). It is suspected that this limitation is the cause of the large discrepancy in the seasonal composites of RSD, as a metric for the interannual variability, between OMI and the models; the latter of which is in closer agreement with that derived from ozonesondes. A general consensus in the interannual variability in tropical tropospheric ozone is however found, with RSD values of over 10 % in some regions and seasons, consistent with the known influence of ~~a number of different teleconnection drivers such as ENSO and the QBO~~ different teleconnections; most notably the QBO which is estimated to influence tropical tropospheric ozone anomalies by as much as 10-20 % (8 ppbv) (Lee et al., 2010). Inconsistencies in a number of the model-OMI and model-ozonesonde differences are also suspected to undermine the issue of resolution (in the case of models) and signal-to-noise ratio (in the case of OMI) in adequately resolving mesoscale features, such as local scale pollution plumes or stratospheric intrusion (tropopause folding) events, although this would be an area warranting further investigation.

Formatted: Font color: Auto

Taking ~~this~~ the above information (from the model-measurement comparison in section 3) into account, the relatively long temporal span of the specified dynamics CCM simulations was utilised to investigate the climatological stratospheric influence on tropospheric ozone and calculate estimated recent changes between 1980-89 and 2001-10. A clear difference in the strength and dominance of the shallow branch of the BDC ~~was found~~ is implied in each model~~.~~, due to the large discrepancy in the burden of ozone in the extratropical lowermost stratosphere (~ 50-100 % more ozone in CMAM compared with EMAC). The characterised biases with respect to ozonesondes indicate that CMAM has a faster, shallower BDC compared to actuality, which can be inferred from the ~~high~~ large lower stratospheric ozone bias (~ +20-60 %), whereas EMAC provides a more realistic simulation of the BDC, albeit perhaps too conservative given a general negative ozone bias (up to 10-20 %) in the lower stratosphere. The difference in BDC simulation has implications for the simulated STE flux of ozone; with preferential downward transport in the subtropics in CMAM compared with the mid-latitudes in EMAC, particularly in the Southern Hemisphere subtropics and during springtime when the difference is as much as 10-25 % from the lower to upper troposphere. Compared to the model results of Lamarque et al. (1999), the CCM simulations examined here are in much closer agreement with ozonesonde measurements, ~~(~~ with biases no larger than 20 %~~)~~, as evidenced on a zonally averaged, monthly basis in Fig. 7 (Fig. ~~S4~~S5)~~. in~~ This contrasts to a systematic underestimation of tropospheric ozone ~~concentrations~~ VMR by as much as 20-50 % in the CTM analysed in their study. Despite a significant fall in the correspondence between the seasonal evolution of the simulated ozone and stratospheric ozone component in the CCMs from the upper to lower troposphere, the results show a significant stratospheric influence on even lower tropospheric ozone – greater than 50 % in the wintertime extratropics, which contrasts with a modest 10-20 % estimated from the CTM in Lamarque et al. (1999).

Both models show an overall, statistically significant increase in ozone between 1980-89 and 2001-10, on the order of ~ 5-10 %, or some 4-6 ppbv over the Northern Hemisphere and 2-6 ppbv over the Southern Hemisphere subtropics, ~~4-6 (2-6) ppbv (~ 5-10 %) across the Northern Hemisphere (Southern Hemisphere subtropics)~~ in the middle to upper troposphere, with a preferential increase over the subtropics in EMAC compared to the extratropics in CMAM (most pronounced in spring). As estimated using stratospheric-tagged ozone ~~simulations~~ tracers from each model, ~~T~~the stratosphere is found to provide a substantial contribution ranging between 1-3 ppbv (~ 20-50 %) in the mid-troposphere (500 hPa) and over 5 ppbv (~ 50-80 %) in the upper troposphere (350 hPa) across the Northern Hemisphere mid-latitudes, with a typical increase of 1-4 ppbv (~ 50-80 %) over the Southern Hemisphere subtropics at both pressure levels. Significant model disagreement however exists, particularly in the extratropical upper troposphere, likely due to ~~high sensitivity to the tropopause~~ known discrepancies in tropopause height (Hegglin et al., 2010) and variability in upper level dynamics which may be further affected by the nudging applied to the models. Estimated changes in ozone and the stratospheric contribution on the other hand are generally small and insignificant in both equatorial and Southern Hemisphere extratropical regions. The spatial pattern of changes in surface ozone in contrast show a very different character, with the largest statistically significant increases over much of south-east Asia (> 6 ppbv) and a general increase of up to 2 ppbv or higher quite widely over Northern Hemisphere oceanic regions, but only very small, non-significant changes across the Southern Hemisphere. The influence from the stratosphere at the surface is seen

to have a strong regional and seasonal dependence, but is estimated to be as much as 1-2 ppbv during spring, which was estimated to be as large as ~ 25-30 % along the northern flank of the Himalayan mountain range and greater than 50 % over a localised, relatively unpolluted region of Eastern Africa and the Western Indian Ocean. The situation is complicated in some regions however where near-zero or slight negative changes in ozone ~~concentration~~VMR are apparent in places such as Western Europe and Eastern North America, corresponding to an observed hiatus or slight fall in precursor emissions.

This study highlights some of the shortcomings of both the EMAC and CMAM CCMs as part of the IGAC/SPARC CCMI activity, as validated with respect to satellite observations from OMI and in situ ozonesonde measurements, in simulating tropospheric ozone. In particular, the importance of a well-resolved stratosphere is clear in attaining a high level of model-measurement agreement and in terms of adequately representing stratospheric influence. For comparisons with satellite observational datasets, a well-resolved stratosphere is of paramount importance for the application of AKs which smooth the vertical distribution of model simulated ozone, by smearing information down from the stratosphere to the troposphere. Using this derived knowledge, this study confirms the strong influence of the stratosphere in modulating tropospheric ozone and provides an indication that such influence may in fact be much larger than previously thought. Furthermore, recent changes in tropospheric ozone are shown to have a large attribution from the stratosphere, which is quantified here in relation to influence of changing precursor emissions. A general increase in the amount of stratospheric ozone in the troposphere between 1980-89 and 2001-10 according to both CCMs, which is statistically significant in some regions of the world such as western Eurasia, eastern North America, the South Pacific and the southern Indian Ocean, would be expected from observed long term changes in the shallow branch of the BDC (Hegglin et al., 2014)~~, in which~~ T~~t~~ransit times have been found to exhibit a steady decrease, primarily due to accelerated transport within this branch of the residual circulation (~ 75 %), with a smaller contribution from a shortening of the transit pathways (~ 25 %) (Bönisch et al., 2011). Indeed, a strengthening of the BDC is postulated to be the main mechanism for an expected increase in STE under future climate change scenarios (Hegglin and Shepherd, 2009; Butchart et al., 2010), in addition to stratospheric ozone recovery (Zeng et al., 2010), which further highlights the need for an improved understanding of the relationship between STE and tropospheric ozone and accurate quantitative estimates. These findings thus have important implications for the enforcement of both current and future air quality regulations, as well as in constraining estimates of tropospheric ozone radiative forcing.

Data Availability

All CCM simulations analysed here are publicly available from CEDA/BADC via the CCMI data archive (www.ceda.ac.uk). L3 data from OMI using the RAL profiling scheme can be provided on request by contacting barry.latter@stfc.ac.uk. Ozonesonde profile data is publicly accessible from the WOUDC database (www.woudc.org).

Author Contribution

RSW (the lead author) designed the research study, undertook the analyses and prepared the manuscript under the close supervision of MIH, with some additional supervisory support from BK. BL produced and provided access to OMI-RAL L3 data, with both BK and BL able to offer technical support on the satellite (OMI) dataset. Similarly, PJ and DP provided technical support in relation to the EMAC and CMAM CCM simulation datasets respectively. All co-authors provided comments and suggestions helping RSW to greatly improve the quality of the manuscript.

Competing Interests

The authors declare that they have no conflict of interest.

Acknowledgments

RSW would like to personally thank the Natural Environmental Research Council (NERC) for funding the research and each co-author in providing their support and expertise in shaping the research study and the design of the manuscript. We acknowledge the modelling groups for making their simulations available for this analysis, the joint WCRP SPARC/IGAC Chemistry-Climate Model Initiative (CCMI) for organizing and coordinating the model data analysis activity, and the British Atmospheric Data Centre (BADC) for collecting and archiving the CCMI model output. The EMAC simulations have been performed at the German Climate Computing Centre (DKRZ) through support from the Bundesministerium für Bildung und Forschung (BMBF). DKRZ and its scientific steering committee are gratefully acknowledged for providing the HPC and data archiving resources for the consortial project ESCiMo (Earth System Chemistry integrated Modelling).

Reference

Akritidis, D., Pozzer, A., Zanis, P., Tyrlis, E., Skerlak, B., Sprenger, M., ~~&~~and Lelieveld, J.: On the role of tropopause folds in summertime tropospheric ozone over the eastern mediterranean and the middle east, Atmos. Chem. Phys., 16(21), 14025-14039, https://doi:10.5194/acp-16-14025-2016, 2016.

Allen, D. J. and Pickering, K. E.: Evaluation of lightning flash rate parameterizations for use in a global chemical transport model~~.~~, J. Geophys. Res. Atmos., 107(D23), 4711, https://doi:10.1029/2002JD002066, 2002

~~Bethan, S., Vaughan, G. and Reid, S. J.: A comparison of ozone and thermal tropopause heights and the impact of tropopause definition on quantifying the ozone content of the troposphere, Q.J.R. Meteorol. Soc., 122: 929-944. doi:10.1002/qj.49712253207, 1996.~~

Banerjee, A., Maycock, A. C., Archibald, A. T., Abraham, N. L., Telford, P., Braesicke, P., and Pyle, J. A.: Drivers of changes in stratospheric and tropospheric ozone between year 2000 and 2100, Atmos. Chem. Phys., 16, 2727-2746, https://https://doi.org/10.5194/acp-16-2727-2016, 2016.

Beekmann, M., Ancellet, G., Megie, G., Smit, H. G. J., and Kley, D.: Intercomparison campaign of vertical ozone profiles including electrochemical sondes of ECC and Brewer-Mast type and a ground based UV-differential absorption lidar, J. Atmos. Chem., 19(3), 259-288, https://doi:10.1007/BF00694614, 1994.

B. Bolin, B.: On the Influence of the Earth's Orography on the General Character of the Westerlies, Tellus, 2:3, 184-195, https://doi:10.3402/tellusa.v2i3.8547, 1950.

Bönisch, H., Engel, A., Birner, T., Hoor, P., Tarasick, D. W., & Ray, E. A.: On the structural changes in the brewer-dobson circulation after 2000, Atmos. Chem. Phys., 11(8), 3937. Retrieved from https://search.proquest.com/docview/867784704?accountid=13460, 2011.

Bönisch, H., Engel, A., Birner, Th., Hoor, P., Tarasick, D. W., and Ray, E. A.: On the structural changes in the Brewer-Dobson circulation after 2000, Atmos. Chem. Phys., 11, 3937-3948, https://doi.org/10.5194/acp-11-3937-2011, 2011.

Brinkop, S., Dameris, M., Jöckel, P., Garny, H., Lossow, S. and Stiller, G.: The millennium water vapour drop in chemistry–climate model simulations, Atmos. Chem. Phys., 16(13), 8125-8140., https://doi:10.5194/acp-16-8125-2016, 2016.

Butchart, N., I. Cionni, V. Eyring, T.G. Shepherd, D.W. Waugh, and H. Akiyoshi, J. et al. Austin, C. Brühl, M.P. Chipperfield, E. Cordero, M. Dameris, R. Deckert, S. Dhomse, S.M. Frith, R.R. Garcia, A. Gettelman, M.A. Giorgetta, D.E. Kinnison, F. Li, E. Mancini, C. McLandress, S. Pawson, G. Pitari, D.A. Plummer, E. Rozanov, F. Sassi, J.F. Scinocca, K. Shibata, B. Steil, and W. Tian: Chemistry–Climate Model Simulations of Twenty-First Century Stratospheric Climate and Circulation Changes. J. Climate, 23, 5349–5374, https://doi:10.1175/2010JCLI3404.1, 2010.

Butchart, N.: The Brewer-Dobson circulation, Rev. Geophys., 52, 157-184, https://doi:10.1002/2013RG000448, 2014.

Charney, J. G. and Eliassen, A.: A Numerical Method for Predicting the Perturbations of the Middle Latitude Westerlies, Tellus, 1:2, 38-54, https://doi:10.3402/tellusa.v1i2.8500, 1949.

Formatted: Font: (Default) +Body (Times New Roman), 1

Formatted: Font: (Default) +Body (Times New Roman), 1

Formatted: Font: (Default) +Body (Times New Roman), 1

Formatted: Font: (Default) Times New Roman

Formatted: Font: (Default) Times New Roman, English (United Kingdom)

Formatted: Font: (Default) Times New Roman

Formatted: Font: (Default) Times New Roman

Formatted: Font: Times New Roman, 10 pt, Not Bold

Formatted: Font: (Default) Times New Roman

Formatted: Font: (Default) Times New Roman, Not Italic

Formatted: Font: (Default) Times New Roman

Formatted: Font: (Default) Times New Roman

Formatted: Font: Times New Roman, 10 pt

Formatted: Font: (Default) Times New Roman, 11 pt

Formatted: Font: Not Bold

Colette, A. and Ancellet, G.: Impact of vertical transport processes on the tropospheric ozone layering above Europe.: Part II: climatological analysis of the past 30 years, Atmos. Environ., 39(29), 5423-5435, https://doi: 10.1016/j.atmosenv.2005.06.015, 2005.

Cooper, O. R., Parrish, D. D., Stohl, A., Trainer, M., Nédélec, P., and Thouret, V., Leblanc, T. et al.: Increasing springtime ozone mixing ratios in the free troposphere over western North America, Nature, 463(7279), 344-348, https://doi:10.1038/nature08708, 2010.

Cooper, O. R., Parrish, D. D., Ziemke, J., Cupeiro, M., Galbally, and I. E., Gilge, S. et al.: Global distribution and trends of tropospheric ozone: An observation-based review, Elem. Sci. Anth. 2, p.29, https://doi:10.12952/journal.elementa.000029, 2014.

Cristofanelli, P., Bracci, A., Sprenger, M., Marinoni, A., Bonafè, U., and Calzolari, F., et al.; Tropospheric ozone variations at the Nepal Climate Observatory-Pyramid (Himalayas, 5079 m asl) and influence of deep stratospheric intrusion events. Atmos. Chem. Phys., 10, 6537-6549, https://doi.org/10.5194/acp-10-6537-2010, 2010.

Dibb, J. E., L. D. Meeker, R. C. Finkel, J. R. Southon, M. W. Caffee, and L. A. Barrie: Estimation of stratospheric input to the Arctic troposphere: ^{7}Be and ^{10}Be in aerosols at Alert, Canada, J. Geophys. Res., 99(D6), 12855–12864, https://doi:10.1029/94JD00742, 1994.

Eichinger, R., Dietmüller, S., Garny, H., Šácha, P., Birner, T. and Bönisch, H., et al.; The influence of mixing on the stratospheric age of air changes in the 21st century, Atmos. Chem. Phys., 19, 921-940, https://doi:10.5194/acp-19-921-2019, 2019.

Eyring, V., Lamarque, J. F., Hess, P., Arfeuille, F., Bowman, K., and Chipperfield, M. P. and Granier, C.et al.: Overview of IGAC/SPARC Chemistry-Climate Model Initiative (CCMI) community simulations in support of upcoming ozone and climate assessments., SPARC Newsletter, 40(January), 48-66, Retrieved From: http://oceanrep.geomar.de/20227/, 2013.

Fiore, A. M., D. J. Jacob, B. D. Field, D. G. Streets, S. D. Fernandes, and C. Jang: Linking ozone pollution and climate change: The case for controlling methane, Geophys. Res. Lett., 29(19), 1919, https://doi:10.1029/2002GL015601, 2002a.

Fiore, A. M., Jacob, D. J., Bey, I., Yantosca, R. M., Field, B. D. and Fusco, A. C. et al.; Background ozone over the United States in summer: Origin, trend, and contribution to pollution episodes. , J. Geophys. Res. Atmos., *107*(D15), doi:10.1029/2001JD000982, 2002b.

Formatted
Formatted
Formatted
Formatted
Formatted
Formatted
Formatted
Field Code Changed
Formatted
Formatted
Formatted
Formatted
Formatted
Formatted
Formatted
Formatted
Formatted
Formatted
Formatted
Formatted
Field Code Changed
Formatted
Formatted
Formatted
Formatted
Formatted
Formatted
Formatted
Formatted
Formatted
Formatted
Formatted
Formatted
Formatted
Formatted
Formatted
Formatted
Formatted
Formatted

Foret, G., Eremenko, M., Cuesta, J., Sellitto, P., Barré, J., and Gaubert, B. et al.: Ozone pollution: What can we see from space? A case study, J. Geophys. Res. Atmos., 119, 8476–8499, https://doi:-10.1002/2013JD021340, 2014.

Gaudel, A., Cooper, O. R., Ancellet, G., Barret, B., Boynard, A., and Burrows, J. P. et al.: Tropospheric Ozone Assessment Report: Present-day distribution and trends of tropospheric ozone relevant to climate and global atmospheric chemistry model evaluation-, Elementa, 6: 39., https://doi:10.1525/elementa.291, 2018.

Greenslade, J. W., Alexander, S. P., Schofield, R., Fisher, J. A. and Klekociuk, A. K.: Stratospheric ozone intrusion events and their impacts on tropospheric ozone in the Southern Hemisphere, Atmos. Chem. Phys., 17(17), 10269-10290, https://doi:10.5194/acp-17-10269-2017, 2017.

Guenther, A., Hewitt, C. N., Erickson, D., Fall, R., Geron, C., and Graedel, T. et al.: A global model of natural volatile organic compound emissions, J. Geophys. Res., 100(D5), 8873–8892, https://doi:-10.1029/94JD02950, 1995.

Haenel, F. J., Stiller, G. P., Von Clarmann, T., Funke, B., Eckert, E., and Glatthor, N. et al.: Reassessment of MIPAS age of air trends and variability, Atmos. Chem. Phys., 15(22), 13161-13176, https://doi:0.5194/acp-15-13161-2015, 2015.

Hegglin, M. I., Brunner, D., Peter, T., Hoor, P., Fischer, H., and Staehelin, J. et al.: Measurements of NO, NO_y, N_2O, and O_3 during SPURT: Implications for transport and chemistry in the lowermost stratosphere, Atmos. Chem. Phys., 6(5), 1331-1350. https://doi:10.5194/acp-6-1331-2006, 2006.

Hegglin, M. I. and Shepherd, T. G.: Large climate-induced changes in ultraviolet index and stratosphere-to-troposphere ozone flux, Nat. Geosci., 2(10), 687-691, https://doi:10.1038/NGEO604, 2009.

Hegglin, M. I., Gettelman, A., Hoor, P., Krichevsky, R., Manney, G. L., and Pan, L. L. et al.: Multimodel assessment of the upper troposphere and lower stratosphere: Extratropics, J. Geophys. Res. Atmos., 115(D3), https://doi:10.1029/2009JD013638, 2010.

Hegglin, M. I., Plummer, D. A., Shepherd, T. G., Scinocca, J. F., Anderson, J., and Froidevaux, L. et al.: Vertical structure of stratospheric water vapour trends derived from merged satellite data, Nat. Geosci., 7(10), 768–776, https://doi:10.1038/NGEO2236, 2014

Hegglin, M. I. and J.-F. Lamarque: The IGAC/SPARC Chemistry-Climate Model Initiative Phase-1 (CCMI-1) model data output, NCAS British Atmospheric Data Centre, 24th September 2018. http://catalogue.ceda.ac.uk/uuid/9cc6b94df0f4469d8066d69b5df879d5, 2015.

~~Hegglin, M. I., Plummer, D. A., Shepherd, T. G., Scinocca, J. F., Anderson, J., and Froidevaux, L. et al.: Vertical structure of stratospheric water vapour trends derived from merged satellite data, Nat. Geosci., 7(10), 768–776, https://doi:10.1038/NGEO2236, 2014~~.

~~Hegglin, M. I. and Shepherd, T. G.: Large climate-induced changes in ultraviolet index and stratosphere-to-troposphere ozone flux, Nat. Geosci., 2(10), 687–691, https://doi:10.1038/NGEO604, 2009.~~

Hess, P. G. and Zbinden, R.: Stratospheric impact on tropospheric ozone variability and trends: 1990–2009, Atmos. Chem. Phys., 13, 649-674, https://doi.org/10.5194/acp-13-649-2013, 2013.

Hoesly, R. M., Smith, S. J., Feng, L., Klimont, Z., Janssens-Maenhout, G., and Pitkanen, T., et al.: Historical (1750–2014) anthropogenic emissions of reactive gases and aerosols from the Community Emissions Data System (CEDS), Geosci. Model Dev. 11(1), 369-408, https://doi: 10.5194/gmd-11-369-2018, 2018.

Holton, J. R., P. H. Haynes, M. E. McIntyre, A. R. Douglass, R. B. Rood, and L. Pfister: Stratosphere-troposphere exchange, Rev. Geophys., 33(4), 403–439, https://doi:10.1029/95RG02097, 1995.

Holton, J. R. and Lelieveld, J.: Stratosphere-troposphere exchange and its role in the budget of tropospheric ozone. In Clouds, chemistry and climate (pp. 173-190)., Springer, Berlin, Heidelberg, 1996.

HTAP, T.: Hemispheric Transport of Air Pollution 2010 Part A: Ozone And Particulate Matter, Air Pollution Studies No. 17, 2010.

Hudman, R. C., Jacob, D. J., Cooper, O. R., Evans, M. J., Heald, C. L., and Park, R. J. ~~and Kita, K.~~et al.: Ozone production in transpacific Asian pollution plumes and implications for ozone air quality in California., J. Geophys. Res. Atmos., 109(D23), https://doi:10.1029/2004JD004974, 2004.

IPCC, Climate Change 2013: The Physical Science Basis. Contribution of Working Group I to the Fifth Assessment Report of the Intergovernmental Panel on Climate Change, [Stocker, T.F., D. Qin, G.-K. Plattner, M. Tignor, S.K. Allen, J. Boschung,

Formatted: Font: (Default) +Body (Times New Roman), 1
Formatted: Font: (Default) Times New Roman
Formatted: English (United Kingdom)
Formatted: Font: (Default) Times New Roman
Formatted: English (United Kingdom)
Formatted: Font: (Default) Times New Roman
Formatted: Font: (Default) Times New Roman
Formatted: Font: Times New Roman, 10 pt
Formatted: Font: (Default) Times New Roman, Not Italic
Formatted: Font: (Default) Times New Roman
Formatted: Font: Times New Roman, 10 pt
Formatted: Font: (Default) Times New Roman
Formatted: Don't adjust space between Latin and Asian te
Don't adjust space between Asian text and numbers
Formatted: Font: (Default) Times New Roman
Formatted: Font: (Default) Times New Roman
Formatted: Font: (Default) Times New Roman, Pattern: C
Formatted: Font: (Default) Times New Roman, Not Italic
Formatted: Font: (Default) Times New Roman

A. Nauels, Y. Xia, V. Bex and P.M. Midgley (eds.)]. Cambridge University Press, Cambridge, United Kingdom and New York, NY, USA, 1535 pp, https://doi:10.1017/CBO9781107415324, 2013.

~~Jöckel, P., H. Tost, A. Pozzer, C. Brühl, J. Buchholz et al.: The atmospheric chemistry general circulation model ECHAM5/MESSy1: consistent simulation of ozone from the surface to the mesosphere. Atmos. Chem. Phys. Discuss. European Geosciences Union, 6(4), 6957-7050, hal-00302020, 2006.~~

Jöckel, P., Tost, H., Pozzer, A., Brühl, C., Buchholz, J., and Ganzeveld, L.et al.: The atmospheric chemistry general circulation model ECHAM5/MESSy1: consistent simulation of ozone from the surface to the mesosphere, Atmos. Chem. Phys., 6, 5067-5104, https://doi.org/10.5194/acp-6-5067-2006, 2006.

Jöckel, P., Tost, H., Pozzer, A., Kunze, M., Kirner, O., and Brenninkmeijer, C. A. et al.: Earth System Chemistry Integrated Modelling (ESCiMo) with the Modular Earth Submodel System (MESSy, version 2.51), Geosci. Model Dev., 8(10), https://doi:10.5194/gmd-9-1153-2016, 2016.

Kerkweg, A., Sander, R., Tost, H., and Jöckel, P.: Technical note: Implementation of prescribed (OFFLEM), calculated (ONLEM), and pseudo-emissions (TNUDGE) of chemical species in the Modular Earth Submodel System (MESSy), Atmos. Chem. Phys., 6, 3603-3609, https://doi.org/10.5194/acp-6-3603-2006, 2006.

~~Komhyr, W. D., R. A. Barnes, G. B. Brothers, J. A. Lathrop, and D. P. Opperman: Electrochemical concentration cell ozonesonde performance evaluation during STOIC 1989, J. Geophys. Res., 100(D5), 9231–9244, doi: 10.1029/94JD02175, 1995.~~

Kolonjari, F., Plummer, D. A., Walker, K. A., Boone, C. D., Elkins, J. W., and Hegglin, M. I. et al.: Assessing stratospheric transport in the CMAM30 simulations using ACE-FTS measurements, Atmos. Chem. Phys., 18, 6801-6828, https://doi.org/10.5194/acp-18-6801-2018, 2018.

Krebsbach, M., Schiller, C., Brunner, D., Günther, G., Hegglin, M. I., and Mottaghy, D. et al: Seasonal cycles and variability of O_3 and H_2O in the UT/LMS during SPURT, Atmos. Chem. Phys., 6(1), 109-125, https://doi:10.5194/acp-6-109-2006, 2006.

Kunze, M., Godolt, M., Langematz, U., Grenfell, J. L., Hamann-Reinus, A. and Rauer, H.: Investigating the early Earth faint young Sun problem with a general circulation model, Planet. Space Sci., *98*, 77-92, https://doi:10.1016/j.pss.2013.09.011, 2014.

Formatted: Font: (Default) Times New Roman

Formatted: Font: Times New Roman, 10 pt

Formatted: Font: Times New Roman, 10 pt

Formatted: Font: Times New Roman, 10 pt

Formatted: Font: (Default) Times New Roman, 11 pt

Formatted: Font: (Default) +Body (Times New Roman), 1

Formatted: Font color: Custom Color(RGB(106,106,106))

Formatted: Font: (Default) +Body (Times New Roman)

Formatted: Font: (Default) +Body (Times New Roman)

Formatted: Font: (Default) +Body (Times New Roman), 1 pt, Not Italic

Formatted: Font: (Default) +Body (Times New Roman)

Formatted: Font: (Default) +Body (Times New Roman)

Formatted: Font: (Default) +Body (Times New Roman)

Formatted: Font: (Default) +Body (Times New Roman)

Lacis, A. A., Wuebbles, D. J., and Logan, J. A.: Radiative forcing of climate by changes in the vertical distribution of ozone, J. Geophys. Res., 95, 9971–9981, https://doi:10.1029/JD095iD07p09971, 1990.

Lamarque, J. F., Hess, P. G. and Tie, X. X.: Three-dimensional model study of the influence of stratosphere-troposphere exchange and its distribution on tropospheric chemistry, J. Geophys. Res. Atmos., 104(D21), 26363-26372, https://doi:10.1029/1999JD900762, 1999.

Lamarque, J. F. and Hess, P. G.: Local Processes. Encyclopedia of Atmospheric Sciences, 4, 262-268, 2003.

Lamarque, J.-F., Bond, T. C., Eyring, V., Granier, C., Heil, A. and Klimont, Z. et al.: Historical (1850–2000) gridded anthropogenic and biomass burning emissions of reactive gases and aerosols: methodology and application, Atmos. Chem. Phys., 10, 7017-7039, https://doi:10.5194/acp-10-7017-2010, 2010.

Langford, A. O.: Stratosphere-troposphere exchange at the subtropical jet: Contribution to the tropospheric ozone budget at midlatitudes, Geophys. Res. Lett., 26(16), 2449-2452, https://doi:10.1029/1999GL900556, 1999.

Lee, S., D. M. Shelow, A. M. Thompson, and S. K. Miller: QBO and ENSO variability in temperature and ozone from SHADOZ, 1998–2005, J. Geophys. Res., 115, D18105, https://doi:10.1029/2009JD013320, 2010.

Lelieveld, J. and Dentener, F. J.: (2000). What controls tropospheric ozone?, J. Geophys. Res. Atmos., 105(D3), 3531-3551, https://doi.org/10.1029/1999JD901011, 2000.

Lelieveld, J., Hoor, P., Jöckel, P., Pozzer, A., Hadjinicolaou, P., and Cammas, J. P. et al.: Severe ozone air pollution in the Persian Gulf region, Atmos. Chem. Phys., 9(4), 1396-1403, https://doi:10.5194/acp-9-1393-2009, 2009.

Levelt, P. F., van den Oord, G. H., Dobber, M. R., Malkki, A., Visser, H., and de Vries, J et al.: The ozone monitoring instrument, IEEE Trans. Geosci. Remote. Sens., 44(5), 1093-1101, https://doi:10.1109/TGRS.2006.872333, 2006.

Levelt, P. F., Joiner, J., Tamminen, J., Veefkind, J. P., Bhartia, P. K., and Stein Zweers, D. C. et al.: The Ozone Monitoring Instrument: overview of 14 years in space, Atmos. Chem. Phys., 18, 5699-5745, https://doi:10.5194/acp-18-5699-2018, 2018.~~Levelt, P. F., Joiner, J. Tamminen, J., Veefkind, P., Bhartia, P. K., Zweers, D. S. et al.: The Ozone Monitoring Instrument: Overview of twelve years in space, Atmos. Chem. Phys., doi:10.5194/acp-2017-487, 2017.~~

Formatted: Normal, Line spacing: single, Pattern: Clear
Formatted: Font: (Default) +Body (Times New Roman), 1
Formatted: Font: (Default) +Body (Times New Roman), 1
Formatted: Font: (Default) +Body (Times New Roman), 1
Formatted: Font: 11 pt, Bold
Formatted: Font: (Default) +Body (Times New Roman)
Formatted: Font: (Default) +Body (Times New Roman)
Formatted: Font: (Default) +Body (Times New Roman), N Italic
Formatted: Font: (Default) +Body (Times New Roman)
Formatted: Font: (Default) +Body (Times New Roman)
Formatted: Font: (Default) +Body (Times New Roman)
Formatted: English (United Kingdom)
Formatted: English (United Kingdom)
Field Code Changed
Formatted: English (United Kingdom)
Formatted: English (United Kingdom)
Formatted: Font: Times New Roman, 10 pt
Formatted: Font: Times New Roman, 10 pt, English (Unit Kingdom)
Formatted: Font: Times New Roman, 10 pt
Formatted: Font: Times New Roman, 10 pt, English (Unit Kingdom)
Formatted: Font: Times New Roman, 10 pt
Formatted: Font: Times New Roman, 10 pt, English (Unit Kingdom)
Formatted: English (United Kingdom)
Formatted: Font: Times New Roman, 10 pt
Formatted: Font: Times New Roman, 10 pt
Formatted: Font: (Default) Times New Roman, English (United Kingdom)
Formatted: Font: (Default) Times New Roman

Li, W., L. Li, R. Fu, Y. Deng, and H. Wang: Changes to the North Atlantic Subtropical High and Its Role in the Intensification of Summer Rainfall Variability in the Southeastern United States, J. Climate, 24, 1499–1506, https://doi:10.1175/2010JCLI3829.1, 2011.

Li, W., Li, L., Ting, M. and Liu, Y: Intensification of Northern Hemisphere subtropical highs in a warming climate, Nat. Geosci., 5(11), 830-834, https://doi:10.1038/NGEO1590, 2012.

Lin, M., Fiore, A. M., Cooper, O. R., Horowitz, L. W., Langford, A. O., and Levy, H. et al.: Springtime high surface ozone events over the western United States: Quantifying the role of stratospheric intrusions, J. Geophys. Res. Atmos., 117(D21), https://doi:10.1029/2012JD018151,- 2012.

Lin, M., Horowitz, L. W., Oltmans, S. J., Fiore, A. M. and Fan, S.: Tropospheric ozone trends at Mauna Loa Observatory tied to decadal climate variability, Nat. Geosci., 7(2), 136-143, https://doi:-10.1038/NGEO2066, 2014.

Lin, M., Fiore, A. M., Horowitz, L. W., Langford, A. O., Oltmans, S. J., and Tarasick, D. et al.: Climate variability modulates western US ozone air quality in spring via deep stratospheric intrusions, Nat. Commun., 6, 7105, https://doi:10.1038/ncomms8105, 2015.

Lin, S. and R.B. Rood: Multidimensional Flux-Form Semi-Lagrangian Transport Schemes,- Mon. Wea. Rev., 124, 2046–2070, https://doi:0.1175/1520-0493(1996)124<2046:MFFSLT>2.0.CO;2, 1996.

Liu, X., Bhartia, P. K., Chance, K., Froidevaux, L., Spurr, R. J. D., and Kurosu, T. P.: Validation of Ozone Monitoring Instrument (OMI) ozone profiles and stratospheric ozone columns with Microwave Limb Sounder (MLS) measurements, Atmos. Chem. Phys., 10, 2539-2549, https://doi:10.5194/acp-10-2539-2010, 2010.

Liu, J., Tarasick, D. W., Fioletov, V. E., McLinden, C., Zhao, T. and Gong, S. et al.,: A global ozone climatology from ozone soundings via trajectory mapping: a stratospheric perspective, Atmos. Chem. Phys., 13, 11441-11464, https://doi.org/10.5194/acp-13-11441-2013, 2013b.

Logan, J. A.: Tropospheric ozone: Seasonal behavior, trends, and anthropogenic influence, J. Geophys. Res., 90(D6), 10463–10482, https://doi:10.1029/JD090iD06p10463, 1985.

Manney, G. L. and Hegglin, M. I.: Seasonal and Regional Variations of Long-Term Changes in Upper-Tropospheric Jets from Reanalyses, J Clim, 31(1), 423-448, https://doi:10.1175/JCLI-D-17-0303.1, 2018.

Formatted: Font: Times New Roman, 10 pt

Formatted: Font: Times New Roman, 10 pt

Formatted: Left, Font Alignment: Top, Pattern: Clear (Wh

Formatted: Font: Times New Roman, 10 pt

Formatted: Font: Times New Roman, 10 pt

Formatted: Font: Times New Roman, 10 pt

Formatted: Font: (Default) Times New Roman, Font color: Custom Color(RGB(106,106,106)), Pattern: Clear

Mauzerall, D. L., Logan, J. A., Jacob, D. J., Anderson, B. E., Blake, D. R., and Bradshaw et al.: Photochemistry in biomass burning plumes and implications for tropospheric ozone over the tropical South Atlantic, J. Geophys. Res. Atmos., 103(D7), 8401-8423, https://doi:10.1029/97JD02612, 1998.

McLandress, C., Shepherd, T. G., Polavarapu, S. and Beagley, S. R.: Is missing orographic gravity wave drag near 60° S the cause of the stratospheric zonal wind biases in chemistry–climate models?, J. Atmos. Sci., 69(3), 802-818, https://doi:10.1175/JAS-D-11-0159.1, 2012.

McLandress, C., J.F. Scinocca, T.G. Shepherd, M.C. Reader, and G.L. Manney: ~~Dynamical Control of the Mesosphere by Orographic and Nonorographic Gravity Wave Drag during the Extended Northern Winters of 2006 and 2009.~~, J. Atmos. Sci., 70, 2152–2169, https://doi:10.1175/JAS-D-12-0297.1, 2013.

Merryfield, W. J., McFarlane, N. and Lazare, M. A generalized hybrid transformation for tracer advection, WGNE Blue Book, WMO, 3, 13-3, 2003.

~~Mielonen, T., De Haan, J. F., Van Peet, J. C. A., Eremenko, M. and Veefkind, J. P.: Towards the retrieval of tropospheric ozone with the Ozone Monitoring Instrument (OMI). Atmos. Meas. Tech., 8(2), 671-687, doi:10.5194/amt-8-671-2015, 2015.~~

Mielonen, T., de Haan, J. F., van Peet, J. C. A., Eremenko, M., and Veefkind, J. P.: Towards the retrieval of tropospheric ozone with the Ozone Monitoring Instrument (OMI), Atmos. Meas. Tech., 8, 671-687, https://doi:10.5194/amt-8-671-2015, 2015.

Miles, G. M., Siddans, R., Kerridge, B. J., Latter, B. G. and Richards, N. A. D.: Tropospheric ozone and ozone profiles retrieved from GOME-2 and their validation, Atmos. Meas. Tech., 8(1), 385-398, https://doi:10.5194/amt-8-385-2015, 2015.

Morgenstern, O., Hegglin, M. I., Rozanov, E., O'Connor, F. M., Abraham, N. L., and Akiyoshi, H. et al.: Review of the global models used within phase 1 of the Chemistry-Climate Model Initiative (CCMI), Geosci. Model Dev., 10(2), 639-671, https://doi:10.5194/gmd-10-639-2017, 2017.

Myhre, G., D. Shindell, F.-M. Bréon, W. Collins, J. Fuglestvedt, and J. Huang, ~~D. Koch, J. F. Lamarque, D. Lee, B. Mendoza, T. Nakajima, A. Robock, G. Stephens, T. Takemura and H. Zhang~~: Anthropogenic and Natural Radiative Forcing. In: Climate Change 2013: The Physical Science Basis. Contribution of Working Group I to the Fifth Assessment Report of the Intergovernmental Panel on Climate Change [Stocker, T.F., D. Qin, G.-K. Plattner, M. Tignor, S.K. Allen, J. Boschung, A.

Formatted: Font: (Default) Times New Roman
Formatted: Font: (Default) Times New Roman
Formatted: Font: (Default) Times New Roman, Not Italic
Formatted: Font: (Default) Times New Roman
Formatted: Font: (Default) Times New Roman, Not Italic
Formatted: Font: (Default) Times New Roman
Formatted: Font: (Default) Times New Roman
Field Code Changed
Formatted: Font: (Default) Times New Roman, 10 pt, Not Italic
Formatted: Font: (Default) Times New Roman
Formatted: Font: Times New Roman, 10 pt
Formatted: Font: Times New Roman, 10 pt
Formatted: Font: (Default) Times New Roman, 11 pt

Nauels, Y. Xia, V. Bex and P.M. Midgley (eds.)]. Cambridge University Press, Cambridge, United Kingdom and New York, NY, USA, 659–740, https://doi:10.1017/-CBO9781107415324.018, 2013.

Nassar, R., Logan, J. A., Worden, H. M., Megretskaia, I. A., Bowman, K. W., and Osterman, G. B. et al.: Validation of Tropospheric Emission Spectrometer (TES) nadir ozone profiles using ozonesonde measurements, J. Geophys. Res. Atmos., 113(D15), https://doi:10.1029/2007JD008819, 2008.

Neu, J. L., Flury, T., Manney, G. L., Santee, M. L., Livesey, N. J. and Worden, J.: Tropospheric ozone variations governed by changes in stratospheric circulation, Nat. Geosci., 7(5), 340, https://doi:10.1038/NGEO2138, 2014.

Paoletti, E., De Marco, A., Beddows, D. C. S., Harrison, R. M., and Manning, W. J. ~~et al.~~: Ozone levels in European and USA cities are increasing more than at rural sites, while peak values are decreasing, Environ. Pollut., 192(x): 295–9, https://doi:10.1016/j.envpol.2014.04.040, 2014.

~~Parrish, D. D., et al. (2014), Long-term changes in lower tropospheric baseline ozone concentrations: Comparing chemistry-climate models and observations at northern midlatitudes, J. Geophys. Res. Atmos., 119, 5719–5736, doi: 10.1002/2013JD021435, 2014.~~

Parrish, D. D., Lamarque, J. F., Naik, V., Horowitz, L., Shindell, D. T., and Staehelin, J. et al.: Long-term changes in lower tropospheric baseline ozone concentrations: Comparing chemistry-climate models and observations at northern midlatitudes, J. Geophys. Res. Atmos., 119(9), 5719-5736, https://doi.org/10.1002/2013JD021435, 2014.

~~Pendlebury, D., Plummer, D., Scinocca, J., Sheese, P., Strong, K., Walker, K. et al.: Comparison of the CMAM30 data set with ACE-FTS and OSIRIS: polar regions. Atmos. Chem. Phys. Discuss., 15(21), 12465-12485, doi:10.5194/acpd-15-11179-2015, 2015.~~

Pendlebury, D., Plummer, D., Scinocca, J., Sheese, P., Strong, K., and Walker, K. et al.: Comparison of the CMAM30 data set with ACE-FTS and OSIRIS: polar regions, Atmos. Chem. Phys., 15, 12465-12485, https://doi.org/10.5194/acp-15-12465-2015, 2015.

Prather, M. J., Zhu, X., Tang, Q., Hsu, J., and Neu, J. L.: An atmospheric chemist in search of the tropopause, J. Geophys. Res. Atmos., 116(D4), https://doi:10.1029/2010JD014939, 2011.

~~Roelofs, G. J. and Lelieveld, J. O. S.: Model study of the influence of cross-tropopause O3 transports on tropospheric O3 levels., Tellus B Chem. Phys. Meteorol.,Tellus B: Chemical and Physical Meteorology, 49(1), 38-55, https://doi:10.3402/tellusb.v49i1.15949, 1997.~~

Formatted: Font: (Default) +Body (Times New Roman)
Formatted: Font: (Default) +Body (Times New Roman), N Italic
Formatted: Font: (Default) +Body (Times New Roman)
Formatted: Font: (Default) +Body (Times New Roman), N Italic
Formatted: Font: (Default) +Body (Times New Roman)
Formatted: Font: (Default) +Body (Times New Roman), 1
Formatted: Font: (Default) +Body (Times New Roman)
Formatted: English (United Kingdom)
Field Code Changed
Formatted: English (United Kingdom)
Formatted: English (United Kingdom)
Formatted: Font: (Default) Times New Roman
Formatted: Font: (Default) Times New Roman
Formatted: Font: (Default) Times New Roman
Formatted: Font: (Default) Times New Roman
Formatted: Font: (Default) Times New Roman
Formatted: Font: (Default) Times New Roman, Not Italic
Formatted: Font: (Default) Times New Roman
Field Code Changed
Formatted: Font: (Default) Times New Roman, 10 pt, Not Bold
Formatted: Font: (Default) Times New Roman
Formatted: Font: Times New Roman, 10 pt
Formatted: Font: Times New Roman, 10 pt
Formatted: Font: Times New Roman, 10 pt
Formatted: Font: (Default) Times New Roman
Formatted: Font: (Default) Times New Roman
Formatted: Font: (Default) Times New Roman
Formatted: Font: (Default) Times New Roman, Not Italic
Formatted: Font: (Default) Times New Roman
Formatted: Font: (Default) Times New Roman, Not Italic
Formatted: Font: (Default) Times New Roman
Formatted: Font: (Default) Times New Roman
Field Code Changed
Formatted: Font: (Default) Times New Roman
Formatted: Font: (Default) Times New Roman

Rayner, N. A., Parker, D. E., Horton, E. B., Folland, C. K., Alexander, L. V., and Rowell, D. P. et al.: Global analyses of sea surface temperature, sea ice, and night marine air temperature since the late nineteenth century, J. Geophys. Res. Atmos., 108(D14), https://doi:10.1029/2002JD002670, 2003.

Revell, L. E., Stenke, A., Tummon, F., Feinberg, A., Rozanov, E., and Peter, T. et al.: Tropospheric ozone in CCMI models and Gaussian process emulation to understand biases in the SOCOLv3 chemistry–climate model, Atmos. Chem. Phys., 18, 16155-16172, https://doi.org/10.5194/acp-18-16155-2018, 2018.

Richards, N. A. D., Arnold, S. R., Chipperfield, M. P., Miles, G., Rap, A., and Siddans, R. et al.: The Mediterranean summertime ozone maximum: global emission sensitivities and radiative impacts, Atmos. Chem. Phys., 13(5), 2331-2345. https://doi:10.5194/acp-13-2331-2013, 2013.

Roelofs, G. J. and Lelieveld, J. O. S.: Model study of the influence of cross-tropopause O3 transports on tropospheric O3 levels, Tellus B Chem. Phys. Meteorol., 49(1), 38-55, https://doi:10.3402/tellusb.v49i1.15949, 1997.

Roscoe, H. K.: The Brewer–Dobson circulation in the stratosphere and mesosphere – Is there a trend?, Adv. Space. Res., 38(11), 2446-245, https://doi:10.1016/j.asr.2006.02.078, 2006.

Sander, R., Baumgaertner, A., Gromov, S., Harder, H., Jöckel, P. and Kerkweg, A. et. al.: The atmospheric chemistry box model CAABA/MECCA-3.0, Geosci Model Dev., 4 (2), 373-380, https://doi:10.5194/gmd-4-373-2011, 2011.

Sander, R., öJJöckel, P., Kirner, O., Kunert, A. T., Landgraf, J., and Pozzer, A.: The photolysis module JVAL-14, compatible with the MESSy standard, and the JVal PreProcessor (JVPP), Geosci. Model Dev., 7, 2653-2662, https://doi.org/10.5194/gmd-7-2653-2014, 2014.

Schenkeveld, V. E., Jaross, G., Marchenko, S., Haffner, D., Kleipool, Q. L., and Rozemeijer, N. C. et al. In-flight performance of the Ozone Monitoring Instrument, Atmos. Meas. Tech., 10(5), 1957-1986, https://doi:10.5194/amt-2016-420, 2017.

Scinocca, J. F., McFarlane, N. A., Lazare, M., Li, J. and Plummer, D.: The CCCma third generation AGCM and its extension into the middle atmosphere, Atmos. Chem. Phys., 8(23), 7055-7074, https://doi:-10.5194/acp-8-7055-2008, 2008.

Seinfeld, J. H. and Pandis, S. N. Atmospheric chemistry and physics: from air pollution to climate change. John Wiley & Sons, 2016.

Formatted: Font: (Default) +Body (Times New Roman), 1

Formatted: Font: (Default) +Body (Times New Roman), 1

Formatted: Font: (Default) +Body (Times New Roman), 1

Formatted: Font: (Default) Times New Roman

Scinocca, J. F., McFarlane, N. A., Lazare, M., Li, J. and Plummer, D.: The CCCma third generation AGCM and its extension into the middle atmosphere, Atmos. Chem. Phys., 8(23), 7055-7074, doi: 10.5194/acp-8-7055-2008, 2008.

Sellitto, P., Bojkov, B. R., Liu, X., Chance, K., and Del Frate, F.: Tropospheric ozone column retrieval at northern mid-latitudes from the Ozone Monitoring Instrument by means of a neural network algorithm, Atmos. Meas. Tech., 4, 2375-2388, https://doi:10.5194/amt-4-2375-2011, 2011.

Shepherd, T. G.: Transport in the middle atmosphere, J. Meteorol. Soc. Jpn., N Ser. II, 85B, 165-191, https://doi: 10.2151/jmsj.85B.165, 2007.

Shepherd, T. G., Plummer, D. A., Scinocca, J. F., Hegglin, M. I., Fioletov, and V. E., Reader, M. C. et al. Reconciliation of halogen-induced ozone loss with the total-column ozone record, Nat. Geosci., 7(6), 443, https://doi:10.1038/NGEO2155, 2014.

Škerlak, B., Sprenger, M. and Wernli, H.: A global climatology of stratosphere-troposphere exchange using the ERA-Interim data set from 1979 to 2011, Atmos. Chem. Phys., 14(2), https://doi:10.5194/acp-14-913-2014, 2014.

Smit, H. G. J., and D. Kley: JOSIE: The 1996 WMO International intercomparison of ozonesondes under quasi flight conditions in the environmental simulation chamber at JuÂ´lich, WMO Global Atmosphere Watch report series, No. 130 (Technical Document No. 926). World Meteorological Organization, Geneva, 1998.

Smit, H. G. J., and W. Straeter: JOSIE-1998, Performance of ECC Ozone Sondes of SPC-6A and ENSCI-Z Type, WMO Global Atmosphere Watch report series, No. 157 (Technical Document No. 1218), World Meteorological Organization, Geneva, 2004a.

Smit, H. G. J., and W. Straeter: JOSIE-2000, Jü¨lich Ozone Sonde Intercomparison Experiment 2000, The 2000 WMO international intercomparison of operating procedures for ECC-ozonesondes at the environmental simulation facility at Ju¨lich, WMO Global Atmosphere Watch report series, No. 158 (Technical Document No. 1225), World Meteorological Organization, Geneva, 2004b.

Son, S. W., Han, B. R., Garfinkel, C. I., Kim, S. Y., Park, R. and Abraham, N. L. et al.: Tropospheric jet response to Antarctic ozone depletion: An update with Chemistry-Climate Model Initiative (CCMI) models, *Environ. Res. Lett.*, *13*(5), 054024, https://doi:10.1088/1748-9326/aabf21, 2018.

Formatted: English (United Kingdom)
Formatted: English (United Kingdom)
Formatted: English (United Kingdom)
Field Code Changed
Formatted: Font: (Default) Times New Roman
Formatted: Line spacing: 1.5 lines
Formatted: Font: (Default) +Body (Times New Roman), 1
Formatted: Line spacing: 1.5 lines
Formatted: Font: (Default) +Body (Times New Roman), 1
Formatted: Font: (Default) +Body (Times New Roman), 1 pt, English (United Kingdom)
Formatted: Font: (Default) +Body (Times New Roman), 1
Formatted: Font: (Default) +Body (Times New Roman), 1 pt, English (United Kingdom)
Formatted: Font: (Default) +Body (Times New Roman), 1
Formatted: Font: (Default) Times New Roman
Formatted: Font: (Default) Times New Roman, English (United Kingdom)
Formatted: Font: (Default) Times New Roman
Formatted: Font: (Default) Times New Roman, English (United Kingdom)
Formatted: Font: (Default) Times New Roman
Formatted: Font: (Default) Times New Roman, English (United Kingdom)
Formatted: Font: (Default) Times New Roman
Formatted: Left, Don't adjust space between Latin and As text, Don't adjust space between Asian text and numbers
Formatted: Font: (Default) Times New Roman
Formatted: Font: (Default) Times New Roman
Field Code Changed
Formatted: Font: (Default) Times New Roman
Formatted: Font: (Default) Times New Roman
Formatted: Font: (Default) Times New Roman, 8 pt, Patte Clear

SPARC: SPARC/IOC/GAW Assessment of Trends in the Vertical Distribution of Ozone. N. Harris, R. Hudson and C. Phillips (eds.), SPARC Report No. 1, WMO Ozone Research and Monitoring Project Report No. 43, available at https://www.sparc-climate.org/publications/sparc-reports/, 1998.

Škerlak, B., Sprenger, M. and Wernli, H.: A global climatology of stratosphere-troposphere exchange using the ERA-Interim data set from 1979 to 2011., Atmos. Chem. Phys., 14(2), https://doi:10.5194/acp-14-913-2014, 2014.

Staley, D. O.: On the mechanism of mass and radioactivity transport from stratosphere to troposphere, J. Atmos. Sci., 19(6), 450-467, https://doi:10.1175/1520-0469(1962)019<0450:OTMOMA>2.0.CO;2, 1962.

Stevenson, D. S., Young, P. J., Naik, V., Lamarque, J. F., Shindell, D. T., and Voulgarakis, A. and Folberth, G. A. et al.: Tropospheric ozone changes, radiative forcing and attribution to emissions in the Atmospheric Chemistry and Climate Model Intercomparison Project (ACCMIP)., Atmos. Chem. Phys., 13(6), 3063-3085, https://doi:10.5194/acp-13-3063-2013, 2013.

Stohl, A., Spichtinger-Rakowsky, N., Bonasoni, P., Feldmann, H., Memmesheimer, M. and Scheel, H. E et al.: The influence of stratospheric intrusions on alpine ozone concentrations., *Atmos. Environ.*, *34*(9), 1323-1354, https://doi:10.1016/S1352-2310(99)00320-9, 2000.

Tarasick, D. W., Carey-Smith, T. K., Hocking, W. K., Moeini, O., He, H. and Liu, J. et al.: Quantifying stratosphere-troposphere transport of ozone using balloon-borne ozonesondes, radar windprofilers and trajectory models., Atmos. Environ., 198, 496-509, https://doi:10.1016/j.atmosenv.2018.10.040, 2019.

Thompson, A. M., Witte, J. C., McPeters, R. D., Oltmans, S. J., Schmidlin, F. J., and Logan, J. A. et al.: Southern Hemisphere Additional Ozonesondes (SHADOZ) 1998–2000 tropical ozone climatology 1. Comparison with Total Ozone Mapping Spectrometer (TOMS) and ground-based measurements, J. Geophys. Res., 108, 8238, https://doi:10.1029/2001JD000967, D2, 2003.

Thompson, A. M., J. C. Witte, H. G. J. Smit, S. J. Oltmans, B. J. Johnson, and V. W. J. H. Kirchhoff, and F. J. Schmidlinet al.: Southern Hemisphere Additional Ozonesondes (SHADOZ) 1998–2004 tropical ozone climatology: 3. Instrumentation, station-to-station variability, and evaluation with simulated flight profiles, J. Geophys. Res., 112, D03304, https://doi:10.1029/2005JD007042, 2007.

Formatted: Font: (Default) Times New Roman
Formatted: Font: (Default) Times New Roman
Formatted: Font: (Default) Times New Roman
Formatted: Font: (Default) Times New Roman
Field Code Changed
Formatted: Font: (Default) Times New Roman
Formatted: Font: (Default) Times New Roman
Formatted: Font: (Default) Times New Roman
Formatted: Font: (Default) Times New Roman
Formatted: Font: (Default) Times New Roman, Not Italic
Formatted: Font: (Default) Times New Roman
Formatted: Font: (Default) Times New Roman, Not Italic
Formatted: Font: (Default) Times New Roman
Formatted: Font: (Default) Times New Roman
Formatted: Font: (Default) Times New Roman
Formatted: Font: (Default) Times New Roman
Field Code Changed

Thompson, A. M., Stone, J. B., Witte, J. C., Miller, S. K., Pierce, R. B. and Chatfield, R. B. et al.: Intercontinental Chemical Transport Experiment Ozonesonde Network Study (IONS) 2004: 1. Summertime upper troposphere/lower stratosphere ozone over northeastern North America, J. Geophys. Res. Atmos., 112(12), [D12S12], https://doi.org/10.1029/2006JD007441, 2007a.

Thompson, A. M., Stone, J. B., Witte, J. C., Miller, S. K., Oltmans, S. J. and Kucsera, T. L. et al.: Intercontinental chemical transport experiment ozonesonde network study (IONS) 2004: 2. Tropospheric ozone budgets and variability over northeastern North America, J. Geophys. Res. Atmos., *112*(D12), https://doi:10.1029/2006JD007670, 2007b.

Thompson, A. M., Miller, S. K., Tilmes, S., Kollonige, D. W., Witte, J. C., and Oltmans, S. J et al.: Southern Hemisphere Additional Ozonesondes (SHADOZ) ozone climatology (2005–2009): Tropospheric and tropical tropopause layer (TTL) profiles with comparisons to OMI-based ozone products, J. Geophys. Res. Atmos., 117(D23), https://doi: 10.1029/2011JD016911, 2012.

Tost, H., Jöckel, P., Kerkweg, A., Sander, R., and Lelieveld, J.: Technical note: A new comprehensive SCAVenging submodel for global atmospheric chemistry modelling, Atmos. Chem. Phys., 6, 565-574, https://doi.org/10.5194/acp-6-565-2006, 2006.

Wasserstein, R. L. and Lazar, N. A.: The ASA's statement on p-values: context, process, and purpose. The American Statistician, 70(2), 129-133, https://doi:10.1080/00031305.2016.1154108, 2016/.

Worden, H. M., Logan, J. A., Worden, J. R., Beer, R., Bowman, K., and Clough, S. A. et al.: Comparisons of Tropospheric Emission Spectrometer (TES) ozone profiles to ozonesondes: Methods and initial results, J. Geophys. Res. Atmos., 112(D3), https://doi:10.1029/2006JD007258, 2007.

Yang, H., G. Chen, Q. Tang, and P. Hess: Quantifying isentropic stratosphere-troposphere exchange of ozone, J. Geophys. Res. Atmos., 121, 3372–3387, https://doi:10.1002/2015JD024180, 2016.

Young, P. J., Archibald, A. T., Bowman, K. W., Lamarque, J. F., Naik, V., and Stevenson, D. S. et al.: Pre-industrial to end 21st century projections of tropospheric ozone from the Atmospheric Chemistry and Climate Model Intercomparison Project (ACCMIP), Atmos. Chem. Phys., 13(4), 2063-2090, https://doi:10.5194/acp-13-2063-2013, 2013.

Zanis, P., Gerasopoulos, E., Priller, A., Schnabel, C., Stohl, A., and Zerefos, C. et al.: An estimate of the impact of stratosphere-to-troposphere transport (STT) on the lower free tropospheric ozone over the Alps using ^{10}Be and ^{7}Be measurements, J. Geophys. Res., 108, 8520, https://doi:10.1029/2002JD002604, D12, 2003.

Formatted
Formatted
Formatted
Formatted
Formatted
Formatted
Formatted
Formatted
Formatted
Formatted
Formatted
Formatted
Formatted
Formatted
Formatted
Formatted
Formatted
Formatted
Formatted
Formatted
Formatted
Formatted
Formatted
Formatted
Formatted
Formatted
Formatted
Formatted
Formatted
Formatted
Formatted
Formatted
Formatted
Formatted
Formatted
Formatted
Formatted
Field Code Changed
Formatted
Formatted
Formatted
Formatted

Zanis, P., Hadjinicolaou, P., Pozzer, A., Tyrlis, E., Dafka, S., and Mihalopoulos, N. et al.: Summertime free-tropospheric ozone pool over the eastern Mediterranean/Middle East, Atmos. Chem. Phys., 14(1), 115-132, https://doi:10.5194/acp-14-115-2014, 2014.

Zeng, G., Morgenstern, O., Braesicke, P. and Pyle, J. A.: Impact of stratospheric ozone recovery on tropospheric ozone and its budget, Geophys. Res. Lett., *37*, L09805, https://doi:10.1029/2010GL042812, 2010.

Zhang, L., Jacob, D. J., Boersma, K. F., Jaffe, D. A., Olson, J. R. and Bowman, K. W. et al.: Transpacific transport of ozone pollution and the effect of recent Asian emission increases on air quality in North America: an integrated analysis using satellite, aircraft, ozonesonde, and surface observations, Atmos. Chem. Phys., 8, 6117-6136, https://doi.org/10.5194/acp-8-6117-2008, 2008.

Ziemke, J. R., Chandra, S., Labow, G. J., Bhartia, P. K., Froidevaux, L. and Witte, J. C.: A global climatology of tropospheric and stratospheric ozone derived from Aura OMI and MLS measurements, Atmos. Chem. Phys., 11(17), 9237-9251, https://doi:10.5194/acp-11-9237-2011, 2011.

Ziemke, J. R. and Chandra, S.: (2012). Development of a climate record of tropospheric and stratospheric column ozone from satellite remote sensing: evidence of an early recovery of global stratospheric ozone, Atmos. Chem. Phys., 12(13), 5737-5753, https://doi:10.5194/acp-12-5737-2012, 2012.

Formatted: Font: (Default) Times New Roman

Formatted: Font: (Default) +Body (Times New Roman), 1

Formatted: Font: (Default) +Body (Times New Roman), 1

Formatted: Font: (Default) +Body (Times New Roman), 1

Formatted: Font color: Custom Color(RGB(106,106,106))